UNIVERSITI MALAYSIA SARAWAK • UNIMAS •

Faculty of Engineering

Characterisation of Ground Coffee Waste-based Biocomposite

Tan Ming Yee

Master of Engineering
2017

Characterisation of Ground Coffee Waste-based Biocomposite

Tan Ming Yee

A thesis submitted

In fulfillment of the requirements for the degree of Master of Engineering

(Mechanical and Manufacturing Engineering)

Faculty of Engineering
UNIVERSITI MALAYSIA SARAWAK
2017

DECLARATION

I hereby declare that the thesis is based on my original work except for quotations and citation, which have been duly acknowledged. The thesis has not been accepted for any degree and is not concurrently submitted in candidature of any other degree.

Signed

____

Name: Tan Ming Yee

Date:

ACKNOWLEDGEMENTS

First and foremost, I would like to thank God for His blessing and strength throughout the course of this research study.

Secondly, I would like to express my deepest gratitude to my supervisor, Dr. Nicholas Kuan Hoo Tien for his ultimate guidance, dedication and advice given throughout the process of completing this research study. His experience and expertise in this research field, as well as constructive insights which supported me eminently throughout the conduction of this project.

Also, I would like to devote my sincere appreciation to my co-supervisor, Professor Dr. Amir Azam Khan for his patient guidance and support in conducting this research work.

Furthermore, thanks to the lab technicians, Mr. Sabariman Bin Bakar from Department of Mechanical and Manufacturing Engineering, Mr. Airul Azhar Bin Jitai from Department of Chemical Engineering and Energy Sustainability, and Mr. Affandi Bin Hj Othman from Civil Engineering for their support and help in this project.

Last but not least, my grateful thanks are also extended to my beloved family and friends for their physical and mental supports, and encouragement for the completion of this project.

ABSTRACT

The escalating awareness for the need of greener and sustainable technologies has resulted in the interest of development of bio-composites. In this study, characterisation of oxo-biodegradable high density polyethylene (oxo-HDPE) and ground coffee waste (GCW) biocomposite had been performed. The composites were fabricated using the GCW reinforced HDPE film followed by a hot compression moulding. Fourier transform infrared spectroscopy (FTIR) spectrum indicated the eradication of lipids, hemicellulose, lignin and impurities from GCW particles after the treatments. Thermogravimetric analysis (TGA) executed improved thermal stability while differential scanning calorimetry (DSC) showed increment in degree of crystallinity for all the treated GCW composites. Water absorption demonstrated the treatments had enhanced the hydrophobicity of the treated GCW composites. Scanning electron microscopy (SEM) revealed a coarser surface for the treated GCW as impurities were removed. Besides that, treated composites gave a better GCW/matrix interface. Tensile and impact properties improved after the treatments as a result of better adhesion between filler/matrix. Specific tensile properties improved further as the composites were lighter in weight and density. Optimised results obtained at the particle size of 64-850 μm during volume fraction of 5% and 10%. Among the treatments conducted, oil extracted GCW composite exhibited the highest mechanical properties due to better adhesion of GCW and Oxo-HDPE. This study had shown the potential of GCW as reinforcement in the development of composite applications.

Keywords: ground coffee waste**,** oxo-biodegradable, biocomposite, mechanical properties, thermal properties

Pencirian Biokomposit Berasaskan Sisa Serbuk Kopi

ABSTRAK

Kesedaran tentang keperluan dan kemampanan teknologi hijau semakin meningkat sehingga mewujudkan kepentingan pembangunan biokomposit. Dalam kajian ini, ciri-ciri polietilena okso-biodegradasi ketumpatan tinggi (oxo-HDPE) dan sisa serbuk kopi (GCW) bio-komposit telah dikaji. Komposit diperbuat dengan menggunakan GCW sebagai pengisi dan polietilena sebagai matriks melalui kaedah pengacuan mampatan panas. Spektrum spektoskopi Fourier transform inframerah (FTIR) menunjukkan pembasmian lipid, hemiselulosa, lignin dan kekotoran dari zarah GCW selepas rawatan kimia. Analisis termogogrimetrik (TGA) yang dilaksanakan mempunyai kestabilan haba yang lebih baik manakala kajian terhadap kalorimetri pengimbasan berbeza (DSC) menunjukkan peningkatan dalam darjah penghabluran untuk semua komposit yang dirawat dengan kimia. Penyerapan air menunjukkan rawatan kimia meningkatkan hidrofobik komposit. Pengimbasan mikroscop electron (SEM) mendedahkan permukaan GCW yang dirawati kimia adalah lebih kasar kerana kotoran telah dibuang. Selain itu, permukaan antara GCW/matrik menjadi lebih baik selepas rawatan kimia. Sifat tegangan dan impak mempunyai lekatan yang lebih baik di antara pengisi/matrik selepas rawatan kimia. Keputusan sifat-sifat tertentu bertambah baik kerana komposit adalah lebih ringan dan kurang tumpat. Keputusan optimum diperolehi pada zarah saiz 64-850 mikron ketika pecahan isipadu 5% dan 10%. Antara rawatan kimia yang dijalankan, komposit GCW mengandungi minyak yang telah diekstrek menunjukkan sifat mekanik terbaik disebabkan oleh lekatan GCW dan Oxo-HDPE yanh lebih baik.. Kajian ini telah menunjukkan potensi GCW sebagai pengisi dalam pembangunan aplikasi komposit.

Kata kunci: *sisa serbuk kopi, okso-biodegradasi, biokomposit, sifat mekanik, sifat haba*

TABLE OF CONTENTS

LIST OF TABLES

LIST OF FIGURES

LIST OF ABBREVIATIONS

AAc	acrylic acid
AN	acrylonitrile
BF	Bamboo flour
CG	Coffee ground
CMC	ceramic matrix composite
COFD	coffee dregs
Composite A	Neat oxo-HDPE
Composite B	GCW with different particle size/oxo-HDPE composites
Composite C	Untreated GCW/oxo-HDPE composites
Composite D	GCW with different treatment time of NaOH/oxo-HDPE composites
Composite E	NaOH treated GCW/oxo-HDPE composites
Composite F	Oil extracted GCW/oxo-HDPE composites
Composite G	Oil extracted + NaOH treated GCW/oxo-HDPE composites
DSC	Differential scanning calorimetry
DTG	Derivative thermogravimetric
EFB	empty fruit bunch
EFB-GF-PP	empty fruit bunch -glass fibre-polypropylene
FTIR	Fourier transform infrared spectroscopy
GCW	Ground coffee waste
GF	Glass fibre
HDPE	high density polyethylene

Hr	Hour
ICO	International organisation of coffee
KOH	Potassium hydroxide
LDPE	low density polyethylene
LiOH	Lithium hydroxide
LLDPE	linear low density polyethylene
MA	Maleated anhydride
MA	Maleic anhydride
MDI	4,4’-Methylene diphenyl diisocyanate
MMC	metal matrix composite
MMVF	Man-made vitreous fibre
NaOH	Sodium hydroxide
NaOH	Sodium hydroxide
NF	Natural fibre
OH	Hydroxide
Oxo-HDPE	Oxo-biodegradable high density polyethylene
PE	Polyethylene
PLA	polylactic acid
PMC	Polymer matrix composite
PP	polypropylene
PS	Polystyrene
PVA	polyvinyl alcohol
RH	rye husk
SEBS	styrene-ethylene-butene

SEM	Scanning electron microscopy
SW	Soft wood
TDPA	totally degradable plastic additive
TGA	Thermogravimetric analysis
UPE	Unsaturated polyester composites
WH	Wheat rusk

CHAPTER 1

INTRODUCTION

1.1 Background of study

Composite material is also known as engineered material. It has been used for thousands of years and its demand is escalating day by day. Composite consists of two parts, reinforcing phase and matrix or binder. The reinforcing phase can be particle, natural or synthetic fibre while matrix can be polymer, ceramic or metal. Composites provide a solution by merging two or more materials that have dissimilar but complementary properties; when combined wisely, the properties of the composites can be enormously superior to that of either material alone (Hossain, 2011). Composite materials are utilised in several aspects, for instance, automotive, aerospace, building, plastic, textile and oilfield application (Malkapuram & Kumar, 2008; Wambua et al., 2003). Besides that, it offers light weight, high strength, stiffness, chemical and temperature resistance, corrosion resistance, durable, design flexibility, low thermal conductivity and high dielectric stability properties. In addition, composite materials contribute to a significant reduction in eco-footprint and CO_2 emission (Clark & Deswarte, 2014). The reduction in CO_2 emission is through the lower weight in transportation, easier installation and less maintenance in construction and continuity of operation in industrial applications, and all of these contribute to this extreme performance (Eucia, 2011).

In the year of 2012, world fibre consumption was estimated at 83 million metric tons, with 31 million tons of natural fibres and 52 million tons of chemical fibre (ICAC, 2012). Yang

(2014) mentioned the fibre production in the year 2013 was approximately 85.5 million tons, including 55.8 millions of synthetic fibre, 29.7 million tons of natural fibres. The total production of fibre is expected to increase 3.7% per annum in 2025 (Yang, 2014). Bernhard and Elmar (2013) reported the global demand for carbon fibre reinforced plastic composite was about 108000 tons in 2015. The demand is expected to double to 208000 tons in year 2020 (Bernhard & Elmar, 2013). The polymer market is monopolised by commodity plastics with 80% consuming materials based on non-renewable petroleum resources (Faruk et al., 2012). The high volume usages of petroleum-based synthetic fibre and polymer matrix in the production of composite have led to the depletion of the natural resources and escalating environmental issues, such as pollution, greenhouse effect and global warming. These consequences have raised the concern on the importance of green technology in restoring our mother nature.

Over the last decades, due to the increased environmental awareness, several studies for the production of biocomposite have been conducted. Widespread research has been undertaken to determine the potential of various natural fibres as reinforcement for biodegradable (a synthetic or renewable) polymer matrices in order to establish greener and better quality composite materials.

1.2 Problem statement

Table 1.1 shows the comparison between natural and synthetic fibres (glass). Petroleum-based synthetic fibres are abrasive to machine. Not only that, it is non-renewable, non-recyclable, non-CO_2 neutral and non-biodegradable. It also impacts the environment as the production causes pollution, health issue, and there is no proper disposal handling after usage.

Synthetic or man-made vitreous fibres (MMVF) such as glass wool, carbon, aramid and rock wool are mostly carcinogenic in nature and may affect our health by increasing the risk of cancer to long-term exposure or inhaled (Mussatto et al., 2011a; Pujol et al., 2013). In comparison to conventional reinforcement (synthetic fibre), natural fibre offers several advantages. Natural fibre is biodegradable, lightweight and renewable resources, economic viability, low density, enhanced energy recovery, abundant, ease of separation, reduced dermal and respiratory irritation, good specific strength and modulus (Arbelaiz et al., 2005; García et al, 2007; Panthapulakkal et al., 2005; Rowell et al., 1997; Taşdemır et al., 2009).

Table 1.1: Comparison between natural and glass fibre (Pickering et al., 2016; Wambua et al., 2003)

	Natural fibres (NF)	**Glass fibres (GF)**
Density	Low	Twice that of natural fibres
Cost	Low	Low, but higher than NF
Renewability	Yes	No
Recyclability	Yes	No
Energy consumption	Low	High
Distribution	Wide	Wide
CO_2 neutral	Yes	No
Abrasion to machines	No	Yes
Health risk when inhaled	No	Yes
Disposal	Biodegradable	Not biodegradable
Production	NF has lower environmental impact than GF	
Reinforced composite (Mechanical)	NF has higher specific strength and stiffness than GF	

However, the use of natural fibre has its limitations. The drawbacks are natural fibre has low melting point, poor adhesion and compatibility between hydrophilic fibre and hydrophobic matrix, and high moisture absorption rate (Faruk et al., 2012; Fidelis et al., 2013;

Kalia et al., 2009). These have resulted in the declining of its mechanical properties. Therefore, modification of natural fibre can be done by physical method (corona treatment, plasma treatment) and chemical method (silane treatment, alkaline treatment, acetylation, meleated coupling and enzyme treatment) to increase the adhesion between fibre and matrix in order to reduce the moisture hydrophilic of natural fibre (Faruk , 2012).

The annual production of the ground coffee waste (GCW) is 6 million tons worldwide (Mussatto et al., 2011b). Malaysia has a population of approximately 30 million and the coffee consumption is about 800 gram per capita (ICO, 2014). Upon preparation of the coffee beverage, GCW is the main waste generated. There is approximately one-half of all of the coffee beans remain as waste after processing (Mussatto et al., 2011b). GCW is an underutilised high nutrient and energy material as it contains a large amount of organic compound which are fatty acid, lignin, cellulose, hemicelluloses and other polysaccharides (Pujol et al., 2013). The existence of high content of organic material and compound from the GCW has adverse environmental effect by disposal to landfill or incineration. The disposal of the GCW should be properly managed to turn it into value-added products. These valuable compounds make it suitable to be used as green natural fillers. Although the amount of waste is in large quantities, very few research was conducted to reuse the wastage. Projects such as "grounds for your garden" organised by Starbucks and "Ground to Ground" are some activities in promoting recycling the GCW. Other than that, GCW is used as growth media for lab insects and earthworms; silage and herbal remedies for livestock, including cattle, buffalo, sheep, pigs and chickens; controlling mosquito larvae (albeit with variable success); treating waste water; a natural antioxidant for treatment of diabetic and cardiovascular disease and compost and mulch materials for gardens and landscapes. In addition, GCW has also been utilised for biofuel production (Caetano et al., 2012), as source of sugar (Mussatto et al., 2011b), as precursor for production of activated carbon (Tsai et al., 2012), as compost (Preethu et al., 2007) and as absorbent for metal ions removal (Fiol et al., 2008). Thus, GCW is selected to be the organic filler reinforcement for biocomposite fabrication in this research work.

Previous work done on GCW composites were focus on silane, coupling agent and maleic anhydride treatment on GCW. The matrix used were polypropylene (PP), polylactic acid (PLA) and polyvinyl alcohol (PVA). The treatments done enhanced the mechanical, thermal properties and water resistance of treated composite compared to untreated (Baek et al., 2013; Garcia-Garcia et al., 2015; Lee et al., 2015; Wu, 2015).

Petroleum-based polymer matrix used is also an important concern. Thermoplastic is used as it has the ability to reform, reshaped and offers better impact and chemical resistance of comparable thermoset. The waste management and environment legislation discourage landfill and incineration of the composite materials while promoting the act of recycling for energy saving and resources. However, the cost involved is expensive, difficult in the separation of reinforcement and matrix, and the mechanical properties of the recycled composite material are degraded. As an alternative, this project work is using oxo-biodegradable HDPE as the polymer matrix. The oxo-biodegradable plastic displays the necessary surplus characteristic of degrading speedily after use and discarding by natural mechanisms and with no undesirable environment concern, at the same time retain all the advantages of the conventional plastic (Gho et al., 2008).

1.3 Aims and objectives

This study embarks on the following objectives:

I. To investigate the microstructure of the untreated and treated ground coffee waste and fabricated composites.

II. To study the thermal analysis and water absorption of the fabricated composites.

III. To examine the mechanical properties of the fabricated composites based on different particle size, volume fraction and chemical treatments of ground coffee waste.

1.4 Scope of study

This research focuses on the characterisation of GCW reinforced oxo-biodegradable high density polyethylene biocomposite that using compression moulding fabrication method. Different particle size (85 to 1180 µm), volume fraction (5% to 20%) and surface medication (alkaline treatment and oil extraction using soxhlet method) of GCW were used in this study.

The microstucture of GCW and its composite has been analysed using fourier transform infrared spectroscopy (FTIR) and scanning electron microscope (SEM), themal analysis using thermogravimetric analysis (TGA) and differential scanning calorimetry (DSC), mechanical properties using tensile and impact test, and physical properties using water absorption.

1.5 Organisation of thesis

The thesis consists of 5 chapters which are an introduction, literature review, methodology, results and discussion, conclusion and recommendations.

Chapter 1 comprises of the background study of the composite material. Brief history, definition and application of composites are discussed. The problem statement and objectives are also included.

Chapter 2 is about the information collection of the composite, natural fibre and matrices. The chemical, mechanical and physical properties of the natural fibres are well studied. Apart from that, various types of chemical treatments are studied to improve the quality of the composite manufactured. Previous work done by other researchers have been reviewed to have a better understanding of the process and knowledge of composite fabrication and characterisation of the composite samples.

Chapter 3 is the methodology on the fabrication of natural fibre reinforced composite. The fabricated composite is characterised physically and mechanical by fourier transform infrared spectroscopy (FTIR), scanning electron microscope (SEM), thermogravimetric analysis (TGA), differential scanning calorimetry (DSC), water absorption, tensile, and impact test.

Chapter 4 discusses the results obtained from the experiments. Results from analysis and performance of the composite fabricated are displayed in table and graph form for easy evaluation.

Chapter 5 covers the conclusion of the study and recommendations for future researchers in order to improve the study.

CHAPTER 2

LITERATURE REVIEW

2.1 Natural fibre

As shown in Figure 2.1, natural fibre can be categorised into organic (plant and animal) and non-organic (mineral). Plant fibres are cellulose based and it is sub-divided into bast, seed, leaf fruit, wood, stalk and grass. Meanwhile, animal fibres are protein based and the examples are angora, catgut, wool, silk and yak. The example of the mineral is asbestos. Asbestos is a type of silicate mineral.

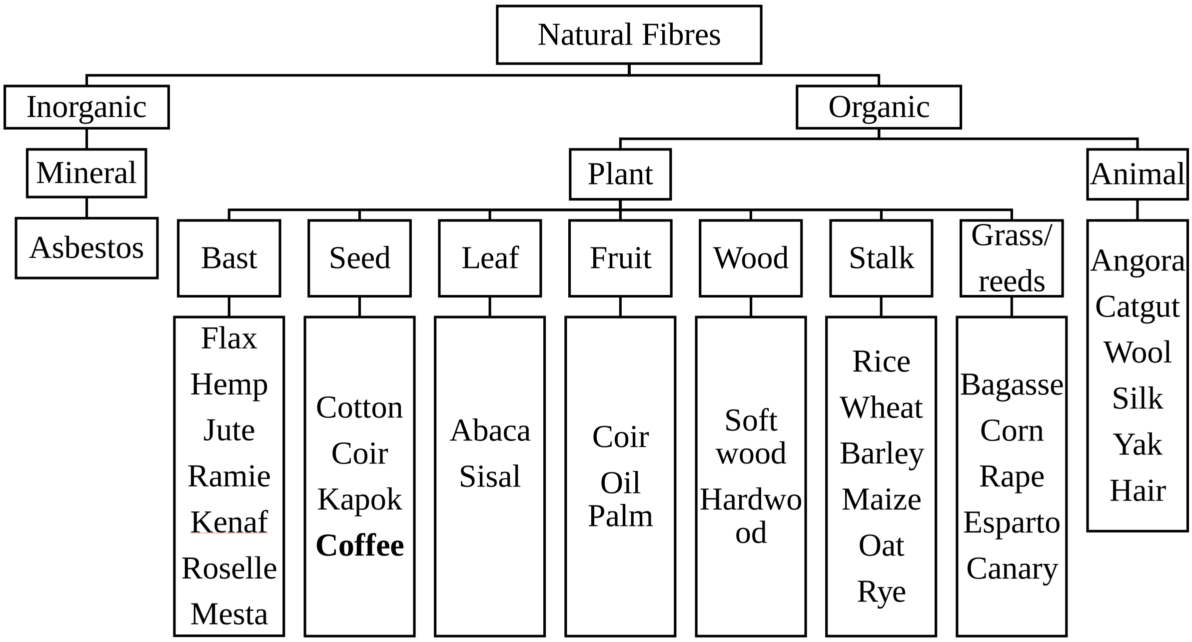

Figure 2.1: Classification of natural fibre (Jawaid & Abdul Khalil, 2011)

2.1.1 Particle reinforced composite

Generally, the reinforcement of composite can be made up of particle-reinforced, fibre-reinforced or structural. Figure 2.2 shows the types of reinforcement of composites. Particle-reinforced can be in the form of large particle or dispersion strengthened. On the other hand, fibre-reinforced can be classified into continuous (aligned) and discontinuous (short). Discontinuous can be further divided into aligned and random oriented. For structural, the reinforcement can be made into laminates or sandwich panels.

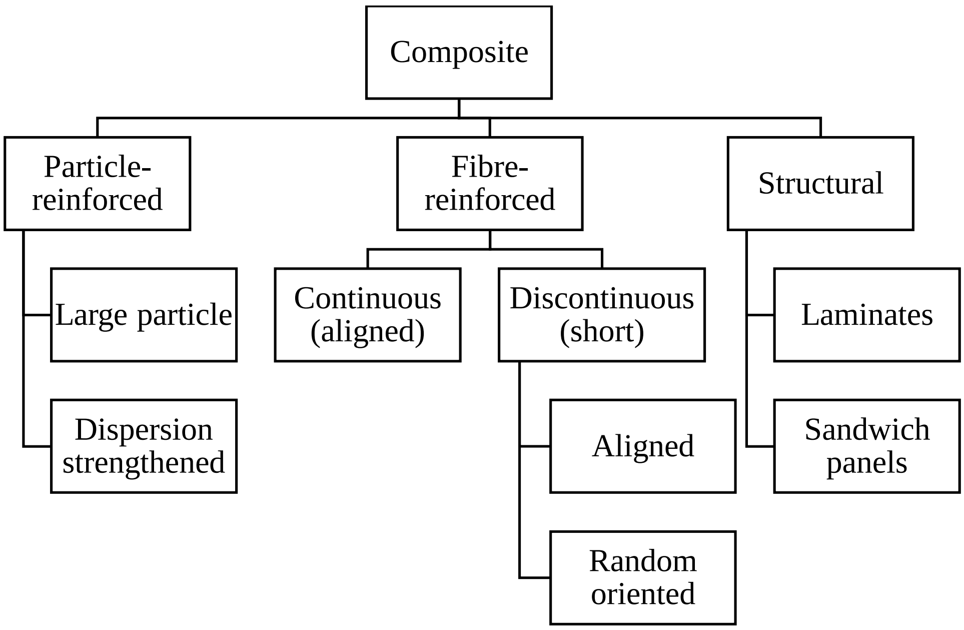

Figure 2.2: Types of reinforcement of composite (Callister & Rethwisch, 2012)

Particle reinforced composite can be classified into two groups which are large-particle and dispersion-strengthened. Large-particle is a type of particle that is unable to be treated on an atomic or molecular level for particle-matrix interactions. Examples of large particles are concrete that is composed of cement the matrix, sand and gravel (the particulates). It has a function of restraining the movement of the matrix when it is well bonded together.

Dispersion-strengthened refers to the diameter of the particles from 10 to 100 nm. The matrix carries a major portion of the applied load while the small particles hinder dislocation motion, limiting plastic deformation. The dispersed phase may be metallic or non-metallic, oxide materials are often used.

Particles have a variety of geometries, however, they should be nearly having an identical dimension in all direction or it may be known as isotropic. Particles can be spherical, platelets, or any other regular or irregular geometry. Particulate composites tend to be weaker and less stiff than continuous fibre composites, nevertheless, they are regularly cheaper. Particulate reinforced composites contain less reinforcement (up to 40 to 50 volume percent) due to processing difficulties and brittleness. For effective reinforcement, the particle should be small and evenly distributed throughout the matrix. The volume fraction of the two phases affects the behaviour, mechanical properties are enriched with rising particulate loading (Callister & Rethwisch, 2012). The properties of the randomly oriented reinforced discontinuous fibres or particles are more isotropic and have a lower strength compared to continuous fibre. However, the particle composites can be produced in an easier and cheaper way compared to fibre reinforced composite through polymer matrix with the fabrication method of compression moulding, extrusion or injection moulding.

Particulate reinforced polymers are used in enormous quantities in various applications. The consumption of particulate reinforcement in Europe was estimated at 4.8 million tons in 2007 (Table 2.1) (Rothon, 2007). The amount of consumption of wood flour and fibre was among the least, 20000 tons. This shows that exploration can still be done to discover new materials in this category since many natural fibres can be used, such as ground coffee waste. Ground coffee waste converts the agro waste into an asset that is valuable.

Table 2.1: Consumption of particulate reinforcement in Europe in 2007 (Rothon, 2007)

Filler	Amount (ton)
Carbon black	2,000,000
Natural calcium carbonate and dolomite	1,500,000
Aluminium hydroxide	250,000
Precipitated silica	225,000
Talc	200,000
Kaolin and clay	200,000
Fumed silica	100,000
Cristobalite, quartz	100,000
Precipitated calcium carbonate	75,000
Calcined clay	50,000
Magnesium hydroxide	20,000
Wollastonite	20,000
Wood flour and fibre	**20,000**

2.1.1.1 *Coffea*

Coffee beans are the seed of the genus of flowering plants, *Coffea*. *Coffea* is a member of the botanical family of Rubiaceace that comprises almost 500 genera and more than 6500 species (Edwin et al., 2006). They are broadly distributed in the tropical and sub-tropical regions.

Coffea is a small tree or shrub with a height of approximately 5 meters. Its shiny dark green colour leaves are 10 to 15 cm long and 6 cm wide. The flowers are white with aromatic smell. The fruit is oval in shape and it is about 1.5 cm in diameter. Figure 2.3 shows *Coffea arabica* tree and Figure 2.4 depicts the coffee cherries turn from green (under ripe) to yellow (ripe) then crimson (very ripe) and finally turn into black (over ripe). Figure 2.5 displays the structure of coffee bean. Most of the coffee cherries have 2 seeds.

The two main cultivated species of coffee beans are *Coffea arabica* and *Coffea canephora*. *Coffea arabica* accounts for 75% to 80% of the world production while *Coffea canephora* or it is also known as Robusta coffee, makes up to approximately 20% of the total production (Ramawat et al., 2014). *Coffea liberica* is less popular whereby it contributes less than 1% of the world coffee production (Illy & Viani, 2005).

Figure 2.3: *Coffea arabica* tree (Powazek, 2013)

Figure 2.4: The colour of coffee cherries from under ripe to over ripe (Powazek, 2013)

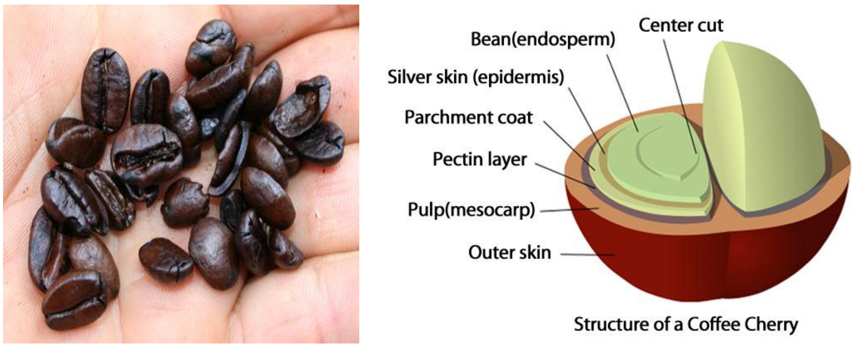

Figure 2.5: Coffee bean (left) and structure of coffee cherry (right) (Powazek, 2013)

Coffea arabica is known as mountain coffee or Arabica coffee. It is self-pollinating, and it is the only tetraploid (2n = 2x = 44) plant (Aga et al., 2003). Tetraploid has 4 sets of chromosomes per cell. It has a higher ratio of cell contents (soluble carbohydrate) to cell wall (fibre). In other words, it has higher water content per cell compared to diploid that has 2 sets of chromosomes per cell. Arabica coffee can be found in the mountains of the Southwestern highland of Ethiopia, the Boma Plateau in Southeastern Sudan and probably Mount Marsabit in northern Kenya (Berthaud & Charrier, 2008; Harlan, 1969; Thomas & Dobkin, 1972). The life span of *Coffea arabica* is up to 100 years and it starts to yield after planting for 3 to 5 years. The fruit takes about 9 months to ripe. The plantation altitude for *Coffea arabica* plant ranges from 600 to 2800 meters with plenty of moisture, rich soil, shade, sun, and the temperature required is approximately 15 ℃ to 24 ℃. Also, it is very sensitive to pest.

Coffea canephora is diploid species (2n = 2x = 22) and it is originated in the upland forests in Ethiopia (Western and Central Africa from Liberia to Tanzania and south to Angola). It is also naturalised in Borneo, French Polynesia, Costa Rica, Nicaragua Jamaica and the Lesser Antilles (Mérot-L'Anthoëne et al., 2014). In comparison to *Coffea arabica*, *Coffea canephora* has twice the amount of caffeine. It can be grown in a lower altitude around 200 to 800 meters and the most importantly it is pest resistance. Other than that, it takes only 10 to 11 months to ripe and ready for harvest.

Coffea liberica is also diploid and it is native to western and central Africa from Liberia to Uganda and Angola. Besides, it can be planted in Seychelles, the Andaman and Nicobar Islands, French Polynesia, Central America, the West Indies, Venezuela, Columbia and Brazil. Liberica takes 8 to 13 months to yield fruits. The peak harvest seasons of Robusta and Liberica fall in January, February and April to June. However, Robusta has another peak harvest season which is from October to December.

Since 1979, Malaysia has started planting coffee. The two species planted in Malaysia are *Coffea canephora* (Robusta) and *Coffea lliberica*. *Coffea liberica* is well-known in Johor and Selangor while the Robusta is found in Northern Peninsular Malaysia, Sabah and Sarawak. In 2009, there are 3000 hectares in the area used for coffee plantation. Harvested coffee cherries are store in a dry place. Coffee beans are dried as fast as possible to yield the best quality beans. Today, Malaysia has a population of approximately 30 million and the consumption of coffee is about 800 grams per capita (ICO, 2014).

Coffee is the second most-traded commodity in the world after petroleum. In accordance to International coffee organisation (2014), the world coffee consumption was about 9 million tons or 149.82 million bags (60 kg per bag) during 2014, an increment of 1.8% than 2013. The total production of coffee during 2015 was about 8.6 million tons or 143.37 million bags (60 kg per bag), an increment of 1.4% compared to the year 2014. The top 5 world leading countries in coffee production are Brazil, Vietnam, Indonesia, Colombia and Ethiopia (ICO, 2014).

It is reported that the annual production of the ground coffee waste is 6 million tons worldwide (Mussatto et al., 2011). After the coffee is extracted in the water, hydrophobic compounds that remain in the coffee ground are oils, lipids, triglycerides and fatty acids; insoluble carbohydrates such as cellulose, hemicelluloses and various indigestible sugars; structural lignin, protective phenolics and wonderful aroma-producing essential oils are also present in coffee (Padmapriya et al., 2013; Pujol et al., 2013). Table 2.2 shows the chemical composition of ground coffee waste.

Table 2.2: Chemical composition of ground coffee waste

Composition of ground coffee waste (% w/w)			References
Cellulose	Hemicellulose	Lignin	
12.4 ± 0.79	39.1 ± 1.94	23.9 ± 1.7	Ballesteros et al., 2014
13.02	-	26.52	Pujol et al., 2013
13.85	-	19.84	Pujol et al., 2013
13.8	-	33.6	Caetano et al., 2012
8.6	36.7	-	Mussatto et al., 2011

2.2 Factor affecting the properties of particulate-polymer composite

The mechanical properties of particulate polymer composite relies on these factors, (Fu et al., 2008)

2.2.1 Particle size

For a given particulate loading, the composite strength rises with decreasing particle size. Particles of smaller size have a greater total surface area. The increasing surface area gives a more effective stress transfer thus it contributes better strength. Under loading, large particles debond easily from the matrix and will lead to premature failure of the part. However, the aggregation tendency of the fillers increases with decreasing particle size (Pukánszky & Móczó, 2004; Suetsugu et al., 1990). The higher the degree of anisotropy (aspect ratio), the higher the strength of the composite (Riley et al., 1990).

2.2.2 Particle-matrix interface adhesion

The adhesion strength of the micro and nanoparticulate composite interface determines the efficiency of stress transfer between matrix and fillers. On behalf of well-bonded particles, the applied stress can be efficiently transferred to the particles from the matrix resulting in higher strength (Hsueh, 1989; Ou et al., 1998). Conversely, for poorly bonded micro-particles, the strength declines by increasing the volume fraction of the particle (Fu & Lauke, 1998; Liang et al., 1997).

2.2.3 Particle loading

There is still no proper principle or theory that can be used to predict the changes in the controlling mechanism in varying composition and component features (Pukanszky & Voros, 1996). With the assumption of perfect adhesion, as the volume fraction of particle increases, the tensile strength increases until the volume fraction reaches its optimum condition.

2.3 Chemical properties of plant fibre

There are more than thousand types of plants on earth with cellulosic fibres. Researchers are still exploring for new and useful natural plant fibres. Natural plant fibres comprise of cellulose fibres, that made up of helically wound cellulose microfibrils, bound together by an amorphous lignin matrix. Fibres can be found in the cell wall of the stem, leaf or seed of a plant. The cell wall is made up of primary wall, secondary wall and lumen. Each fibre has its unique, complex, layered structure comprising a thin primary wall. The primary wall consists of two layers that are an outer and inner layer. The microfibrils arrangement in the primary wall increases assembles from outer to inner surface. The primary wall deposited the plant growth surrounding the secondary wall. The secondary wall has 3 layers (inner, middle and outer). The thickest middle layer decides the mechanical properties of the fibre. The microfibrils in the inner layer of the secondary wall are aligned in two or more orientation while middle layer has comparatively homogeneous orientation. In contrast, the outer layer has a cross-helical (S helix and Z helix) structure of orientation. The chemistry and structure of fibres define their characteristics, functionalities and processing efficiencies. The structure of natural fibre is shown in Figure 2.6.

Plant fibres consist of cellulose, hemicelluloses, lignins, aromatics, waxes, lipids, ash, and water soluble compounds (Mussig, 2010). The chemical composition of plant fibre has its particular behaviour in the cell wall. Cellulose gives strength and stiff crystalline region; cellulose and hemicelluloses form semi-crystalline region and contribute to flexibility; amorphous region of lignin grants toughness and cohesion (Sjostrom, 1993).

The properties of natural fibres are influenced by various factors. These include variety, climate, harvest, maturity, retting degree, decortications, disintegration (mechanical, steam explosion treatment), fibre modification, textile and technical processes (spinning and carding) (Kalia et al., 2009).

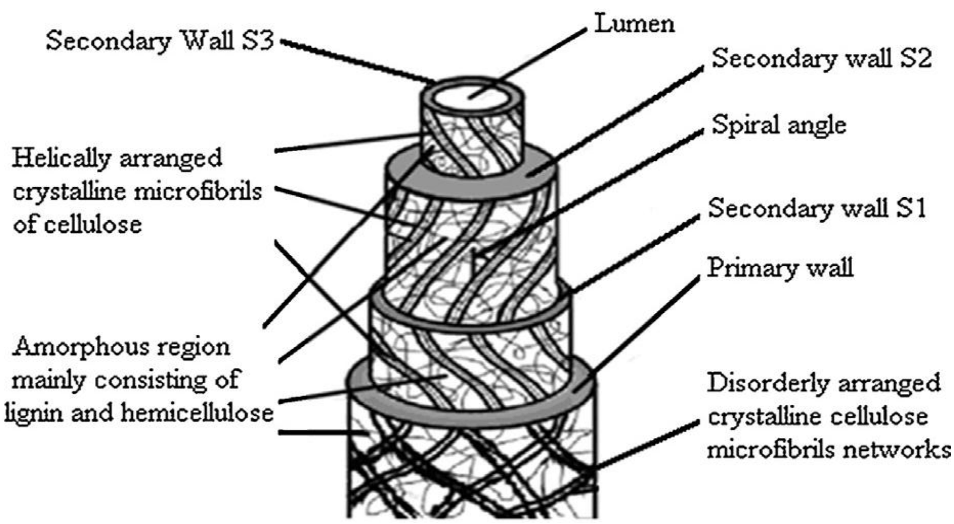

Figure 2.6: Structure of natural fibre (Rong et al., 2001)

2.3.1 Cellulose

Cellulose is the key component of plant cell walls and it is the utmost abundant organic polymer around the globe. It is produced through the process of photosynthesis. Cellulose comprises of C, H and O with the general formula $C_6H_{10}O_5$ (Figure 2.7). Approximately 60% to 70% of the cellulose is present in most natural cellulosic fibres (Akil et al., 2011; Thakur, 2013). Cellulose is mostly found in the leaves and stalks where cotton fibre has a cellulose content up to 95%, and wood is about 50%.

Cellulose is a linear, non-branched carbohydrate polymer of glucose with its simplest form of 1-4 linked β-d-anhydroglucopyranose (Akil et al., 2011; Nelson & Cox, 2013). The repeating unit of cellulose is recognised as cellobiose. Cellulose is connected to another cellulose unit through 1 and 4 carbon as well as intermolecular hydrogen bonds to form a long and straight chain. Cellulose is found in plant cell walls as microfibrils, which have typically a diameter of 2 to 20 nm and 100-40000 nm long. When thousands of glucose unit bond together, crystalline structure will be formed with intramolecular hydrogen bonds providing a stable, hydrophobic polymer with high tensile strength fibre. The length of different types of chains is subjected to the source of cellulose. Cellulose is not water soluble due to widespread intra- and inter-molecular hydrogen bonding and it is a highly crystalline polymer (Medronho & Lindman, 2014).

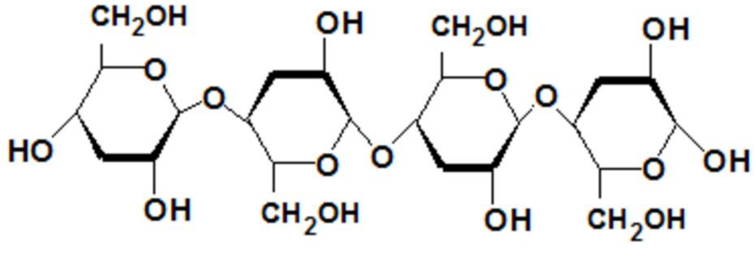

Figure 2.7: Structure of cellulose (Nishiyama et al., 2002)

2.3.2 Hemicelluloses

Hemicellulose is the second most abundant biopolymer on earth. It is heteropolymer of pentose (xylose and arabinose), hexoses (glucose, galactose, mannose) and sugar acids (uronic acid) that are a constituent in primary and secondary cell wall (Peng et al., 2012). Hemicellulose comprises of various distinct sugar meanwhile cellulose contains only anhydrous glucose. There are about 25% to 30% hemicelluloses in a plant.

Hemicellulose is a short and branched chain of sugar build up of an arrangement of 6-ring carbon ring sugars. The important monomers of hemicellulose are shown in Figure 2.8. The degree of polymerisation of cellulose (7000-15000 glucose molecules per polymer) is better than hemicelluloses (500-3000 sugar units per polymer) for ten to hundred times (Bledzki & Gassan, 1999). Thus, it has smaller molecular weight than cellulose. Hemicellulose found in natural fibres is believed to act as a compatibiliser between cellulose and lignin as it remains accomplice with cellulose after lignin has been extracted. However, it has no chemical relationship to cellulose.

Hemicellulose is usually known as a matrix component and it is located in the middle lamella that binds the primary and secondary cell wall of fibres (Focher, 1992). The embodiment of cellulose and hemicellulose network impart rigidity to cell walls.

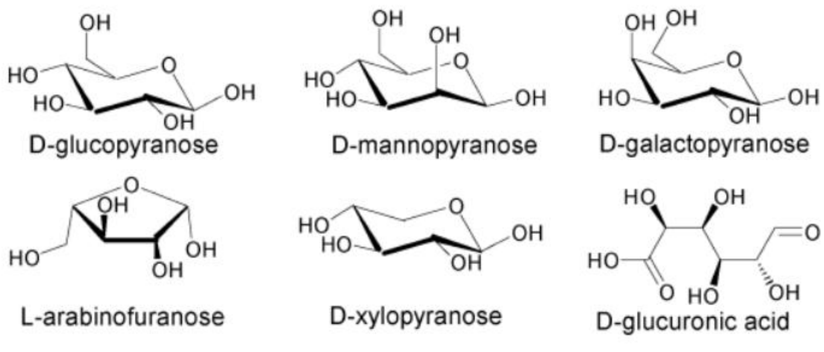

Figure 2.8: The important monomers of hemicellulose (Hansen & Plackett, 2008)

2.3.3 Lignin

Lignin, a fibrous, tasteless material, is insoluble in water and alcohol but soluble in weak alkaline solution and can be precipitated from solution using acid (de Candolle, 1813). It is also oxidised easily and condensable with phenol (Bismarck et al., 2005). Lignin is a sophisticated hydrocarbon polymer that comprises of aliphatic and aromatic ring structures with a huge molecular weight where hydroxyl, methoxyl and carbonyl groups are found in it. The structure of lignin in unit is 4-hydroxy-3-methoxy phenylpropane as shown in Figure 2.9.

The function of lignin is to keep the water in fibre and serve as a protection against microbial pathogens of cell walls. Other than that, it acts as a stiffener to provide stems its protection from gravity forces and the wind. In addition, it provides strength and rigidity by holding and binding the cellulose fibres as a cementitious material. Lignin is a thermoplastic polymer that has a glass transition temperature of approximately 90 ℃ and melting temperature of about 170 ℃ (Thomas et al., 2011). The occurrence of the phenolic group makes lignin more reactive to polymer matrix and coupling agent than cellulose.

In comparison to cellulose and hemicellulose, lignin has crosslinking sites along the propane chain, throughout the C4 oxygen and at the vacant aromatic ring carbon. The cross-link builds up an amorphous structure of lignin. Bledzki and Gassan (1999) stated that the mechanical properties of isotropic hydrophobic lignin are markedly lower than the cellulose (Bledzki & Gassan, 1999).

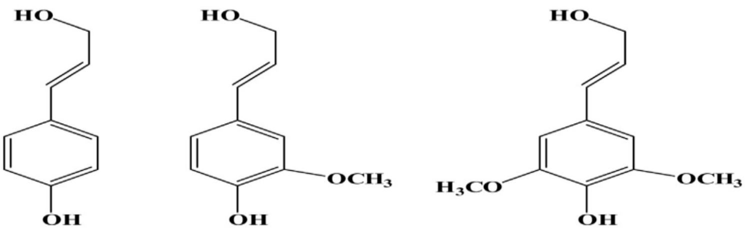

Figure 2.9: Structure of lignin (from left to right: Coumaryl alcohol, Coniferyl alcohol, Sinapyl alcohol) (Bismarck et al., 2005)

2.3.4 Pectin

Pectin, a biopolymer consists of polygalacturon acid. Pectin illustrates a family of oligosaccharides and polysaccharides that have the same features however are dissimilar in their fine structure (Willats et al., 2006). It is a main element of the outer cell wall (middle lamella) that is permeable together with other non-structural carbohydrates that bind the cell together and soluble in water only after partial neutralisation with alkali or ammonium hydroxide (Bledzki & Gassan, 1999; Stamboulis et al., 2001). Pectin plays an important role by allowing primary cell wall extension, plant growth and flexibility. Pectin may be broken down by the use of enzymes such as pectinase and laccase.

2.3.5 Waxes

Waxes are among the most abundant of all natural lipids. It consists of a long chain fatty acid connected through an ester-oxygen to a long chain of alcohol. It is water and numerous acid insoluble such as palmitic acid, oleaginous and stearic acid and solid at biological temperatures. Waxes exist in fibres and it can be extracted using organic solution (Bledzki & Gassan, 1999). Waxes have hydrophobic nature thus they are able to limit the diffusion of water. Waxes surface stem and leave to prevent water loss.

2.4 Mechanical properties and physical properties of natural fibre

Mechanical testing plays a vital role in assessing crucial properties of engineering materials along with establishing new materials. It is used to supervise the quality of materials used in design and construction. Table 2.3 shows the chemical and physical properties of cellulose-based natural fibre versus man-made synthetic fibre.

Table 2.3: Chemical and physical properties of cellulose-based natural fibre versus man-made synthetic fibre

Fibre	Chemical properties					Physical properties				References
	Cellulose (%)	**Hemicellulose (%)**	**Lignin (%)**	**Wax (%)**	**Moisture (%)**	**Density (g/cm^3)**	**Elongation %**	**Tensile Strength (MPa)**	**Young's modulus (GPa)**	
Cotton	82.7	5.7	–	–	1	1.5-1.6	7–8	287-800	5.5-12.6	Bledzki & Gassan, 1997, Chand & Rohatgi, 1994
Coir	36–43	0.15–0.25	41–45	–	–	1.15	15-40	131-175	4-6	Bledzki et al., 1996, Chand & Rohatgi, 1994, Varma et al., 1984
Jute	64.4	12	11.8	0.7	1.1	1.3	1.5–1.8	393–773	26.5	Bisanda & Ansell, 1992, Bledzki et al., 1996, Sridhar et al., 1982
Flax	64.1	16.7	2	1.5–3.3	3.9	1.5	2.7–3.2	345-1035	27.6	Bledzki et al., 1996, Sridhar et al., 1982
Hemp	74.4	17.9	3.7	–	–	1.47	2–4	690	70	Bledzki et al., 1996, Omar Faruk et al., 2012
Sisal	60–78	10.0–14.2	8.0–14	2	10–22	1.33-1.5	2–7	363-700	9.0-38	Dittenber & Gangarao, 2012, Joseph et al., 1999
Kenaf	31–72	20.3–21.5	8–19	–	–	1.4	1.6	930	53	Dittenber & Gangarao, 2012, Omar Faruk et al., 2012
Ramie	68.6–85	13.1	0.6	0.3	7.5–17	1.0-1.55	1.2-4	400-1000	44–128	Bisanda & Ansell, 1992, Dittenber & Gangarao, 2012, Omar Faruk et al., 2012, Sridhar et al., 1982, Varma et al., 1986
Softwood	30-60	20-30	21-37	–	–	1.5	4.4	600-1020	18-40	Michell & Willis, 1978, Spence et al., 2010, Tsoumis, 1991
Hardwood	31-64	25-40	14-34	–	–	1.2	–	–	37.9	Tsoumis, 1991

Table 2.3 Continued

Fibre	Chemical properties					Physical properties				References
	Cellulose (%)	**Hemicellulose (%)**	**Lignin (%)**	**Wax (%)**	**Moisture (%)**	**Density (g/cm^3)**	**Elongation %**	**Tensile Strength (MPa)**	**Young's modulus (GPa)**	
Pineapple leaf	70–83	–	5–12.7	–	11.8	0.8-1.6	1.6-14.5	180-1627	34–82	Chand & Rohatgi, 1994, Dittenber & Gangarao, 2012
Banana	63-64	19	5	–	10-11	1.35	1–3.5	529–759	8	Geethamma et al., 1998, Joseph et al., 2002
Oil Palm	65	10.12	17.5	4	–	1.55	25	248	3.2	Omar Faruk et al., 2012
Bamboo	73.83	12.49	10.15	3.16	–	0.91	1.4	503	35.91	Bledzki et al., 1996
Bagasse	41.6	25.1	20.3	–	–	1.2	1.1	20–290	19–27	Kim & Day, 2011
Wheat straw	34.5	21.3	17.5	–	–	1.45	–	–	–	Fu et al., 2010
Sago waste	40	13.1	4.5	–	–	–	–	–	–	Lee et al., 2014
Corn stover	34.5	27.7	17.8	–	–	–	–	–	–	Kumar et al., 2011
Rice husk	53.2	4.6	19.7	–	–	–	–	–	–	Ang et al., 2011
Switch grass	38.9	28.9	31.7	–	–	–	–	–	–	Kumar et al., 2011
Pandanus	37.3	34.4	24	–	–	–	–	–	–	Sheltami et al., 2012
Spent coffee ground	12.4	39.1	23.9	–	–	–	–	–	–	Ballesteros et al., 2014
E-glass	–	–	–	–	–	2.5	0.5	2000–3500	70	Bledzki et al., 1996, Saechtling, 1995
S-glass	–	–	–	–	–	2.5	2.8	4570	86	Bisanda & Ansell, 1992, Saechtling, 1995
Aramid	–	–	–	–	–	1.4	3.3–3.7	3000–3150	63–67	Bledzki et al., 1996, Saechtling, 1995
Carbon	–	–	–	–	–	1.7	1.4–1.8	4000	230–240	Bledzki et al., 1996,

2.5 Matrices for composite

The matrix of composite acts as an important medium to attach the reinforcement together gives the composite shape and keeps them correctly positioned to maximise its mechanical properties. It also protects the surface of reinforced fibres from environment attack, such as moisture and chemical. Other than that, it transfers the stress from one phase to other phase and provides slight tensile load-carrying capacity for the composite structure. The matrix used for the fabrication of composite can be categorised into three groups, that are metal matrix composite (MMC), ceramic matrix composite (CMC) and polymer matrix composite (PMC).

MMC means the matrix used for the composite is made up of metal such as aluminium, magnesium and titanium; while the reinforcement can be particles, short or long fibre, such as silicon carbide. MMC shows improvement in properties, such as wear characteristic, creep performance and resistance to thermal distortion (Clyne & Withers, 1995). Furthermore, it offers high specific stiffness and high operating temperatures. The drawbacks of MMC are high cost of material, expensive processing, cost lower ductility and toughness.

Meanwhile, CMC comprises short fibres or whiskers bounded together in a ceramic matrix. Examples of the fibre and matrix are carbon, silicon carbide, alumina, mullite and boron nitride. CMC is used to enhance the fracture toughness and used in a very high temperature environment. CMC has light weight, high moduli, high compressive strength, high temperature capability, high hardness and strength, excellent wear, corrosion resistance, low thermal conductivity and high chemical stability. However, ceramic is brittle. Processing of CMC requires high temperature, thus it limits the choice of reinforcement. Apart from that, high processing temperature has resulted in complexity in manufacturing thus increases the production cost. Moreover, the dissimilarity in the coefficients of thermal expansion between the matrix and the reinforcement leads to thermal stresses on cooling from the processing temperature.

PMC consists of short or long fibres embedded by polymer matrix. The reinforcement of fibre gives strength to the fabricated composite while the matrix acts as a support. Strong fibrous network reinforced polymer composite offers high strength, high stiffness, high fracture toughness, good abrasion resistance, chemical resistance, moisture resistance, good puncture resistance, good corrosion resistance and low cost. The disadvantages of PMC are low thermal resistance and high coefficient of thermal expansion. The properties of the composite are affected by the properties of the fibres, orientation of the fibres, concentration of the fibres and the properties of the matrix. PMC is the leading and most diverse used composite nowadays by reason of its ease of fabrication, low cost and good properties.

There are two types of PMC namely, thermoset and thermoplastic. Thermoset is in a liquid state and it is uncured at room temperature, allowing easy impregnation of reinforcing fibres, for instance, fibre glass, carbon fibre or Kevlar. Examples of thermoset resin are polyester, vinyl ester, urethane, phenolic, epoxies and polyamide. They have good properties as they serve as a superb resistance to solvents, corrosives, heat and high temperature, fatigue strength, tailored elasticity, outstanding adhesion, finishing and low raw material cost. Apart from that, it is easy to be fabricated. However, thermoset does not melt or reform upon cooling. This is because it has chemical cross-link to the polymer chains. Hence, the whole matrix is connected to form a three-dimensional network. Consequently, it is very hard to recycle thermoset resin.

Thermoplastic is in a solid state at room temperature and it has high molecular weight. It can be remelted and remoulded when heat and pressure are applied as its polymers are links by intermolecular interactions or van der Waals forces, forming linear or branched structures.

The examples are polyethylene (PE), polypropylene (PP), polyvinyl chloride (PVC) and Polystyrene (PS). Moreover, thermoplastic has 10 times higher for impact resistance compared to a thermoset. Thermoplastic polymer is preferable compared to thermoset as it is recyclable (Hull & Clyne, 1996). The concept of recycling polymer based products gained attention at the end of 1970's due to the oil crises. Recycle refers to the capacity of a material to be used as a source for the new product. The recycling methods employed are remoulding and remelting, chemical recycling, thermal recycling, mechanical recycling and re-melting-casting. The waste management and environment legislation discourage landfill and incineration of the composite materials while promoting the act of recycling for energy saving and resources. However, the cost involved is expensive as it faces difficulty in separation of reinforcement and matrix. The mechanical properties of the recycled composite material are degraded. Thus, research and development have been done continuously in order to discover a low cost, effective recycling technology to separate and recycle the composites.

2.5.1 Polyethylene (PE)

Polyethylene (PE) is the greatest common plastic used in the industries. The yearly global production is 80 million tons (Kingston et al., 2014). Polymerisation of ethylene gas ($H_2C{=}CH_2$) creates PE. Ethylene is generally created from petroleum sources, but it is produced by dehydration of ethanol. PE consists of long chains of the building block of ethylene monomer. The chemical formula of PE is as shown in Figure 2.10. PE is often chosen whenever moisture resistance and low cost products are required.

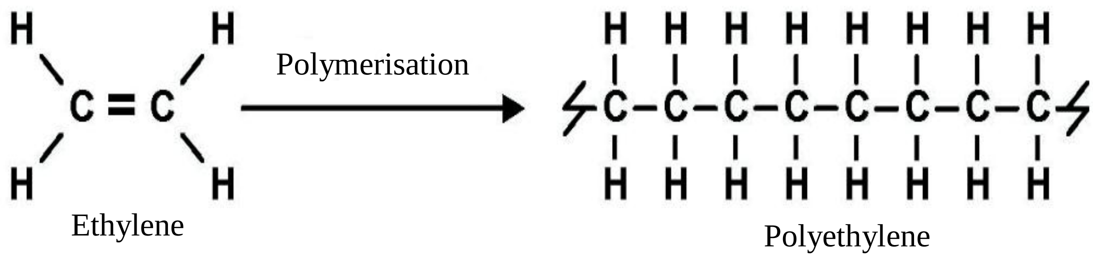

Figure 2.10: Structure of polyethylene

PE can be subcategorised into three groups which are high density polyethylene (HDPE), linear low density polyethylene (LLDPE) and low density polyethylene (LDPE). Common commercial grades of medium and high density PE has a melting point of 120 ℃ to 180 ℃ while for commercial low density polyethylene, it ranges from 105 ℃ to 115 ℃. The mechanical properties of the PE are subjected to its variables. For instance the extent and the type of branching, the crystal structure and the molecular weight. It is used to produce grocery bags, shampoo bottles, children's toy and bullet proof jacket.

PE is usually made of petroleum or natural gas and without special treatment, it will not degrade. Bio-derived PE can be produced by sugar cane, sugar beet or corn. Bio-derived PE is chemically and physically similar to traditional PE, it can be recycled. Bio derivation of polyethylene reduces the emission of greenhouse gases. Alternative ways like, hydro-biodegradable plastic and oxo-biodegradable PE provide the solution where they are biodegradable. Hydro-biodegradable plastic is made from starch based polymers derived from tapioca, corn potato or wheat. Meanwhile, oxo-biodegradable plastic is conventional petroleum-based products with some addictive that hasten degradation.

2.5.1.1 Oxo-biodegradable HDPE

Oxo-biodegradable plastics are shown in Figure 2.11 are a by-product of oil or natural gas containing totally degradable plastic additive (TDPA). TDPA is very small in amount, with approximately 2% to 3% of fatty acids compounds of specific transition metal salts (not heavy metal) such as iron, nickel, cobalt or manganese. They are added to commodity resin as they are a very reactive ingredient. Based on a study conducted by UK Food Standards Agency (2003) on Vitamin and Mineral, it is proven that the metal salts utilised in TDPA plastic are essential fundamentals required for healthy plant and human growth (UK Food Standards Agency, 2003). The metal salts are able to speed up the normal degradation process by the factor of 10. The salts catalyse the degradation process so that it degrades abiotically at the end of its useful life in the occurrence of oxygen faster than ordinary plastic (Joseph et al., 2002; Siracusa et al., 2008a). The European Standards Organisation, CEN defines oxo-biodegradation as degradation resulting from oxidative and cell-mediated phenomena, either simultaneously or successively. Oxo-biodegradable plastic products are evaluated in accordance to ASTM D7954-04 as standard guidelines for exposing and testing plastic that degrade in the environment by a combination of oxidation and biodegradation (Scott, 2009). After the additives have diminished the molecular structure to a level that allows living micro-organisms approach to the carbon and hydrogen, it will be depleted by bacteria and fungi. This process endures until the material has biodegraded to nothing more than CO_2, water, and it does not leave fragments of petro-polymers in the soil. Additionally, oxo-biodegradable plastic passes all the usual ecotoxicity tests, including seed germination, plant growth and organism survival (daphnia, earthworms) tests carried out in accordance with ON S 2200 and ON S 2300 national standards (Scott, 2009).

Figure 2.11: Oxo-biodegradable plastics

In contrast, hydro-biodegradable plastic produces from vegetable biodegrades faster than oxo-biodegradable plastic. However, it is 12 times more expensive than the conventional plastic. In addition, it requires new machinery and it must be produced 5 times thicker to get the same strength as conventional plastic (Tan, 2010). On the contrary, the oxo-biodegradable plastic is cheaper and it has better physical properties and can be manufactured using existing plastic processing equipment. For instance, each oxo-biodegradable garbage bag costs RM 0.30 whereas, for each conventional plastic, it costs RM 0.29.

The demand of oxo-biodegradable plastic is 0.36 million metric tons (2007) and it is predicted to rise to 3.45 million metric tons in 2020 (Faruk et al., 2012). In addition, the useful life of oxo-biodegradable plastic can be preset at manufacture, and it is able to be manufactured by the current technology machinery and workforce in the factories with no additional cost. The oxo-biodegradable plastic retains all the benefits of the conventional plastic at the same time displays extra characteristic of degrading hastily after use and disposal, by natural mechanisms and with no undesirable environment concerns. For manufacturing safety, research has been conducted to govern the exposure to TDPA additive throughout the manufacture of both the additive and product. Outcomes indicated neither the air nor the process water was polluted with the constituents of TDPA and the factory exposure levels were fall in the range of allowable limits (Gho et al., 2008). Table 2.4 shows the comparison of oxo-biodegradable and hydro-biodegradable plastics.

Table 2.4: Comparison of oxo-biodegradable and hydro-biodegradable plastics (Scott, 2009)

Oxo-biodegradable	Hydro-biodegradable
Usually made from a by-product of oil refining	Made from fossil fuel-derived polymers and starch
Can be recycled as part of a normal plastic waste stream	Damages recycle stream unless extracted from feedstock
Can be made from recycled plastic	Cannot be made from recyclate
Emits CO_2 slowly while degrading and forms biomass	Emits CO_2 rapidly while degrading
Inert deep in landfill	Can emit methane in landfill
Can use the same machinery as for conventional plastic	Needs special machinery
Suitable for use in high-speed machinery	Not suitable
Can be compostable	Compostable
Little or no on-cost	Four or five times more expensive than conventional plastic
Same strength as conventional plastic	Weaker than conventional plastic
Same weight as conventional plastic	Heavier
Leak-proof	Prone to leakage
Degrades anywhere on land or sea	Degrades only in high-microbial environment
Time to degrade can be set at manufacture	Cannot be controlled
Safe for food contact	Safe for food contact
No PCB's Organo-chlorines, or "heavy metals"	No PCB's Organo-chlorines, or "heavy metals"
Can be incinerated with high energy-recovery	Can be incinerated, but lower calorific value
Production uses no fertilisers, pesticides or water	Production uses fertilisers, pesticides and water
No genetically modified ingredients	Possibility of GM ingredients
No limit on availability of feedstock	Limited availability of feedstock
Demand for oxo-biodegradable plastics does not drive up cost of fuel for vehicles	Demand for hydro-biodegradable plastics drives up price of human and animal foodstuffs

2.6 Modification of natural fibre (Chemical Treatment)

The usage of natural fibre as reinforcement in the fabrication of composite to replace synthetic fibre has become more popular nowadays to emphasise the importance of concerning the environmental problems. Hydrophilic natural fibre and hydrophobic matrix often lead to poor adhesion and incompatibility between fibre and matrix. Moreover, natural fibre has high moisture absorption behaviour. Thus, modification of natural fibre has to be done to improve the properties of the composite produced. Numerous modifications can be applied for example oil extraction, mercerisation, enzyme, acetylation, and coupling agent.

2.6.1 Oil extraction

Soxhlet extractor is made up of a percolator that circulates the solvent, a thimble to retain the solid to be laved and a siphon mechanism that periodically empties the thimble. The assembly of a soxhlet extractor is condenser at the top, glassware that acts as the reservoir places in between and round bottom flask at the bottom. Soxhlet extraction is designed when the chosen compound has a limited solubility in a solvent, and the impurity is insoluble in that solvent. The process efficiently recycle a small volume of solvent used. This is a low cost oil extraction method. Oil extracted from the samples through soxhlet method can be used to produce biodiesel, synthesis of bioplastic or other possible applications. The samples left behind are always being thrown away. These samples have the potential to be used as reinforcement for composites fabrication.

Rozman et al., (2001) conducted a study on the effect of oil extraction of the oil palm empty fruit bunch (EFB) on the mechanical properties of polypropylene-oil palm empty fruit bunch-glass fibre hybrid composites. EFB extraction was conducted by refluxing the EFB fibres in a solvent mixture of toluene, acetone, and ethanol, with the volume proportion of 4:1:1, for 3 hours. The extracted EFB fibres were dried in an oven at 105 ℃ for 5 hours. Oil extraction EFB composites significantly improved the tensile, flexural, toughness and ductility properties than those without extraction. As shown in SEM micrographs (Figure 2.12), the extracted is embedded tighter in the matrix compared to untreated. This is due to the removal of oil residues on the EFB fibres that enhance the compatibility and better bridging between fibres and the matrix interfacial regions. The oil extraction contributed to the development of continuous interfacial region between EFB and PP matrix, and an improvement in the ductility of the matrix. The extracted surface appeared to be coarser than the untreated surface as a result of the removal of an oil layer on the surface of the fibre.

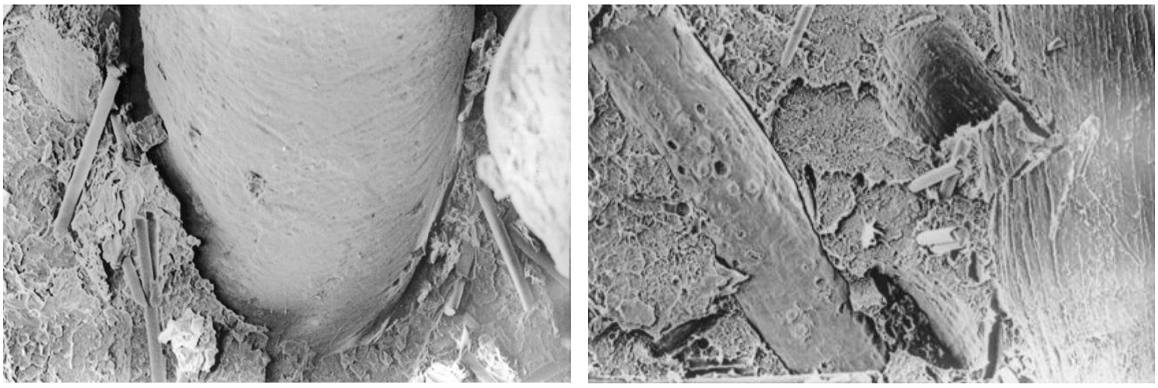

(a) (b)

Figure 2.12: SEM micrograph for composites with a) unextracted EFB-GF-PP b) extracted EFB-GF-PP (Rozman et al., 2001)

Sibele Piedade and Luis Claudio (2013) conducted thermal properties and morphology of high-density polyethylene filled with coffee dregs. The coffee dregs (COFD) were extracted by soxhlet, using 20 g of integral COFD and 80% formic acid as solvent, at a ratio of 1/6, for 12 hours. Based on thermogravimetric performed, the extracted COFD was decreasing in the thermal stability of the composite. This represented the removal of lignin that acted as a thermal protection material. The existence of COFD in the composites did not cause degradation of the material in the common temperature range used (180-200 ℃) for thermoforming articles. The T_{max} and T_{final} stayed very close to pure HDPE. Alternatively, differential scanning calorimetry (DSC) curve revealed 12% reduction in melting enthalpy than the pure HDPE. This demonstrated an interference of the filler in the crystalline packing of the polymer. The reduction might be due to the penetration of the molten polymer into the voids among the COFD dendroids. It might have hindered the diffusion of the molecules to the centres of crystallisation. The crystallisation temperature (T_c) of the composite persisted nearly the same of the HDPE (Sibele Piedade & Luis Claudio, 2013).

2.6.2 Alkaline treatment

Alkaline treatment is also known as mercerisation, a process where the natural fibre is immersed in a concentrated strong base aqueous solution, such as NaOH, LiOH and KOH to create enormous swelling with resultant changes in the fine structure, dimension, morphology and mechanical properties (ASTM D1965) (Aboul-Fadl et al., 1985). The surface treatment disrupts the hydrogen bonding in the network thus increase the surface roughness and yield enhanced mechanical interlocking and increases the quantity of cellulose exposed on the fibre surface, thus increasing the number of likely reaction sites for coupling.

Alkaline treatment is very useful in removing hemicellulose, a slight effect on lignin, waxes, oils and alpha-cellulose. It also depolymerised cellulose and exposed short length crystallites (Mohanty et al., 2001). After the hemicellulose has been removed, the interfibrillar region becomes less dense and less rigid. Thus, the fibrils are able to reorganise themselves along the path of tensile deformation and result in better load sharing when the natural fibres are being stretched. Therefore, the mechanical properties are enhanced. There is a regular elimination of microvoids after the removal of lignin. The middle lamella joins the ultimate cells become more plastic and homogeneous. It is reported that alkaline treatment is able to increase the percentage of crystallinity index as the cementing materials are removed and result in a better packing of cellulose chain. In addition, alkaline treatment decreases the spiral angle (Bledzki & Gassan, 1999). Alkaline treatment is a simple, low cost and effective chemical treatment. The reaction is shown in Equation 2.1,

$$\text{Fibre-OH} + \text{NaOH} \rightarrow \text{Fibre-O-Na}^{+} + H_2O \tag{2.1}$$

Arrakhiz et al., (2013) conducted a study on tensile, and flexural properties of alkaline treated alfa, coir and bagasse reinforced polypropylene. The composites were fabricated using Leistritz ZSE-18 twin screw extruder then Engel e-Victory injection moulding with a 40 tons platen force. The crushed natural fibre was washed carefully with water then kept for 48 hours in a 1.6 mol/l sodium hydroxide aqueous solution. The natural fibres were then removed from the caustic solution and rapidly treated with 100 ml acetic acid. After that, it was air-dried for 24 hours. The size of the natural fibres used is shown in Table 2.5.

Table 2.5: Size of the natural fibre (Arrakhiz et al., 2013)

Type of natural fibres	Average diameter (µm)	Average length (µm)	Aspect ratio
Alfa	135	1300	10
Coir	198	1245	6
Bagasse	201	805	4

In comparison to pure polypropylene (PP), the increased in fibre loading had led to a decreased in tensile strength for all of the natural fibres tested. The tensile strength of coir/PP composite were the highest among the three types of natural fibres. This was because of the lower cellulose and higher lignin contents among the natural fibres. The Young's modulus measured increased with fibre loading (0 wt% to 30 wt%). All of the fibres were having a linear increased in Young's modulus with fibre loading. This was because of the high fibre tensile modulus compared to neat PP (Nam et al., 2011).

Flexural strength remained nearly persistent for all composites. This could be attributed to the good wetting of the treated fibre by the PP matrix. The flexural modulus improved with fibre loading for alfa/PP composite (+46.5%), Coir/PP composite (+47%) and Bagasse/PP composite (+30%). The result showed a good stress transfer from the low modulus PP to the high modulus treated fibres. A good interface between fibre and matrix under the compressive stresses established in sections of the specimen during bending also explained the increased in modulus (Liu et al., 2009). Besides that, the mechanical properties were affected by the aspect ratio of the natural fibres used. It can be seen that aspect ratio greater than 6 shows better improvement in mechanical properties.

Anbukarasi and Kalaiselvam (2015) also studied the effect of chemical treatment on the mechanical behaviour of luffa (300 μm) reinforced epoxy composites. Alkaline treatment was conducted by soaking the fibres in 2% NaOH for 1 hour at room temperature. In contrast to untreated luffa fibre composite, the tensile strength for mercerised luffa fibre composite improved for every particle loading. The highest tensile strength obtained was at 40 wt%. Alkaline treatment is the interruption of hydrogen bonding in the network structure of fibre and increases its surface roughness. The treatment removes a firm quantity of lignin, wax and oils wrapping the external surface of the fibre cell wall, depolymerises cellulose and depicts the short length crystallites (Mohanty et al., 2001). Mercerisation endorses the ionisation of the hydroxyl group to the alkoxide (Agrawal et al., 2000). Therefore, improved mechanical interlocking, increase the quantity of cellulose exposed to the fibre surface and result in increasing number of possible reaction sites (Valadez-Gonzalez et al., 1999).

The flexural strength improved for every particle loading after the treatment. The maximum flexural strength obtained was at 40 wt%. This had shown the effectiveness of the treatment conducted. Although the flexural strength improved with particle loading, it was still lower than the unfilled epoxy. This may due to the agglomeration of the fibre led to an overlap of the fibre and result in the chance of the air entrapment that contributed to poor stress transfer. Rokbi et al., (2011) reported alfa fibre showed improvement in both flexural strength and modulus at 10% NaOH for 24 hours. Meanwhile, 5% NaOH for 48 hours contributed to decrement in flexural properties as a result of the reduction of lignin that binds the cellulose fibrils together (Rokbi et al., 2011).

The impact strength of mercerised luffa fibre composite improved for every particle loading compared to untreated luffa fibre composite. The highest impact strength obtained was at 40 wt%. Alkaline treatment increased the surface roughness of the fibre surface result in better fibre/matrix adhesion. The discontinuity particle fibre reinforced epoxy had weakened the material as the homogeneity of the material was declined. In comparison to untreated fibre, alkaline treated fibre also resulted in better dispersion and stress transfer thus improved the impact strength. Obasi et al., (2014) reported alkali treated oil palm press fibre reinforced epoxy was having a similar trend where impact strength improved with increasing particle loading. The treatment of the oil palm press fibre improved the compatibility and promotes the ability to dissipate energy during fracture (Obasi et al., 2014).

Singha et al., (2013) reported the mechanical properties of untreated and modified grewia optiva fibres (90 µm) reinforced unsaturated polyester matrix based biocomposites using fabrication method of a combination of hand layout and compression moulding. The tensile testing conducted according to ASTM D3039. For untreated grewia optiva fibre, the effect of particle loading (0%, 10%, 20%, 30% and 40%) was studied. The tensile strength of unfilled UPE was 18.7 MPa. As particle loading increased, the tensile strength increased and reached an optimum condition during untreated particle loading 30% with an improvement of 25%. The increased in the tensile strength with the proportion of reinforcement was owing to the enhancement of load transfer between matrix and fibre interface. Conversely, composites declined in tensile properties beyond optimum values as a result of agglomeration of fibres. Agglomeration generated flaws and created voids between fibre and matrix thus diminishing tensile strength (Yang et al., 2004). The surface modification of fibres done was alkali treatment, silane treatment, benzoyl chloride and acrylonitrile (AN) and acrylic acid (AAc) graft polymerisation. The tensile strength was the highest when reinforced with benzoylated fibres followed by Grewia optiva-g-poly(AN), silanated fibres, Grewia optiva-g-poly(AAc), mercerised and raw grewia optiva fibres reinforced composites. The optimum condition obtained was at 30% particle loading for all the surface modifications. The tensile strength improved 21%, 14%, 12%, 11% and 10% with particle loading compared to untreated fibre. Benzoylation treatment aimed to decrease the hydrophilic nature of treated fibre and improved its interaction with the hydrophobic matrix. Benzoylation improved the fibre-matrix adhesion, water resistance and thermal stability (Li et al., 2007). Thus, increased the strength of the composite. Benzoylation increased the hydrophobicity of the fibre compared to silanated and grewia optiva-g-poly(AN) (Mohanty et al., 2000). Graft copolymerisation of AN and AAc initiated free radicals to react with the cellulose molecules by dehydrogenation and oxidation. The activated free radical sites interacted with the monomer of the matrix to enhance the interlocking efficiency at the interface (Kalia et al., 2009). Grewia optiva-g-poly(AAc) fibre reinforced polymer composites demonstrated the lowest tensile strength of the treated fibres because of the existence of polar pendants -OH groups on grafted poly (AAc) chains that led to weaker interfacial adhesion between matrix and fibre. Other researchers reported AAC enhanced the stress transferability at the interface and therefore improved composite properties (Li et al., 2007; Zahran & Rehan, 2006). The rough surface topology of mercerised composites improved adhesive characteristics between fibre and matrix. Mercerised fibre also increased in the effective surface area resulted in higher aspect ratio. Silane treatment was used to improve fibre hydrophobicity and fibre-matrix adhesion in order to yield better mechanical properties. Similar trend result reported by another researcher (Raj et al., 1989). For raw fibre, hydrophilic -OH groups on fibre surface make it less compatible with hydrophobic UPE. Therefore, resulted in poor fibre/matrix adhesion and lower tensile strengths as compared to grafted fibre. Study on rice husk/post-consumer polyethylene composites showed no significant on tensile strength with mercerisation and acetylation treatment (Fávaro et al., 2010).

The thermal properties of grewia optiva fibres (90 μm) reinforced unsaturated polyester matrix based composites are depicted in Figure 2.13. TGA of optimised samples of raw, mercerised, silanated, benzoylated, grewia optiva-g-poly(AN) and grewia optiva-gpoly(AAc) particle fibres reinforced UPE composites was carried out in the nitrogen atmosphere at a heating rate of 15 ℃/min, temperature ranges from 20 ℃ to 1000 ℃. There were three stages of weight loss linked with the TG curve. The level of degradation of surface modified grewia optiva/UPE composites was less than the untreated. The first stage, up to 200 ℃, corresponded to a maximum weight loss of 10%. The second stage with more than 70 wt% of loss, up to 500 ℃ while the final stage extended to about 800 ℃ in association with a loss that may reach 20 wt%. The thermal decomposition of cellulose began to occur at 210-260 ℃ by dehydration followed by main endothermic reaction of depolymerisation with DTG peaks that vary from 310 ℃ to approximately 450 ℃. Hemicellulose was detected to decompose at a maximum temperature at 290 ℃ and up to 150 kJ/mol of activation energy. Meanwhile, lignin decomposed at 280 ℃ to 520 ℃ and up to 229 kJ/mol of activation energy (Nguyen et al., 2007a, 2007b). Thermal stability of treated fibre composites improved as extra intermolecular bonding between fibre and matrix. This increased in degradation temperature was credited to the strong interface formed through chemical modification of fibres. The silanated based composites obtained the maximum thermal stability. This was related to the better interaction between fibre and matrix as strong covalent bonds between $H_2N-(CH_2)_3$- groups of silane and OH groups of cellulose were formed (Singha et al., 2013). Major degradation occurred at temperature 300 ℃ to 400 ℃ and the improvement of the thermal stability of these fibres after treatment ensure the ability to be utilised with engineering polymers for enhanced performance and thus broaden the applications of natural fibre composite.

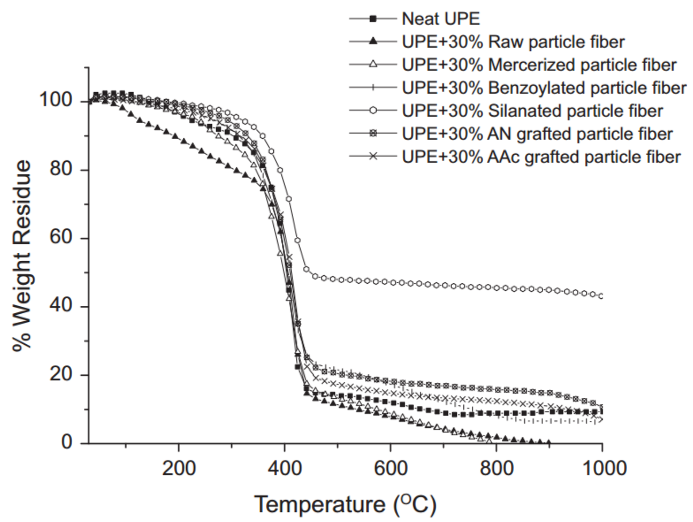

Figure 2.13: TGA thermograms of neat UPE and its composites reinforced with raw and different surface modified surface modified grewia optiva fibres (Singha et al., 2013)

Mwaikambo and Ansell (2002) utilised FTIR to study the chemical modification of hemp, jute and kapok fibre by alkalisation. The result showed that alkalisation modified plant fibres promoted the development of fibre-resin adhesion. This resulted in an increment in the interfacial energy and therefore improved the mechanical and thermal stability of the composites (Mwaikambo & Ansell, 2002).

Alkaline treatment reduced the presence of hydrogen bonding. This was attributable to the removal of the hydroxyl groups. Thus, it increased the –OH concentration. Figure 2.14 and Figure 2.15 depicted the evident of improved intensity between 1000 and 1500 cm^{-1} peaks compared to untreated fibre that represented hemicelluloses. Other than that, peaks range 3200 to 3600 cm^{-1} referred to hydrogen bonding with the carboxyl groups or fatty acids on the fibre surface. Figure 2.14 and Figure 2.15 showed a reduction in the area of these peaks after treatment.

Peaks range from 1736 and 1740 cm^{-1} indicated the existence of carboxylic acid. These peaks disappeared after treatment as a result of deesterification (Sun et al., 1999). The presence of C=O bonds (fatty acid in oils) of hemicellulose detected at around 1654 cm^{-1} was removed easily by the treatment especially for sisal and jute while hemp and kapok were less affected. During the peak at 1384 cm^{-1} and 1245 to 1259 cm^{-1} showed the presence of lignin and hemicelluloses (Mwaikambo & Ansell, 1999; Runcang Sun et al., 1999). As the concentration of the treatment increased, the diminishing area at peak 1384 cm^{-1} getting bigger. Peaks at 1245 to 1259 cm^{-1} represented removal hemicellulose only. This proved that it is harder to remove lignin content in fibre during alkaline treatment.

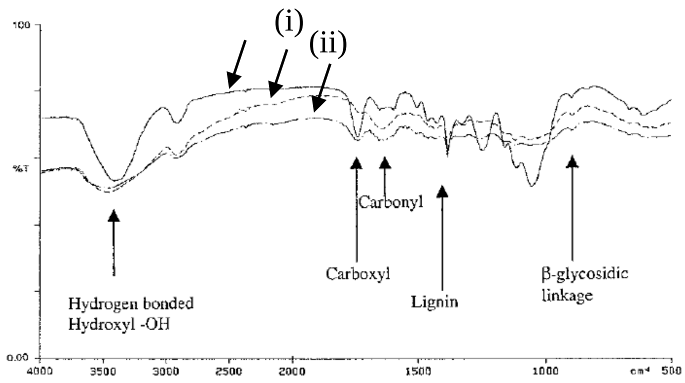

Figure 2.14: FTIR spectra of (i) untreated hemp fibre, (ii) untreated sisal fibre, and (iii) untreated kapok fibre (Mwaikambo & Ansell, 2002)

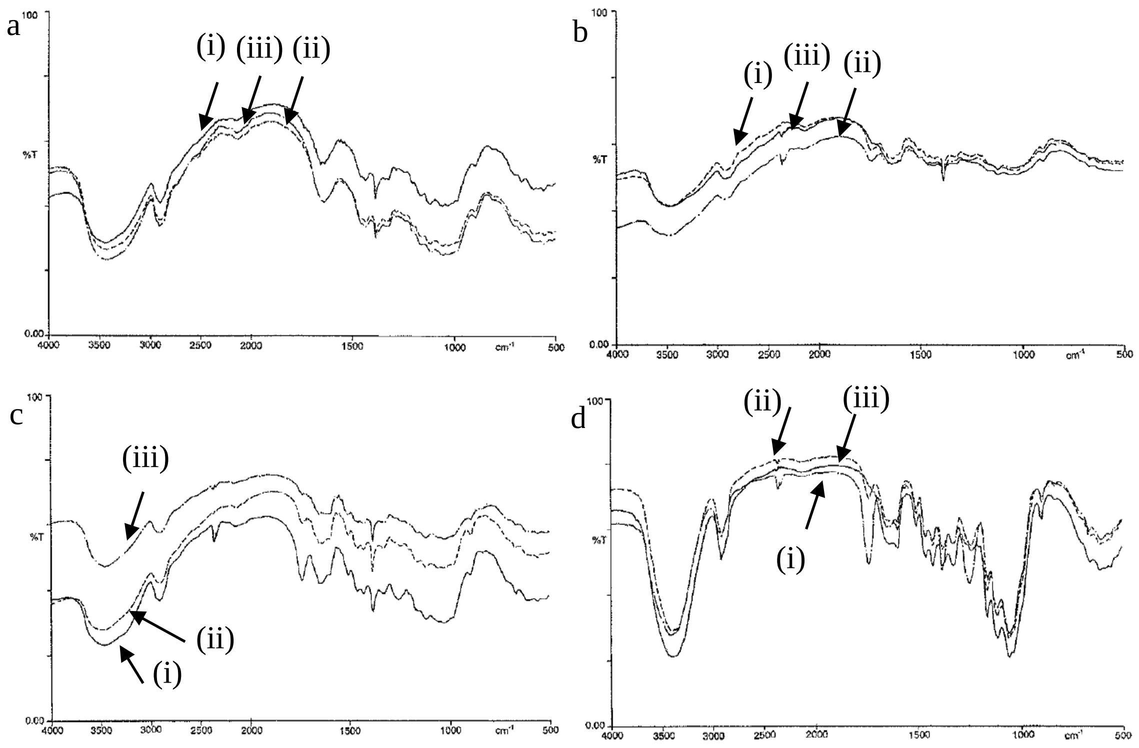

Figure 2.15: (a) Infrared spectra of hemp fibre: (i) 0.8% NaOH, (ii) 8% NaOH, (iii) 30% NaOH, (b) Infrared spectra of sisal fibre: (i) 2% NaOH, (ii) 4% NaOH, (iii) 6%NaOH, (c) Infrared spectra of jute fibre: (i) untreated (ii) 2% NaOH, (iii) 4% NaOH and (d) Infrared spectra of kapok fibre: (i) untreated, (ii) 6% NaOH, (iii) 30%NaOH (Mwaikambo & Ansell, 2002)

Alkaline treatment enhanced fibre strength (Beckermann & Pickering, 2009; Bera et al., 2010). Besides that, the treatment improves properties, such as interfacial shear strength (IFSS), tensile strength, Young's modulus, failure strain, impact strength, fracture toughness and flexural properties of composites as well as thermal stability and long-term moisture resistance were reported using alkali treated natural fibre reinforced composites (Bera et al., 2010; Goda et al., 2006; Gomes et al., 2007; Islam et al., 2010; Kabir et al., 2012; Nor Azowa Ibrahim et al., 2010). For crystallisable matrices, alkaline treated fibre affects the degree of matrix crystallinity as the exposed cellulose performing as a nucleation site for crystalline polymer (Sawpan et al., 2011).

2.6.3 Acetylation

Acetylation is a reaction that presents an acetyl functional group ($COCH_3$) into a chemical group. The reaction involves the substitution of the hydrogen atom of a hydroxyl group with an acetyl group that produces acetate. The purpose of acetylation is to coat the surface of the natural fibres become more hydrophobic with -OH groups (Figure 2.16). Acetylation is able to lessen the hygroscopic nature of natural fibres and improves the dimensional and thermal stability of composites (Sreekala et al., 2000). The equation of acetylation treatment is shown in Equation 2.2. Commonly acetylation is preceded by an alkaline treatment.

$$\text{Fibre-OH} + CH_3\text{-C(=O)-O-C(=O)-}CH_3 \rightarrow \text{Fibre-OCOCH}_3 + CH_3COO \qquad (2.2)$$

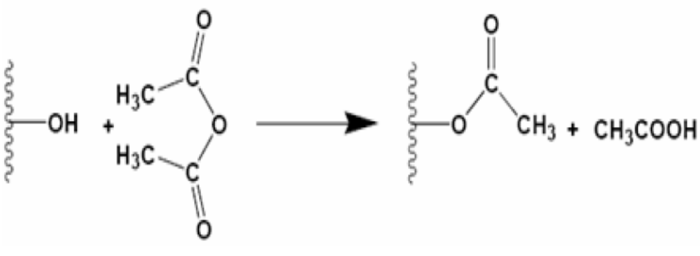

Figure 2.16: Structure of acetylation process (Pickering et al., 2016)

Bledzki et al., (2008) performed a study on the effects of acetylation on properties of flax fibre reinforced polypropylene composite. The flax fibres were having a length of 6 to 8 mm. The flax fibres were immersed in the demineralised water for an hour, filtered and placed in a round bottom flask, comprising acetylating solution. Acetylating solution was prepared with a combination of 250 ml toluene, 125 ml of acetic acid anhydride and a small amount of 60% perchloric acid at temperature, 60 ℃ for 1 to 3 hours. The fibres were washed periodically using distilled water until it returned to pH 7. Then, modified fibres were air dried. The fabrication of composite was using mixer injection moulding.

Tensile and flexural strengths of composites increased with degree of acetylation up to 18% and then decreased. The improvement was because of the removal of lignin and extractives, a slight increase in cellulose content and a small amount of hemicellulose transforming to acetylated hemicellulose. After 18% acetylation treatment, the celluloses were degraded and internal cracks and damages occurred in the fibre. Acetylation treatment also removed waxy materials, improved the adhesion between matrix and fibre, and surface free energy that contributed to better properties. Tensile and flexural strength properties improved 20 to 35% using maleated polypropylene-MaH as a result of the formation of ester bonds.

The result for flexural modulus was having the same trend as tensile and flexural strength. The improvement was due to the removal of the outer surface; increased cellulose content and effective surface area increased interfacial adhesion and physical, and chemical changes induced by fibre treatment. Fibrillation and diameter reduction of flax fibre also affect the flexural modulus. The flexural strengths increased 20% for MAH treatment due to better interfacial interaction between fibre and matrix. Flexural modulus also improved for MAH treatment.

Increasing the degree of acetylation has led to decrement in Charpy impact strength. The sturdy interface and the decrease in toughness of composites were the main reasons respond to the results. The introduction of MAH treatment did not show any improvement but impact results were decreased further. Owning to the local internal deformation and increment in brittleness of the composite materials (Bledzki et al., 2008).

Hung et al., (2016) examined the effect of wood acetylation on the mechanical properties and creep resistance of wood/recycled-polypropylene composites using time-temperature superposition principle. Flexural and tensile strength of the composites increased with particle loading up to 13%. Besides, the TTSP-predicted creep compliance curve fit well with the long-term experimental data. The creep resistance of acetylated composites showed better results than the untreated composites (Hung et al., 2016).

2.6.4 Coupling agent

Coupling agent is a chemical element that is able to react with the reinforcement and the matrix of a composite material. It offers a chemical bond between two different materials, generally an inorganic and an organic to promote a stronger bond at the interface. Maleated coupling can modify the surface of the natural fibre and at the same time, it enhances the adhesion bonding between the matrix and the fibre then strengthen the composite. Figure 2.17 shows the reaction for MAPP treatment.

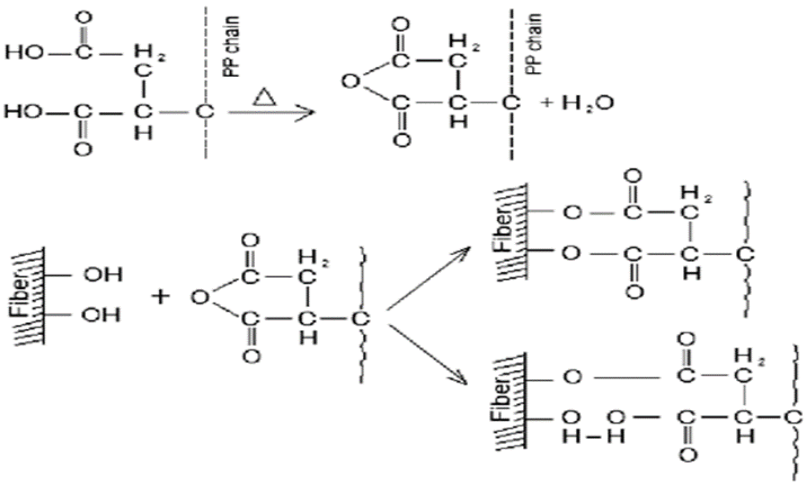

Figure 2.17: The reaction of cellulose fibre with hot MAPP copolymer (Bledzki et al., 1996)

Kakou et al., (2014) studied the effect of coupling agent (maleated polypropylene, MAPP) on properties of high density polyethylene composites reinforced with oil palm fibres. The composites were fabricated by twin-screw extrusion followed by compression moulding. The oil palm fibres were having an average diameter of 50 µm and 750 µm giving L/D ratio of 15. Tensile and impact test were conducted to determine the effect of fibre and compatiliser content. The volume fraction of oil palm fibres used were 30 wt% and 40 wt% with coupling agent concentration 0, 2, 4, 6 wt%.

The neat HDPE had the highest tensile strength of 22.5 MPa. The result of 30 wt% of fibre content showed a better result compare to 40 wt% volume fraction while coupling agent performed the best during 4 wt%. When more fibre/fibre interaction during higher volume fraction, it blocked efficient stress transfer between the fibre and matrix. Other than that, it was harder to obtain good dispersion of fibre into the polymer matrix when volume fraction increased. Using a 6 wt% of coupling agent resulted in lower tensile strength because of the self-entanglement among coupling agent chains rather with the polymer matrix. The lower tensile strength was due to the fragile character of natural fibres and short fibrillar of the palm fibres that initiated cracks during tensile deformation (Shinoj et al., 2011). The enhancement in tensile strength for the treated fibre composite was due to the formation of a chemical bridge between the oil palm fibres and the HDPE matrix. Thus, resulted in better interaction.

The increased in fibre contents from 30 to 40 wt% lead to the increase of young modulus of 40% and 50%, respectively at 4 wt% coupling agent compared to untreated fibre. The existence of ester bonds between the fibre and maleic anhydride function in the coupling agent and inherent stiffness of the fibres resulted in the improvement of the modulus (Mamun & Bledzki, 2013; Shinoj et al., 2011).

The impact strength of 40 wt% of oil palm fibre was higher compared to 30 wt%. This showed that oil palm fibres played a significant role in the toughening processes. Impact strength improves with fibre volume fraction. The optimum impact strength of 40 wt% with 4 wt% coupling agent. The composite with more fibre content was more fragile. This problem can be solved by using coupling agent with the polymeric part with rubber character like styrene-ethylene-butene (SEBS-g-MA) styrene grafted with maleic anhydride (Nekhlaoui et al., 2014). The results presented that compitalised composites have superior stiffness owing to enhance interfacial adhesion between the fibres and the matrix. In addition, better fibre dispersion by reason of chemical bonding. The optimal MAPP content was 4%.

Another researcher reported similar results that tensile, flexural strength, stiffness and impact strength of PP matrix composites using MAPP treatment (Franco-Marquès et al., 2011). It gave nearly twofold the composite strength compared to silane treatment (Bera et al., 2010). MA grafted PLA improved the mechanical and thermal properties of the composites (Avella et al., 2008; Kang et al., 2014; Yu et al., 2014). Overall, Maleic anhydride (MA) grafted polymer is the most commonly used coupling agent that yielded promising results.

Baek et al., (2013) utilised coffee ground (CG) and bamboo flour (BF) as reinforcement to polylactic acid (PLA) bio-based polymer. The method of production was using twin screw extruder then injection moulding. Coupling agent, MDI (4,4'-Methylene diphenyl diisocyanate) was used to enhance the interface bond between the matrix and natural fibre. The tensile strength of both the CG/PLA and BF/PLA composite decreased with the increase of natural fibre filler content. Pure PLA was having a strength of 60.1 MPa. The use of the natural fibre loading from 10 wt% to 40 wt% showed a decrease of tensile strength from 48 MPa to 27.5 MPa for BF/PLA. CG/PLA also exhibited an alike trend of reduction. The tensile strength showed a reduction of 20.1% to 54.3% compared to neat PLA. This was because of the weak interface between the reinforcement and matrix. Thus, hinder stress propagation. The tensile strength of BF/PLA was better than CG/PLA because of the holocellulose and lignin content of BF was higher compared to CG. Natural fillers comprise of cellulose, hemicellulose and lignin. Lignin serves as a stiffening agent for the cellulose molecules within the bio-flour cell wall. Hence, the lignin and cellulose content of bio-flour marks the tensile strength of the fabricated composites.

MDI treatment for 1, 3 and 5 phr improved the tensile strength for both BF/PLA and CG/PLA composite from 34.6 to 54 MPa and 27.5 to 37.3 MPa. BF/PLA composite performed better than CG/PLA. The isocyanate groups from MDI that respond to the hydroxyl group of BF and CG result in graft copolymer of PLA and natural fibre with a urethane linkage. Therefore, MDI enhanced the interface bonding between matrix fibre and natural fibre.

The flexural strength showed a similar pattern result to tensile strength. The flexural strength of pure PLA was 106 MPa. The increase of natural fibres loading from 10 wt% to 40 wt% led to a decrement in flexural strength for both BF/PLA and CG/PLA. CG/PLA showed a decline from 80 MPa to 42.3 MPa. MDI treatment significantly improved the flexural strength for both BF/PLA and CG/PLA composite with a rise of 30% compared to untreated. During 5 phr of MDI content, CG/PLA composite had improved 42% while BF/PLA composite 70.5%. The reaction among the isocyanate groups of MDI and hydroxyl or carbonyl groups of PLA and hydroxyl group of the natural fibre BF/PLA composite resulted in higher flexural strength as it has more hydroxyl group than CG which formed more urethane linkage.

The elongation of the CG/PLA composite is longer than pure PLA. The increased in the elongation was due to the presence of the oil component of the ether extract in CG. The result of MDI treatment showed that 5% having the highest flexural modulus. Flexural modulus defines as the ratio of stress to strain in flexural deformation. Untreated CG resulted in poor interface. After treatment, internal bonding of CG and PLA improved.

2.6.5 Enzyme

Enzyme is a biological catalyst which catalyses the chemical reaction occurring in living organism. Hemicellulase, laccase, xylanase, pectinase, cellulose and fungamix are the example of the enzyme used. Enzyme technology has gained the attention in processing natural fibre as it is environmentally friendly, the reaction catalysed are very precise with a focused performance, energy and water saving, enhanced product quality and potential process integration.

In accordance to the study done by Mamun and Bledzki (2013), micro fibres (wheat husk (WH), rye husk (RH) and softwood (SW) reinforced polylactide (PLA) and polypropylene (PP) composites were fabricated using a high speed mixer followed by injection moulding with a fibre load of 40 wt%. The use of novamix which is a mixture of lipase, protease and amylase-xylanase enzymes ratio 1:1:2 (Mamun & Bledzki, 2013).

For unmodified fibres, SW-PP composite showed the highest tensile strength that was 30% and 15% higher than RH-PP and WH-PP composites, respectively. After the modification of enzyme, the tensile strength of WH-PP composite increased 30% while RH-PP composite increased 25%. Another treatment using MAPP was conducted. However, the result showed that enzyme modification yields a better result. On the other hand, the enzyme modification for both WH-PLA and RH-PLA composites depicted an increase of around 15%, respectively compared to untreated fibre. The enhancement in tensile strength was owing to the decrease of the particle size, better interface and an increasing of the average molecular weight of fibre by eliminating the amorphous and undesired materials.

The flexural strength of WH-PP composite was 32% higher than that of RH-PP composite and 25% lower than that of SW-PP. After enzyme treatment, the flexural strength improved 27% for WH-PP and 32% RH-PP composites. For PLA composites, enzyme treatment showed 25% increment in flexural strength for both WH-PLA and RH-PLA composites. The flexural modulus also showed similar results where enzyme treated microfibers gave higher flexural modulus compared to untreated. This was because of the increase of the effective surface area of the fibres, enhanced interface, a reduction of the particle and physic-chemical changes as a result of the modification made.

The notched Charpy impact strength of WH-PP showed 25% and 30% better than RH-PP and SW-PP, respectively. For both PP and PLA composites, the impact strength improved slightly after modification of enzyme. The improvement of fibre flexibility had resulted in composite flexibility. Impact property slightly reduced for MAPP composites as it increased the brittleness of the composites. As a conclusion, enzyme treatment performed better than MAPP coupling for these particular types of composites.

Another study conducted by Bledzki and Mamun (2010) on polypropylene composites with an enzyme (fungamix) modified abaca fibre. Tensile and flexural strength were found to be about 45% and 35% better after the treatment. The improvement of these properties is owning to the elimination of outer surface; increase the accessible surface area and interfacial adhesion, and physical-chemical changes induced by fibre treatment. Fibrillation and diameter reduction of abaca fibre after the treatment might affect the properties of composites too. Fungamix modified composites showed elongation at break for tensile and flexural improved 90% and 85%, respectively in compared to unmodified composites. The untreated fibre comprises waxy and cuticle materials its surface. These materials were thermally degraded and produced free radicals when undergoing melt mixing process. These free radicals diminished the matrix's molecular weight and eventually decreased the elongation at break. The notched Charpy impact strength improved 10-25% as the enzyme treatment enhanced the toughness of the composites. The moisture absorption property of the modified composites was 45% lower than the unmodified. The enzyme treatment was able to remove surface extractives, fat, protein, lignin and hemicellulose without destroying fibre surface and structure. Thus, it was able to provide better adhesion between fibre and matrix and led to a reduction in moisture absorption. TGA conducted showed that the thermal stability improved by 8 °C for modified composites. The increase of decomposition temperature of treated fibre as a result of the elimination of smaller molecules (molecular weight) from fibre surface (Bledzki et al., 2010). These enzymatic modified composites outperformed when compare to MAPP treated composites. Enzymatic treatment was inspected with hemp fibre and flax fibre (Lipp-Symonowicz et al., 2004; Pickering et al., 2007; Saleem et al., 2008). The enzyme technology could be cost effective and enhanced product quality in contrast to maleated and silane modification.

2.7 Fabrication method

Natural fibre is incapable of resisting temperature higher than 150 ℃ for long processing duration while short-term exposures to temperatures up to 220 ℃. Temperature higher than 220 ℃ leads to discolouration, volatile release, poor interfacial adhesion and embrittlement of the cellulose component. The thermal decomposition of the fibres produces volatiles and the obtained composites reveal low mechanical properties (Holbery & Houston, 2006).

Moisture content in natural fibre during processing is another factor that could greatly worsen degradation. The moisture content of natural fibres is typically between 6% and 12% by weight. It has to be reduced to less than 3% in order to obtain good quality mouldings. Moreover, the fibres are likely to swell when visible to humidity, that contributed to a reduction in mechanical properties of composite (Biagiotti et al., 2004; Saheb & Jog, 1999).

The correct processing methods are subjected to numerous parameters. These are part geometry, complexity, size, the properties of the fibres and polymers, the defined fibre orientation, the quantity and quality of the product and not all processing methods are applicable to all materials.

There are various processing techniques for natural fibre thermoplastic composites such as extrusion, injection moulding, thermoforming, compression method, cold pressing, heating, direct long fibre reinforced thermoplastic, filament winding, foam moulding, rotational moulding, calendaring and co-extrusion.

The most familiar used methods for natural fibre composites are extrusion, injection moulding and compression moulding. The fabrication method used in this research study is through compression moulding. It is a standard manufacturing for laboratory studies of natural fibre reinforced thermoplastic composite.

2.7.1 Compression moulding

Figure 2.18 shows the structure of compression moulding. Compression moulding is a process where the moulded material, generally preheated, is first placed in an open, heated mould cavity. Then, the material charge prepared is placed onto the lower mould half. After that, the mould is closed and pressed with a pressure by hydraulic moulding press. The pressure is applied to force the material into contact with all mould areas. At the same time, heat and pressure are maintained until the moulding material has cured.

Compression moulding of natural fibre reinforced composite is the most frequently utilised method to produce automotive parts, such as hoods, fenders, scoops, spoilers, battery trays and air deflectors. Many manufacturers use compression moulding because of cost effectiveness and efficiency. It is cheaper compared to transfer moulding and injection moulding. This method of fabrication yields high strength, complex parts in a wide variety of sizes. Also, it has net size and shape, two outstanding finished surfaces, and excellent part-to-part repeatability for the fabricated product. Thus, trimming and finishing costs are minimised. In addition, it saves the cost of material as waste is reduced.

The compression moulding technique has verified appropriate for the production of thermoplastic composites. The mechanical properties and dimensional stability of compression moulded composites are subjected by the design of the mould cavity, location of the charge and processing parameters for instance compound temperature, mould cooling or heating rate, closing speeds and the filler loading.

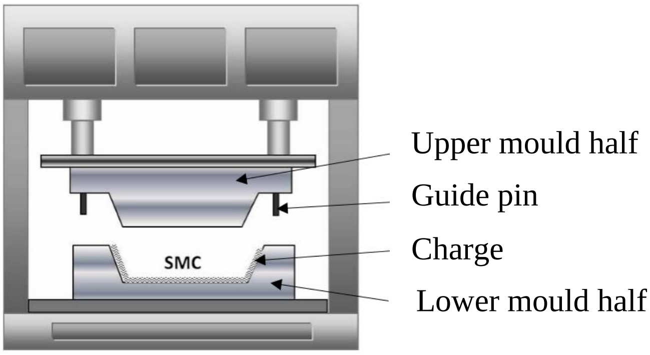

Figure 2.18: Schematic representation of compression moulding

2.7.2 Injection moulding

Figure 2.19 shows the schematic representation of injection moulding. Injection moulding is a manufacturing process for fabricating parts by injecting material into a mould. Plastic material in the form of pellet is loaded into the barrel that is surrounded by the heating element. The material flows up the reciprocating screw and it is forced under high pressure into a mould cavity through the nozzle. The molten polymer remains in the mould cavity through holding pressure, cooling, pressing and then formed into solid shape ejected out of the mould.

Injection moulding is applied generally for thermoplastics but elastomers and thermosets. Injection moulding requires high initial tooling cost. Residual stress in thermoplastic matrix composites because of pressure gradients, non-uniform temperature profiles, polymer chain alignment and dissimilarities in fibre and matrix thermal expansion coefficients can diminish composite strength (Ho et al., 2012). Owing to the viscosity requirements, injection moulding of natural fibre composites is restricted to composites of less than 40% fibre loading. Fibre attrition in injection moulding as for extrusion diminishes the length of the fibre during processing.

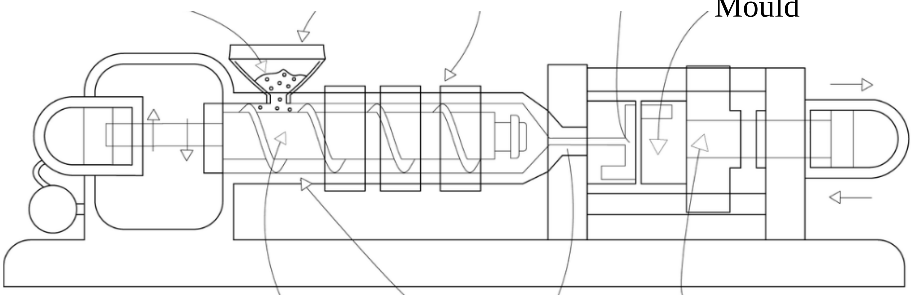

Figure 2.19: Schematic representation of injection moulding

2.7.3 Extrusion

Extrusion is a process of fabricating long products of a persistent cross-section, such as rods, sheets, pipes, films and wire insulation coating forcing soften polymer through a die with an opening. Its working principle is alike to injection moulding. The key dissimilarity between the two machines is in screw operation. For extrusion, the extruder screw (single or two rotating screws) rotates continuously giving an output of continuous long product (pipe, rod, and sheet). Extrusion also requires high initial tooling cost. Apart from that, more parameters need to be addressed in using injection moulding and extruder compared to compression moulding. Optimum parameters should be studied to ensure the quality of the samples produced. High screw speed may lead to air entrapment, excessive melt temperatures and fibre breakage. Meanwhile, Low speed contributes to poor mixing and inadequate wetting of the fibres. Twin rotating screw systems provide better dispersion of fibres and better mechanical performance compared to single rotating screw extruders (Malkapuram et al., 2009).

2.8 Conclusion

To sum up, this chapter discussed on types of natural fibre incudes seed fibre, *coffea*, types of matrices, factor affecting the properties of particulate polymer composites, modification of natural fibre and fabrication method for polymer composite.

Ground coffee waste is chosen as it is available abundantly and its characteristic shows that it has the potential to be used as reinforcement of composite and Oxo-HDPE is used as it has promising properties and it is biodegradable.

Based on the different types of treatments discussed, alkaline treatment and oil extraction have been chosen. Both of the treatments are cost effective, easy and efficient. Alkaline treatment is able to remove unwanted impurities within the reinforcement. This has increased the surface roughness, exposed more active sites to be bonded to the matrix and better arrangement of the fibrillar region that led to a better properties. Oil extraction is not commonly used by other researchers. Oil extraction is very good in removing lignin. The removal of the oil on the surface of the reinforcement can significantly improve the properties and adhesion of the reinforcement and matrix. The use of very small amount of NaOH and n-hexane in both treatments will not harm the environment. Although coupling agent and enzyme are very effective, the use of coupling agent is not environmental friendly whilst enzyme is very expensive. Acetylation is not chosen as it requires a large amount of acetic acid to yield the same result of small amount of NaOH used (Tan, Wu, Chan, & Lim, 2014). -

The fabrication technique used is compression moulding as it is easy to operate, the equipment is cheap, less maintenance required, easily available and yields promising result.

CHAPTER 3

METHODOLOGY

3.1 Introduction

This project utilised ground coffee waste (GCW) as discontinuously particulate reinforced oxo-biodegradable high density polyethylene (oxo-HDPE) matrix for composite fabrication. Based on the study, types of treatments undergone by GCW were shown in Figure 3.1. The fabricated composites were undergone characterisation including microstructure, thermal and mechanical and physical testing shown in Figure 3.2.

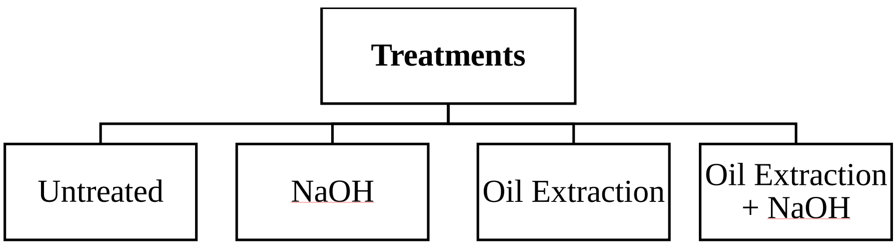

Figure 3.1: Types of treatments of GCW

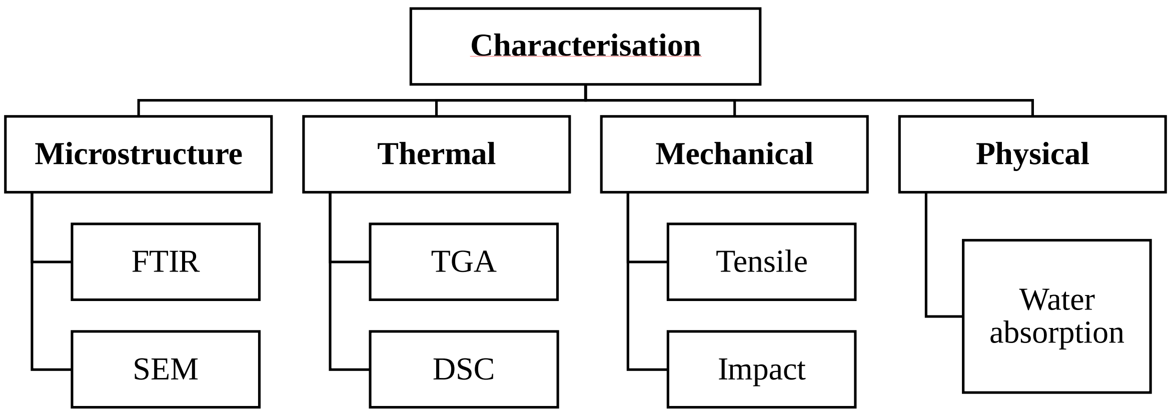

Figure 3.2: Characterisation of composite

3.2 Material investigation

3.2.1 Filler preparation

Ground coffee waste (GCW) (Arabica) was collected from local Café (Figure 3.3). Collected GCW was washed to remove the contaminant and dried at 105 °C for 24 hours to 1-2% moisture content. The sieving analysis was performed by automatic shaker to separate the size of ground coffee waste in groups (64-425 μm, 426-850 μm, 851-1180 μm and mixed size) (Figure 3.4). Then, GCW were kept in a desiccator.

Figure 3.3: Collected GCW

Figure 3.4: Sieved analysis by automatic shaker

3.2.2 Matrix preparation

A commercial oxo-biodegradable high density polyethylene (oxo-HDPE) thin film with a thickness of 22 µm (density 0.96 g/mL @ 23 °C) was used as matrix. Figure 3.5 shows the oxo-HDPE films arranged in the mould.

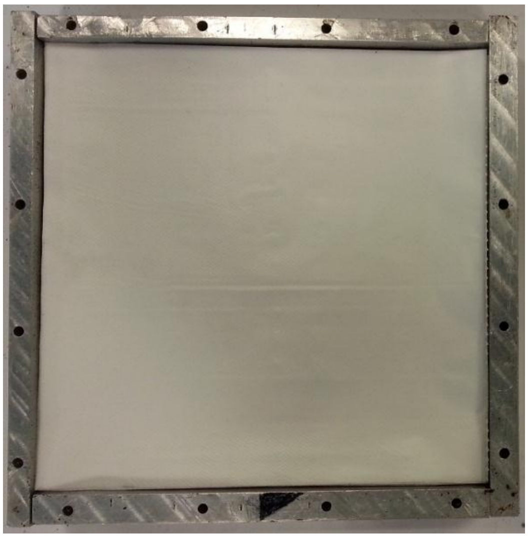

Figure 3.5: The oxo-HDPE films were arranged in the mould

3.2.3 Alkaline treatment

GCW were soaked into 1 % concentration of NaOH solution (0.25 molarity) for 1, 6, 12 and 24 hours at room temperature. After that, the GCW were washed with distilled water until the GCW return to pH 7 (Figure 3.6). The treated GCW were dried in an oven at 105 °C for 24 hours to remove the moisture content. Dried treated GCW were kept in the desiccator.

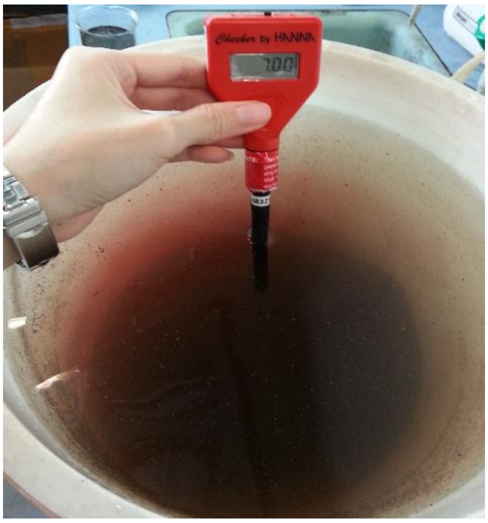

Figure 3.6: The pH meter shows the reading of the solution

3.2.4 Oil extraction (Soxhlet)

The schematic diagram and basic set-up of soxhlet extractor are shown in Figure 3.7 and Figure 3.8. A thimble-shaped filter filled with 200 g of GCW is then placed into the reservoir. The round bottom flask is filled with 800 ml of extraction solvent (n-hexane). After that, the soxhlet extractor is being set-up whereby condenser at the top, reservoir places in between and round bottom flask at the bottom as seen in Figure 3.7. Cold running water is switched on to activate the condenser. The solvent is heated up from the bottom of the flask at a reaction temperature of 80 ℃ to 95 ℃. As the solvent boils, the cool water in the condenser will flow to return its drip into the thimble. This will allow the soluble components of GCW to be extracted. When the solvent fills the reservoir, it will rise up the siphon tube on the side of the extractor. When the solvent level exceeds the siphon tube, the siphon will empty the reservoir. The cycle will start again after the solvent is boiling again. The solvent is heated for 3 hours to enhance the effectiveness throughout the process. Oil extracted GCW were dried in the oven at 105℃ for 24 hours to remove the moisture content. Dried oil extracted GCW were kept in the desiccator.

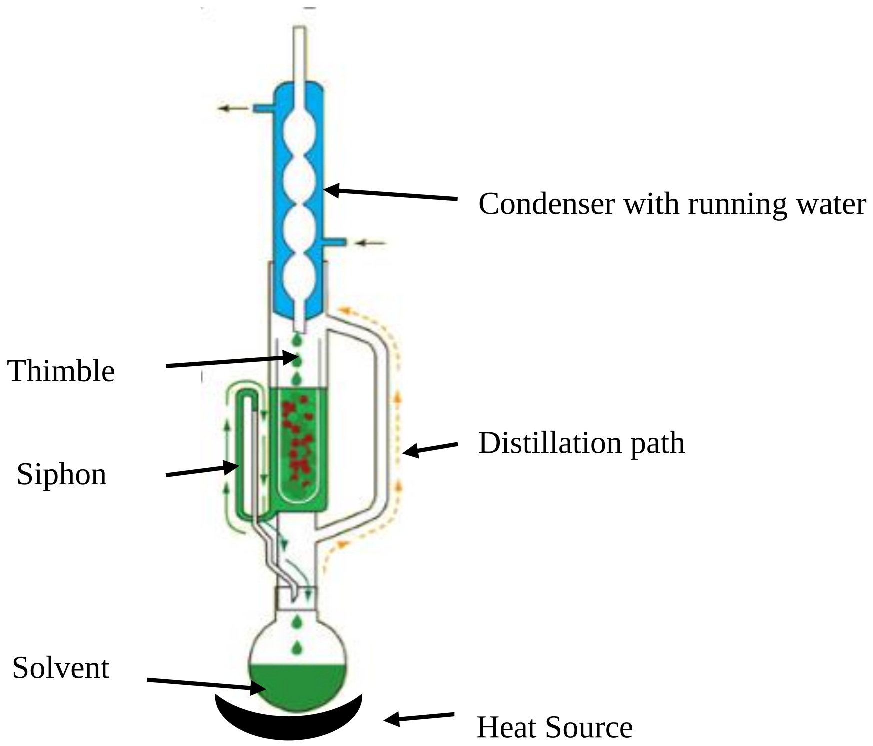

Figure 3.7: Schematic diagram of soxhlet extractor

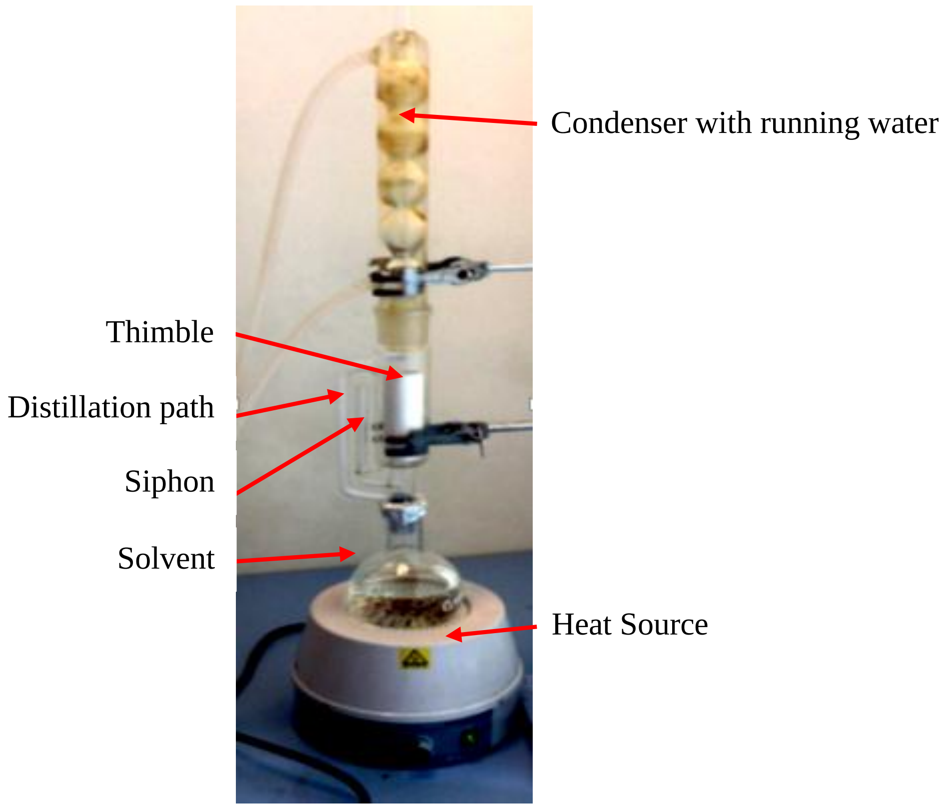

Figure 3.8: Set-up of soxhlet extraction

3.2.5 Oil extraction + alkaline treatment

Oil extracted GCW were soaked into 1% concentration of NaOH solution (0.25 molarity) for 24 hours at room temperature. After that, treated GCW were washed with distilled water until it returned to pH 7. The treated GCW were dried in an oven at 105 °C for 24 hours to remove the moisture content. Dried treated GCW were kept in the desiccator.

3.3 Composite fabrication

Ground coffee waste (GCW) is manually sieved in between oxo-HDPE thin films. Then, it is sent for compression moulding in a hydraulic press machine at approximately 3 MPa at 150 °C. The preparation and arrangement of the composites were shown in Figure 3.9 and Figure 3.10. The hot press machine is shown in Figure 3.11. A total of 25 types of composites were prepared in this research. Figure 3.12 shows the samples of fabricated composite panels while Table 3.1 depicts the summary of the composites investigated in this study. The composites were divided into seven categories. Composite type A is neat oxo-HDPE, type B is different particle size of untreated GCW/oxo-HDPE composites (fine, medium, coarse and mixed size), type C, D, F and G are untreated GCW, oil extracted GCW, mercerised GCW, and oil extracted + mercerised GCW reinforced oxo-HDPE composites of different volume fraction (5%, 10%, 15% and 20%) and type E is 10% volume fraction of mercerised GCW with different treatment time (1, 6, 12 and 24 hr) reinforced oxo-HDPE composites.

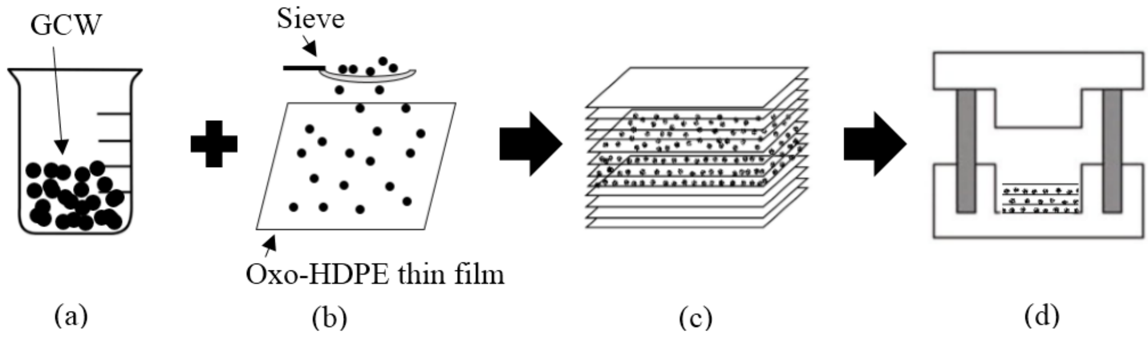

Figure 3.9: Schematic representation of the preparation of GCW/ oxo-HDPE composite and samples of fabricated composite (a) Ground coffee waste, (b) sieving + Oxo-HDPE, (c) Mixing with different ratio, (d) Compression moulding

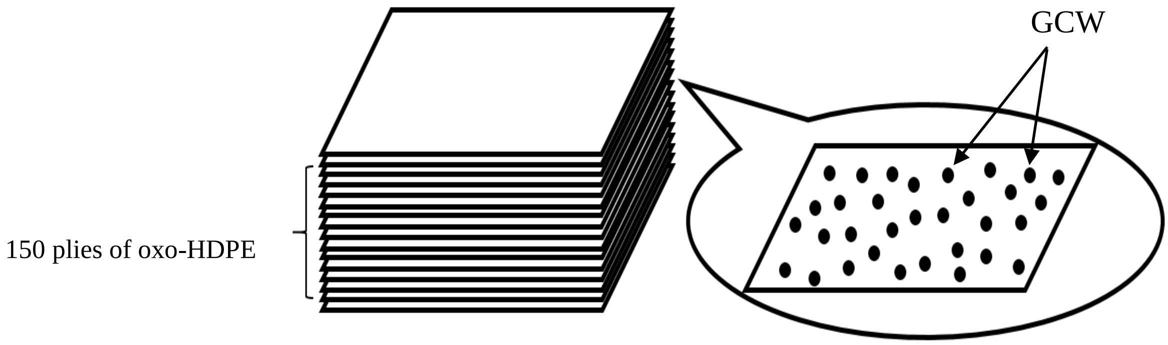

Figure 3.10: The arrangement of the GCW/oxo-HDPE composite

Figure 3.11: Hot press machine

Figure 3.12: Ground coffee waste reinforced oxo-HDPE composite panels

Table 3.1: Summary of the composites investigated in this study

Composite	Sample	Stacking Sequence	Volume of GCW (%)	Volume of oxo-HDPE (%)
A1	Oxo-HDPE (PE)	150PE	0	100
B1	Untreated FGCW5/oxo-HDPE	150PE + 5FUG	5	95
B2	Untreated MGCW5/oxo-HDPE	150PE + 5MUG	5	95
B3	Untreated CGCW5/oxo-HDPE	150PE + 5CUG	5	95
B4	Untreated MiGCW5/oxo-HDPE	150PE + 5MiUG	5	95
C1	Untreated GCW5/oxo-HDPE	150PE + 5UG	5	95
C2	Untreated GCW10/oxo-HDPE	150PE + 10UG	10	90
C3	Untreated GCW15/oxo-HDPE	150PE + 15UG	15	85
C4	Untreated GCW20/oxo-HDPE	150PE + 20UG	20	80
D1	1% 1NaOH10GCW/oxo-HDPE	150PE + 10NG1	10	90
D2	1% 6NaOH10GCW/oxo-HDPE	150PE + 10NG6	10	90
D3	1% 12NaOH10GCW/oxo-HDPE	150PE + 10NG12	10	90
D4	1% 24NaOH10GCW/oxo-HDPE	150PE + 10NG24	10	90
E1	1% NaOH5GCW/oxo-HDPE	150PE + 5NG	5	95
E2	1% NaOH10GCW/oxo-HDPE	150PE + 10NG	10	90
E3	1% NaOH15GCW/oxo-HDPE	150PE + 15NG	15	85
E4	1% NaOH20FCW/oxo-HDPE	150PE + 20NG	20	80
F1	Oil Extraction GCW5/oxo-HDPE	150PE + 5OG	5	95
F2	Oil Extraction GCW10/oxo-HDPE	150PE + 10OG	10	90
F3	Oil Extraction GCW15/oxo-HDPE	150PE + 15OG	15	85
F4	Oil Extraction GCW20/oxo-HDPE	150PE + 20OG	20	80
G1	Oil Extraction + NaOH5GCW/oxo-HDPE	150PE + 5ONG	5	95
G2	Oil Extraction + NaOH1GCW/oxo-HDPE	150PE + 10ONG	10	90
G3	Oil Extraction + NaOH15GCW/oxo-HDPE	150PE + 15ONG	15	85
G4	Oil Extraction + NaOH20GCW/oxo-HDPE	150PE + 20ONG	20	80

* B1 = Fine GCW (65-425 µm)

B2 = Medium GCW (426-850 µm)

B3 = Coarse GCW (851-1180 µm)

B4 = Mixed size GCW (65-1180 µm)

3.4 Mechanical testing

3.4.1 Tensile testing

Schematic representation of tensile testing is presented in Figure 3.13. Properties that are directly measured via a tensile test are ultimate tensile strength, maximum elongation and reduction in area (He & Pei, 2013; Reviews, 2012). From these data, the test yields the result concerning Young's modulus, Poisson's ratio, yield strength and strain-hardening characteristics of the specimen. The tensile strength, ultimate tensile strength and failure strain can be calculated using Equation 3.1 and Equation 3.2 (ASTM D3039/D3039M, 2000),

$$Stress, \sigma = \frac{F}{A} \tag{3.1}$$

Where,

$\sigma = stress\ (MPa)$

$F = lateral\ axial\ tensile\ load\ on\ specimen\ (N)$

$A = Cross\ sectional\ area\ of\ the\ specimen\ (m^2)$

$$Strain, \varepsilon = \frac{\Delta l}{l_o} = \frac{l - l_o}{l_o} \tag{3.2}$$

Where,

$\varepsilon = Strain\ (\frac{mm}{mm})$

$\Delta l = Change\ in\ length, l - l_o\ (mm)$

$l_o = Initial\ length\ of\ the\ specimen\ (mm)$

Young's modulus is also identified as tensile modulus or elastic modulus. It is a measure of the stiffness of an elastic material or its slope in elastic region of stress-strain graph. The formula used is Equation 3.3,

$$Young\ modulus, \epsilon = \frac{\Delta Stress}{\Delta Strain} = \frac{\Delta\sigma}{\Delta\varepsilon}(GPa) \tag{3.3}$$

Tensile properties were conducted using a Shimadzu universal testing machine model AG-300K IS MS (Figure 3.13). The dimension of the test specimen 200 mm x 25 mm was measured (Figure 3.14a). In order to keep track of the gauge length (100 mm), two symbols were marked on the tensile specimen. The load was monitored by a load cell. The test was conducted at a crosshead displacement rate of 1 mm/minute (Figure 3.14b). Five different samples were subjected to the tensile test. The computer accumulated load (N) versus elongation (mm) data. Stress, strain and Young's modulus were calculated using Equation 3.1, Equation 3.2 and Equation 3.3.

Figure 3.13: Shimadzu universal testing machine model AG-300K IS MS

5 cm

(a) (b)

Figure 3.14: a) Tensile specimens and b) Specimen during tensile testing

3.4.2 Low velocity impact test (ASTM D3763-15)

Schematic representation of the operation of a drop weight impact tester is shown in Figure 3.15. A mass is dropped vertically onto a test specimen until it fractures or breaks. A tube or rail is used to guide the falling mass. Drop weight impact tester can be used for both low and high energy applications. In comparison to Charpy and Izod impact test, drop weight impact testing can collect a greater amount of data of the behaviour of the composites fabricated. Drop weight impact testing also permits diverse configurations to be used. Thus, drop weight testing is a preferable method applied using low velocity impact testing. Drop weight testing outcomes can be improved from post-impact testing. Impact properties can be calculated by Equation 3.4 (ASTM D3763, 2012),

$$Impact\ energy, E = mg\left(h_{initial} - h_{final}\right) = \frac{1}{2}mv^2 \tag{3.4}$$

Where,

$m = mass\ (kg)$

$g = gravitational\ field\ strength, 9.81\ Nkg^{-1}$

$h_{initial} - h_{final} = distance\ between\ the\ mass\ at\ its\ height\ position$

$and\ the\ test\ specimen\ directly\ below\ it\ (m)$

$v = impact\ velocity\ (ms^{-1})$

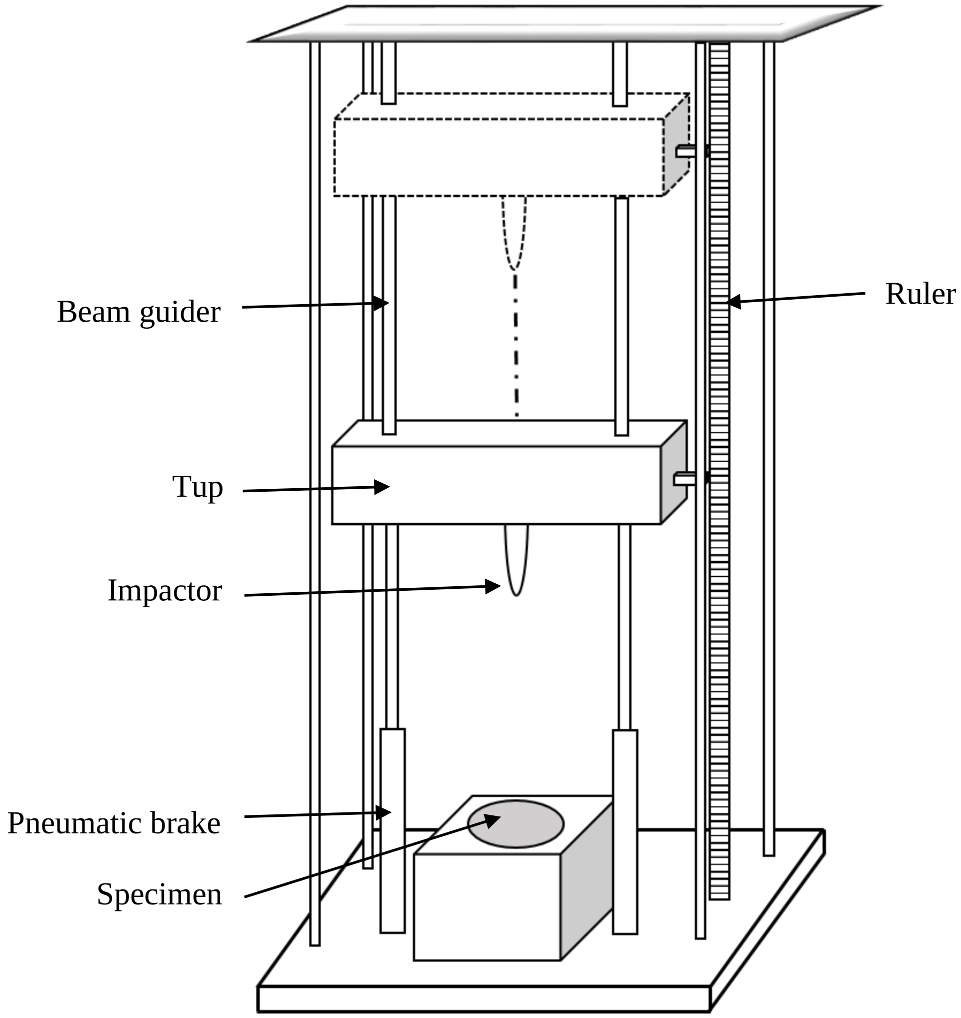

Figure 3.15: Schematic representation of operation of a drop weight impact test machine

Dart drop impact properties were characterised using Instron 9250HV in accordance to ASTM D3763-15 (Figure 3.16). The sample specimen was cut into the size of 5 cm x 5 cm. The specimen was clamped along its edges in the test machine. A mass was raised to the desired height, initial drop height, H (0.5 m) and locked into place. The dart weight (3.47 kg) having a radius of 12.88 mm with hemisphere head was used. The velocity was recorded in the range of 3.00 to 3.20 m/s. The machine was set to its correct configuration. The mass was released, impacting the sample specimen. Force, energy or displacement versus time graph was plotted.

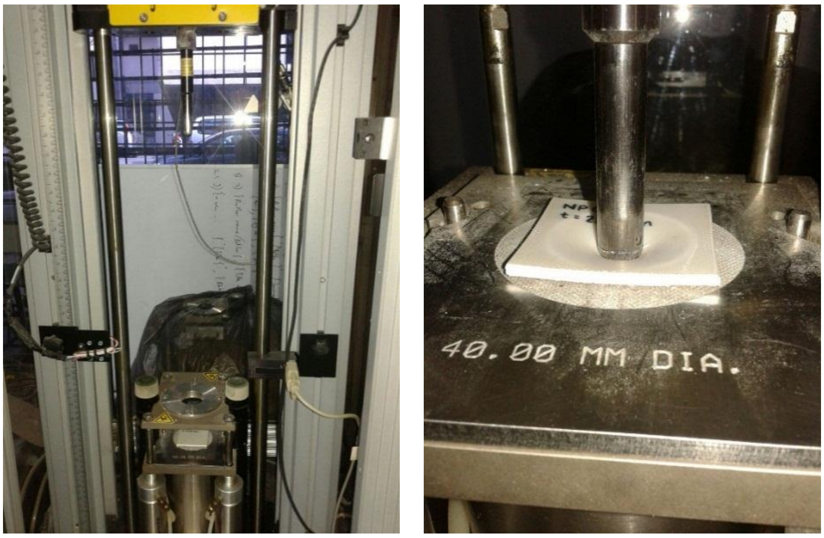

Figure 3.16: Instron 9250HV

3.5 Microstructural analysis

3.5.1 Fourier Transform Infrared (FTIR) spectroscopy analysis

Fourier Transform InfraRed (FTIR) is a technique of infrared spectroscopy. It is an efficient method for the surface and interface characterisations of lignocellulosic fibres and composites (Fan, Dai, & Huang, 2012).

The working principle of the FTIR is shown in Figure 3.17. First of all, the infrared energy is emitted from the glowing black-body source. This beam permits through an aperture that controls the amount of energy absorbed by the sample and the detector. After that, the beam enters the interferometer where the spectral encoding occurs. The interferogram signal leaves the interferometer. The beam would then pass through the sample compartment. This is where it is transmitted through or reflected off of the surface of the sample. Specific frequencies of energy of distinctively characteristic of the sample are absorbed. Next, the beam continues to pass through the detector for final measurement. The detectors used are intended to measure the special interferogram signal. Lastly, the measured signal is digitised and sent to the computer. The final infrared spectrum characterises a molecular fingerprint of the sample with absorption peak that resembles the frequencies of vibrations between the bonds of the atoms. The material is then obtainable to the user for interpretation and manipulation. Furthermore, the size of the peaks in the spectrum demonstrates the amount of material present (Nicolet & All, 2001).

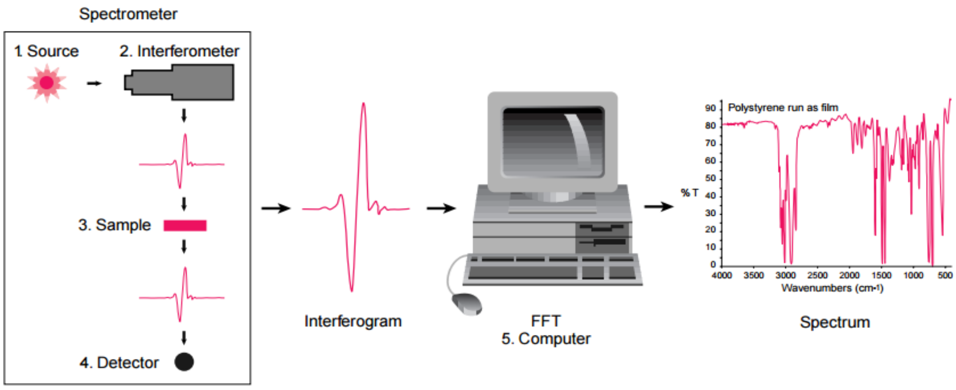

Figure 3.17: Process flow of FTIR spectroscopy analysis (Nicolet & All, 2001)

The untreated and treated GCW were analysed using fourier transform infrared spectroscopy (FTIR) using an IRAffinity-1 from. About 20 mg of GCW were put onto the surface of the ATR. Each sample was subjected to 20 scans in the range of 600-4000 cm^{-1}. Spectra generated was interpreted and compared.

3.5.2 Scanning Electron Microscope (SEM)

Figure 3.18 shows the schematic diagram of a SEM. Scanning electron microscope (SEM) creates images of a sample by scanning it with a focused electron beam instead of light. The surface of the sample is scanned with an electron beam, and the reflected (or back-scattered) beam of electrons is gathered, and then showed at the same scanning rate on a cathode ray tube. The image of the screen that can be photographed symbolises the surface features of the sample. The surface may or may not be polished and etched. However, it must be electrically conductive. A thin metallic surface coating must be applied to non-conductive samples (Callister & Rethwisch, 2012).

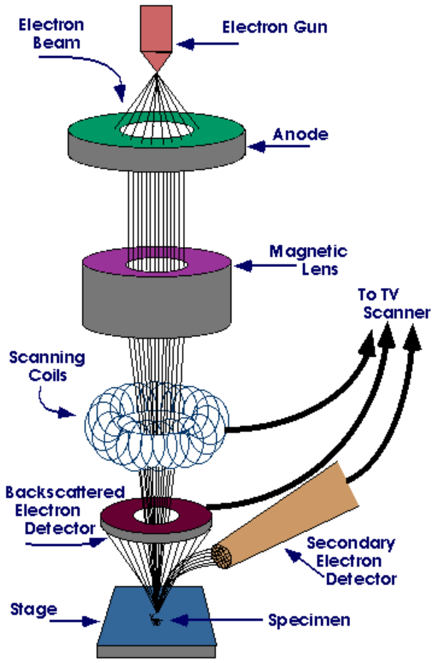

Figure 3.18: Schematic of a SEM (Callister & Rethwisch, 2012)

All the tensile composites were investigated using a table top SEM (Hitachi TM3030) with 15 kV electron with a coating, a charge-up reduction mode. The specimen was coated with a layer of gold prior to analysis.

3.6 Thermal analysis

3.6.1 Thermogravimetric Analysis (TGA)

Thermogravimetric analyser (TGA) is an essential laboratory tool used for material characterisation. It is a technique of thermal analysis in which changes in physical and chemical properties of materials are used as a function of increasing temperature (with constant heating rate), or as a function of time (with constant temperature and/or constant mass loss) (Coats & Redfern, 1963). In other words, TGA measures the weight of a sample as it is heated or cooled in a furnace.

As shown in Figure 3.19, TGA has a sample pan that is supported by a precision balance. The pan is situated in a furnace and is heated or cooled when the experiment is conducted. The mass of the sample is supervised throughout the experiment. A sample purge gas (inert gas or reactive gas) controls the sample environment, flows over the sample and exits through an exhaust (*TGA A Beginner's Guide*, 2010). TGA is able to give valuable information on selecting materials for certain end-use applications, product performance prediction and product quality improvement.

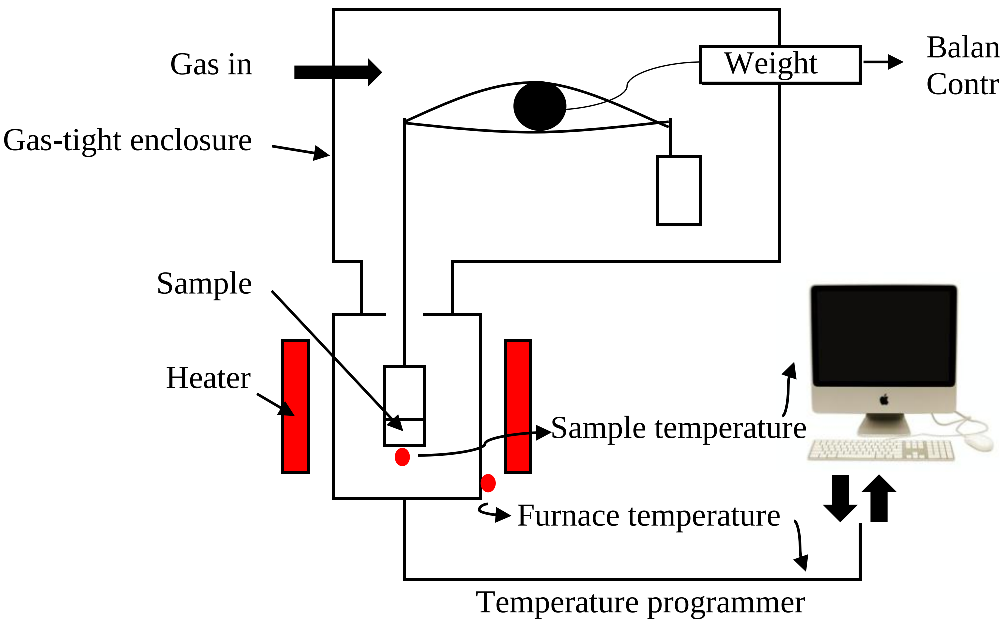

Figure 3.19: Thermogravimetric analysis instrumentation

The untreated and treated GCW composites were undergone thermogravimetric analysis via Netzsch TG 200 F3 Tarsus. About 20 mg of the composite was prepared and put into the crucible. The temperature range used from 30 ℃ to 600 ℃, at a heating rate of 10 ℃ min^{-1} under nitrogen atmosphere. The mass loss, initial degradation temperature (T_{onset}), maximun degradation temperature ($T_{\max}$), and final degradation temperature (T_{final}) were determined.

3.6.2 Differential Scanning Calorimetry (DSC)

Differential scanning calorimetry (DSC) is well-defined as the measurement of the variation of the difference in the heat flow rate to the sample and to a reference sample though they are subjected to a controlled temperature program (Höhne et al., 2003). In the other words, it is a tool of thermal analysis that express how a heat capacity of a material is changed by temperature. This permits the detection of transitions such as melts, glass transitions, phase changes and curing. This tool has been utilised in various industries such as polymers, paper, printing, manufacturing, semiconductor, electronics, pharmaceuticals and food.

Figure 3.20 shows a schematic diagram of DSC. When conducting an experiment, the sample is added in one of the pans while the other one is left empty. They are positioned on a thermoelectric disk encircled by a furnace controlled by a computer system at a certain specific rate. The system is maintained at nearly constant temperature during the experiment. The temperature of the sample holder rises proportionally as a function of time. The reference sample should have a definite heat capacity over the range of temperatures to be studied.

The untreated and treated GCW composites were analysed using differential scanning calorimetry (DSC), Perkin-Elmer equipment DSC 8000 model. About 20 mg of the composite was prepared. The temperature range used from 50 ℃ to 180 ℃, at a heating rate of

20 ℃ min^{-1}, under nitrogen atmosphere. The sample was heated from 50℃ to 180℃, leaving the material at 180 ℃ for 2 min; the second cycle was done using a cooling rate of 20℃ min^{-1}, until 50℃; in the third cycle, the sample was heated from 50℃ to 180℃, at a heating rate of 20 ℃ min^{-1}. The crystalline melting temperature (T_m) and degree of crystallinity (X_c) of the HDPE were obtained considering the second heating curves. The degree of crystallinity, X_c was determined using the Equation 3.5,

$$Degree\ of\ crystallinity, x_c(\%) = \frac{\Delta H_m}{\Delta H^0{}_m \times w} \times 100\% \qquad (3.5)$$

where, ΔH_m is the heat of fusion of GCW/oxo-HDPE composite, $\Delta H^0{}_m$ is the theoretical heat of fusion of 100% crystallinity HDPE (290 Jg^{-1}) (Sibele Piedade & Luis Claudio, 2013) and w is the volume fraction of oxo-HDPE in the composite.

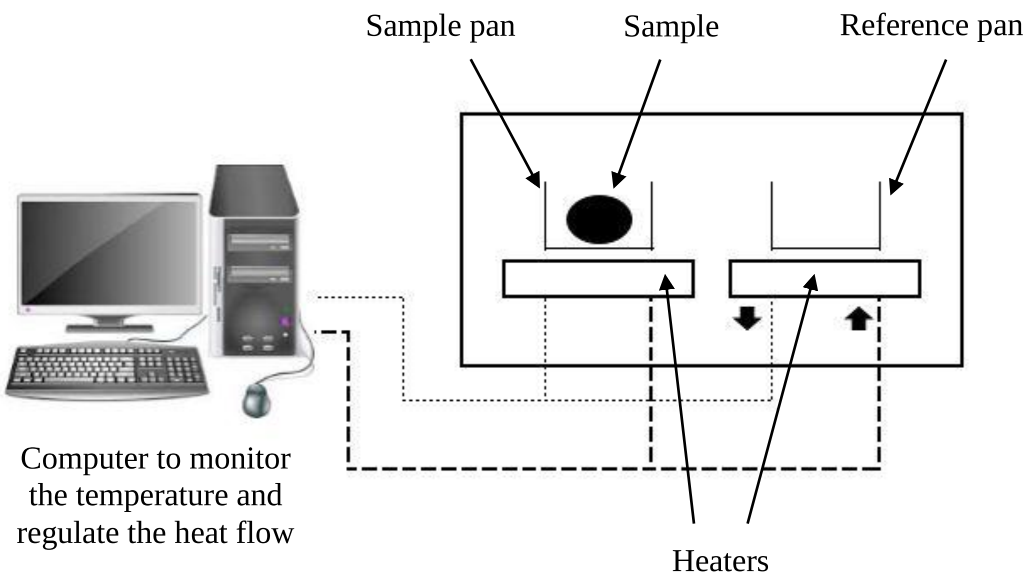

Figure 3.20: Schematic diagram of DSC

3.7 Water absorption test

Water absorption test was carried out in accordance to ASTM D570-98. Test specimens were in the size of 76.2 mm x 25.4 mm. 6 specimens were prepared for each type of sample. The specimens were immersed entirely in a container of distilled water at temperature 23 ± 1 ℃ (Figure 3.21). The specimens were weighed after 2 hours and repeated every 24 hours accordingly. The specimens shall be removed from the water one at a time. All the samples were wiped with a dry cloth immediately and weighed to the nearest 0.001g. Percentage of water absorption was measured using Equation 3.6 (ASTM D570-98, 2010),

$$Percentage\ of\ water\ absorption, \% = \frac{W_{final} - W_{initial}}{W_{initial}} x\ 100\% \qquad (3.6)$$

where W_{final} is the final weight at certain immersion period and $W_{initial}$ is the initial weight of the sample before immersion. The percentage of weight gained against time was then plotted.

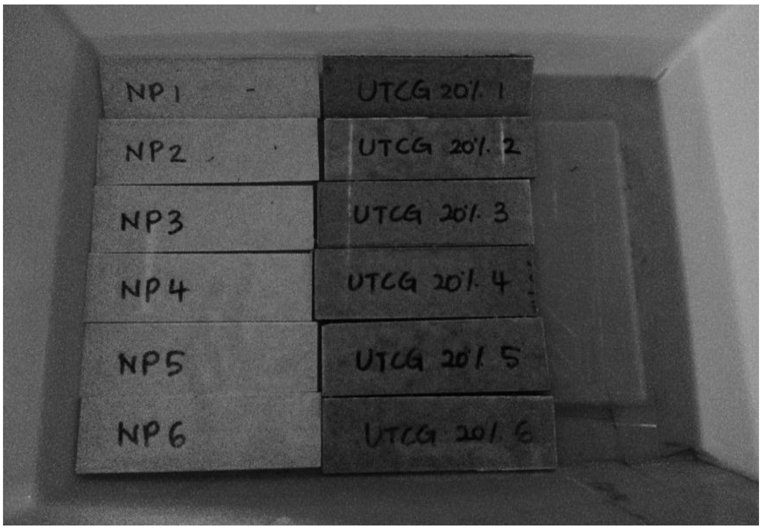

Figure 3.21: Samples of water absorption test

3.8 Preliminary study of material selection

Preliminary study has been done to study the optimum size of GCW to be used as the reinforcement of the composite.

3.8.1 Effect of particle size

3.8.1.1 Sieve analysis

Sieve analysis was performed to study the particle size distribution of ground coffee waste (GCW). About 530 g of GCW was used in the sieving experiment. The result is presented in Figure 3.22. The GCW was in the range of particle size 64 to 1180 µm. A total mass of 57 % of the GCW was fallen in the range of 601-850 µm, followed by 20% for 426-600 µm and 17% for 851-1180 µm. The remaining of the GCW was less than 425 µm.

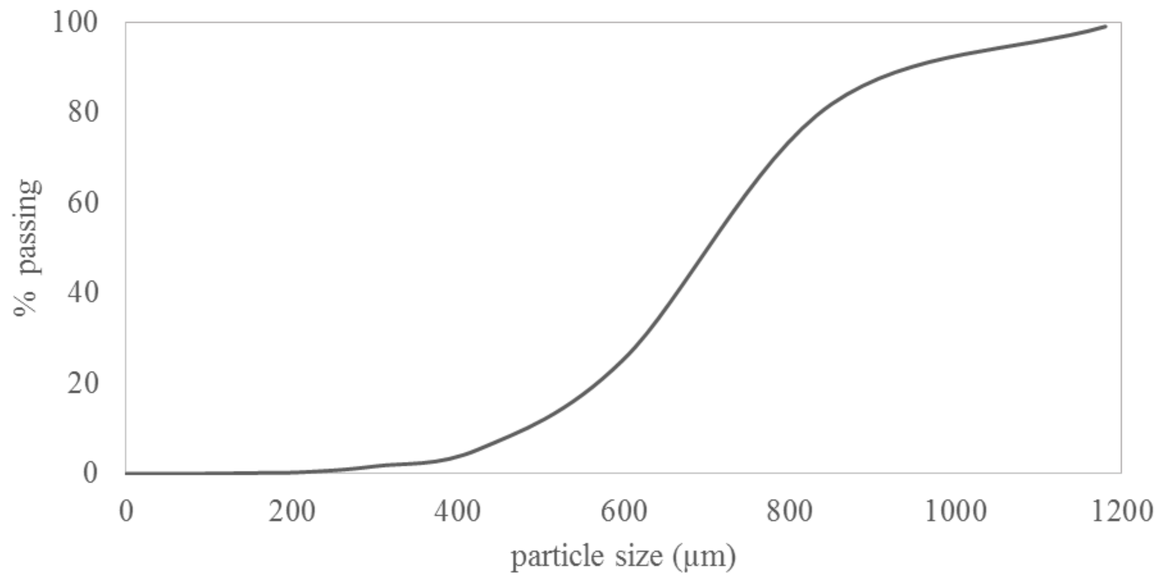

Figure 3.22: Sieve analysis of GCW according to particle size

3.6.1.2 Tensile test

Based on the result from sieve analysis, GCW was distributed into 4 batches, which were fine (65-425 μm), medium (426-850 μm), coarse (851-1180 μm) and mixed size (640-1180 μm). The tensile test was conducted to determine the tensile properties for different size of untreated GCW composite (composite type B).

Figure 3.23 shows the variation of the stress-strain graph of untreated GCW/oxo-HDPE composite using different size at crosshead displacement rates of 1 mm/min. Neat oxo-biodegradable high density polyethylene (oxo-HDPE) was fabricated to act as the reference having the highest tensile strength and modulus of 18.89 MPa, 1107 MPa. Tensile properties suffered a slight decrease with the inclusion of GCW. This might due to the reason of poor interface between hydrophilic untreated GCW and hydrophobic oxo-HDPE.

Ductility is the amount of plastic deformation that a material can undergo before failure. It can be measured in terms of percentage elongation in length at break or percentage reduction in cross-sectional area. As shown in Figure 3.23, the ductility of the untreated GCW was reduced compared to Neat oxo-HDPE. HDPE is a soft and tough material having high crystallinity that enables it to have more plastic behaviour since it restructured itself as it is elongated. Thus, oxo-HDPE showed a very long necking and crazing behaviour that gave a high strain, or might not break at all. The addition of the particle has a function of restraining the movement of the matrix. Thus, the ductility decreased after the inclusion of the GCW particle. The ductility (elongation at break) of the composite increased with decreasing particle size. Bigger particle size initiated cracks propagation easily, yielding a decreasing trend of ductility as the particle size increased.

As shown in Figure 3.24 and Figure 3.25, the tensile strength and modulus declined as the particle size increased. The highest tensile strength was at particle size of 65-425 µm, 14.79 MPa followed by particle size of 426-850 µm, 14.29 MPa , then, mixed size, 12.83 MPa and finally particle size of 851-1180 µm, 11.98 MPa, declination of 21 to 37% in comparison to neat oxo-HDPE respectively. Meanwhile, for tensile modulus, in comparison of particle size to neat oxo-HDPE, the tensile modulus of particle size of 65-425 µm, 426-850 µm, 851-1180 µm and mixed size were decreased by 10%, 15%, 22% and 24%, respectively. For a given particulate volume fraction, the composite tensile strength and modulus increased with decreasing particle size (Pukánszky, 1993). Particles of smaller size had a higher total surface area for a given volume fraction. The increasing surface area gave a more efficient stress transfer thus giving higher strength. During loading, large particles debond easily from the matrix that led to premature failure of the part.

GCW with an irregular cross section having a low aspect ratio (<2) also contributed to declining strength (Fernandes et al., 2013; Rozman et al., 1998). Aspect ratio (length to diameter ratio) shows a greater effect on tensile properties than the particle size (Stark & Rowlands, 2003). A high aspect ratio was expected as it was an indication of strength properties. It acted to control the fibre dispersion, fibre-matrix adhesion and optimum performance of the composites (De & White, 1996). GCW with low aspect ratio led to weak stress transfer from the matrix to the fibre. Thus, resulted in poor tensile properties.

Based on the particle size studied, GCW particle size of 64-850 µm were further study by incorporation different volume fraction of untreated and treated GCW reinforced composites. This range of particle size was selected as it offered better tensile properties and ductility. The summary data for composite type B is shown in Table 3.2.

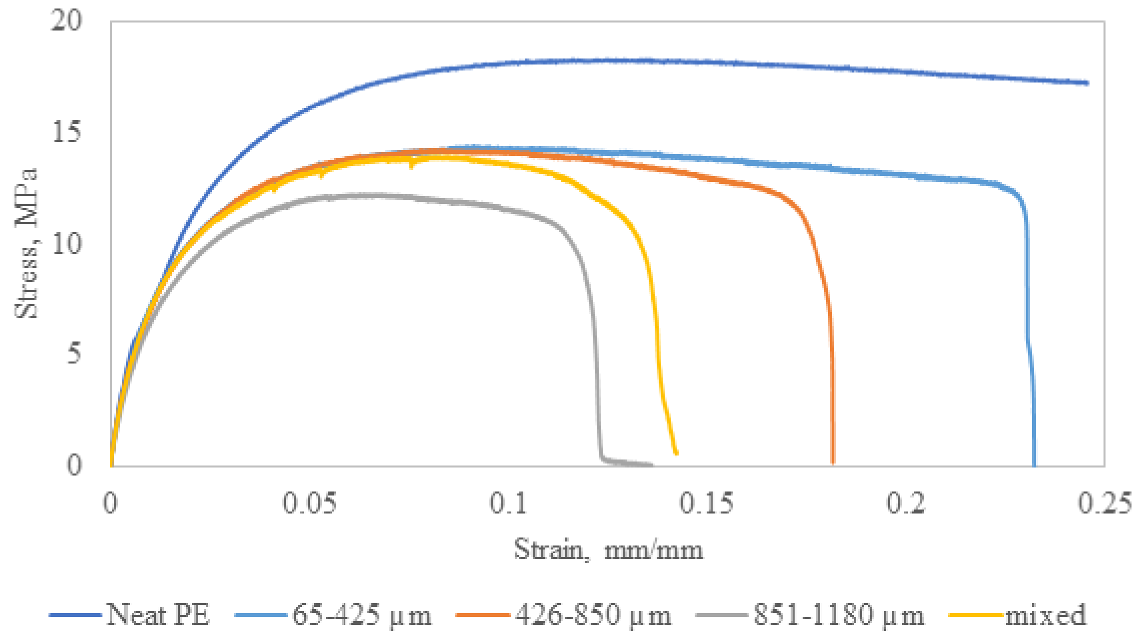

Figure 3.23: The variation of the stress-strain for untreated GCW/oxo-HDPE composite using different particle size at crosshead displacement rates of 1 mm/min

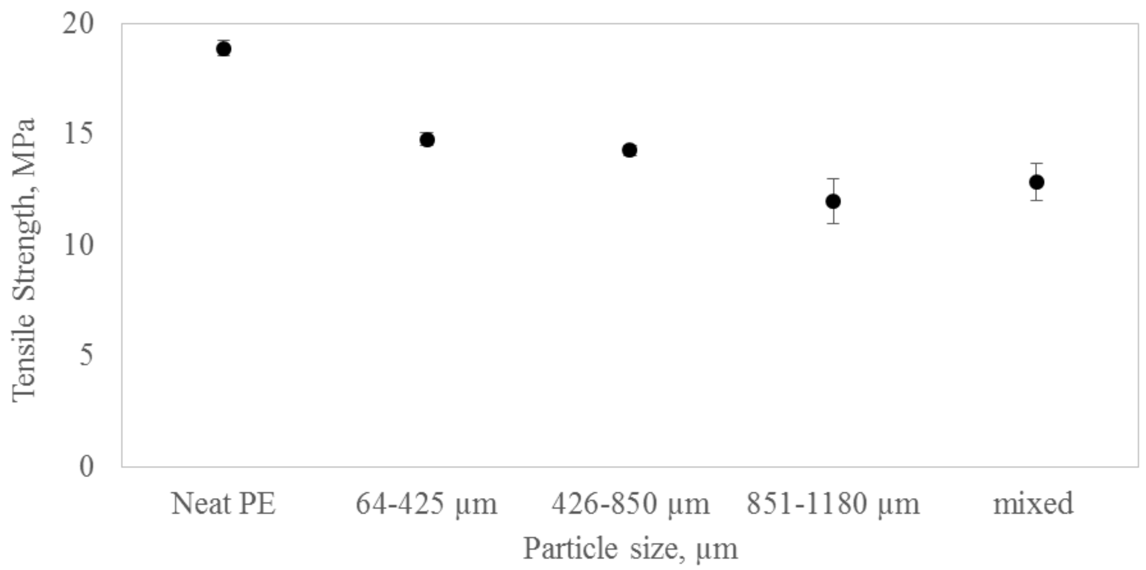

Figure 3.24: The variation of the tensile strength for untreated GCW/oxo-HDPE composite using different particle size at crosshead displacement rates of 1 mm/min

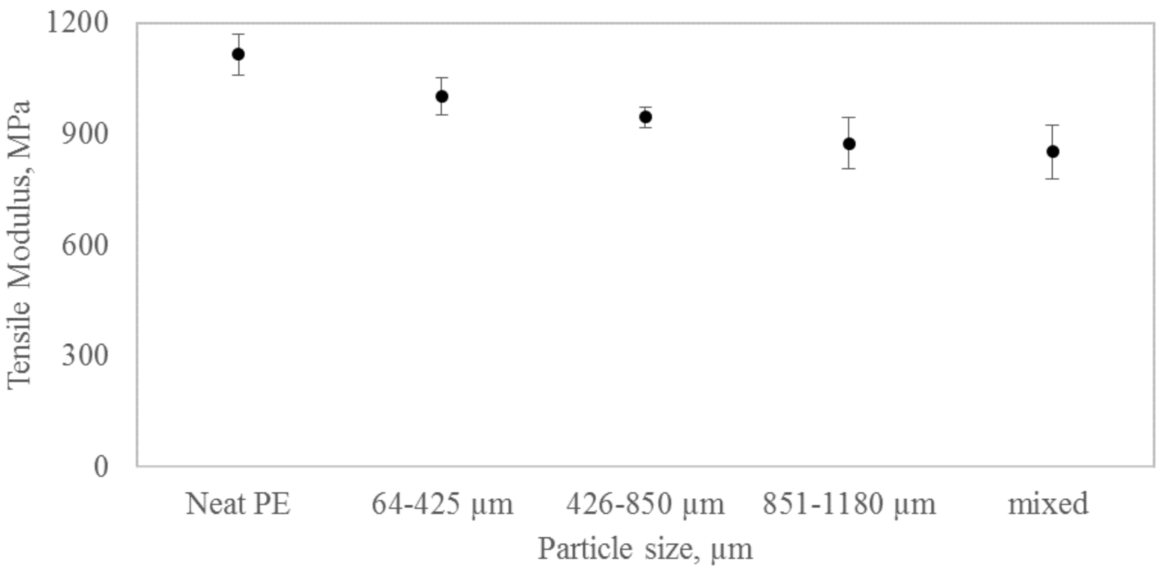

Figure 3.25: The variation of the tensile modulus for untreated GCW/oxo-HDPE using different particle size at crosshead displacement rates of 1 mm/min

Table 3.2: Tensile properties of different particle size of untreated GCW/oxo-HDPE composite

Composite	**Filler Vol. (%)**	**Tensile Strength (MPa)**	**Tensile Modulus (MPa)**
Neat oxo-HDPE	0	18.89 (0.35)	1107.18 (67.57)
64-425 µm	5	14.79 (0.31)	1001.32 (49.96)
426-850 µm	5	14.28 (0.22)	945.17 (28.58)
851-1180 µm	5	11.98 (0.99)	874.81 (70.16)
mixed	5	12.83 (0.84)	852.20 (73.02)

CHAPTER 4

RESULTS AND DISCUSSION

Figure 4.1 shows an overview of testing conducted for all the composite laminates. This chapter discussed the outcome based on three categories, which were the effect of untreated and alkaline treatment on the composites, the effect of oil extraction and oil extraction + alkaline treatment on the composites, and the overall results comparison for all the fabricated composites.

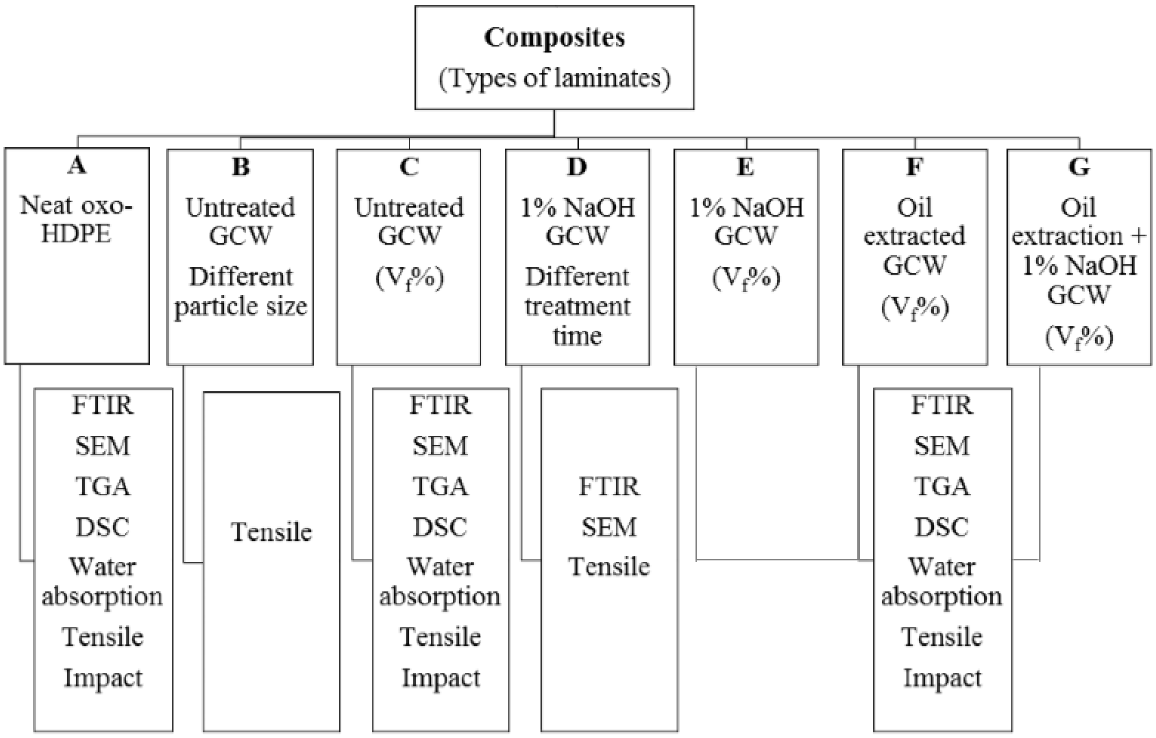

Figure 4.1: Overview of testing conducted for all the fabricated laminates

4.1 Comparison of untreated and NaOH treated GCW/oxo-HDPE composites

4.1.1 Fourier transform infrared spectroscopy (FTIR)

Figure 4.2 represents the FTIR spectra of untreated GCW, and NaOH treated GCW as a function of duration. Peaks in the range of 3000-3600 cm^{-1} and 1500-1600 cm^{-1} showed the absorption of –OH bending and stretching region. As the treatment time increased from 0 to 24 hours, 3100-3600 cm^{-1} region exhibited a higher intensity with the presence of a higher –OH intensity on the surface of treated GCW, which mean it offered an active interaction site between treated GCW and oxo-HDPE matrix. During mercerisation, cellulose I changed to cellulose II (Varshney & Naithani, 2011). Untreated GCW having peak at 3351 cm^{-1} which was cellulose I, O(3)H-O(5) bonds. Cellulose II peaks at 3307, 3311, 3319 cm^{-1} (OH inter H-bond and OH intra H-bond) after mercerisation (Kondo, 2004). Two sharp peaks at 2859 and 2923 cm^{-1} represented the existence of the methyl and methylene group that accredited to asymmetric and symmetric stretching of C-H bonds in aliphatic chains. These peaks have been formerly recognised in roasted Arabica and Robusta coffee (Kemsley et al., 1995), roasted coffee husks (Reis et al., 2013) and known as the presence of caffeine (Craig et al., 2012; Paradkar & Irudayaraj, 2002). The same peaks have been attributed to the presence of the lipids in corn and corn flour sample (Cremer & Kaletunç, 2003). Highly soluble caffeine has been extracted upon preparation of a coffee beverage. Thus, these peaks can be attributed to a huge amount of lipids in the coffee sample. After alkaline treatment, the area of these two peaks was reduced since the lipid reduced. The characteristic GCW peak at 1728 and 1651 cm^{-1}, attributed to the acyl ester hemicellulose, aldehyde lignin or carbonyl lipid, disappeared after alkaline treatment (Kemsley et al., 1995; Matuana et al., 2001). The reduction of hemicellulose and lignin content evident from the decreasing in 1250 cm^{-1} and 1120 cm^{-1}

bands were compared to untreated GCW. The details of band wavelength and associated chemical group are as shown in Table 4.1.

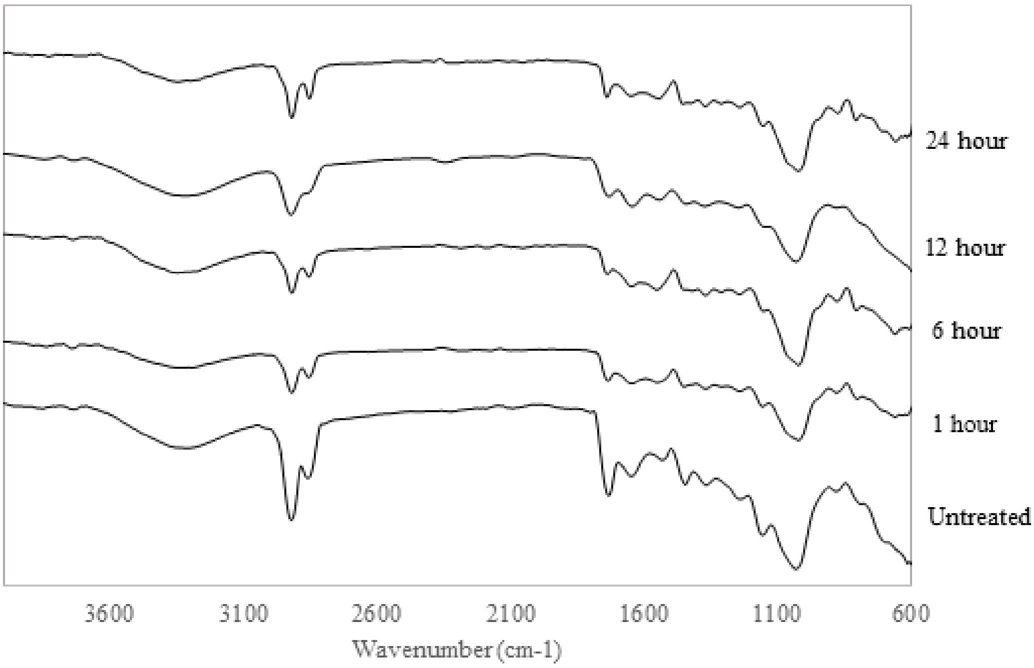

Figure 4.2: FTIR Spectra of untreated GCW, and NaOH treated GCW in different treatment time

Table 4.1: FTIR spectra of GCW as a function of treatment duration (hours)

Band wavelength (cm^{-1})	Associated chemical group	1% NaOH Treatment				
		0 hr	1 hr	6 hr	12 hr	24 hr
3100-3500	-OH intensity	Low	High	High	High	High
2923	Lignin	Present	Reduced	Reduced	Reduced	Reduced
2859	Lignin	Present	Reduced	Reduced	Reduced	Reduced
1728	Hemicellulose, lignin, lipid, pectin and wax	Present	Reduced	Reduced	Reduced	Reduced
1651	Hemicellulose, lignin, lipid, pectin and wax	Present	Reduced	Reduced	Reduced	Reduced
1250	Hemicellulose, Lignin	Present	Reduced	Reduced	Reduced	Reduced
1100	Lignin	Present	Reduced	Reduced	Reduced	Reduced

4.1.2 Scanning electron microscopy (SEM)

Figure 4.3 depicts the SEM images of untreated and NaOH treated GCW fillers with different treatment time. Untreated GCW shows a smoother surface compare with NaOH treated GCW. As the time increased from 0 to 1, 6, 12 and 24 hours, more uneven concave surfaces appeared as the impurities were removed. The impurities were hemicellulose, lignin, pectin, wax and lipid as discussed in both FTIR and TGA results. As a consequence, the surface of GCW was actually getting rougher. The rougher surfaces were able to provide a better adhesion between GCW particle/matrix.

Figure 4.4 illustrates the SEM images corresponding to fracture surfaces from tensile testing of 10% volume fraction of untreated GCW and NaOH treated GCW reinforced composites. For untreated GCW, a gap can be seen on the fractured surface in between the untreated GCW and oxo-HDPE due to poor GCW particle/matrix adhesion. The adhesion between the GCW and oxo-HDPE was improved with NaOH treatment as the rougher surface that led to a better impregnation of the matrix.

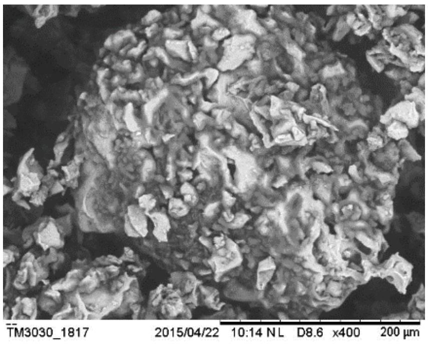

(a)

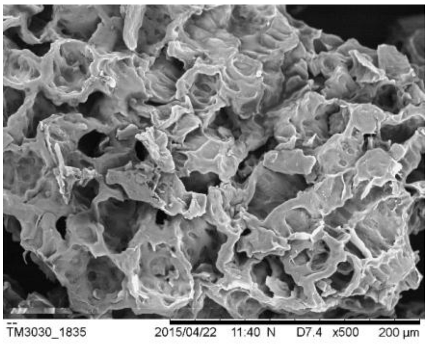

(b)

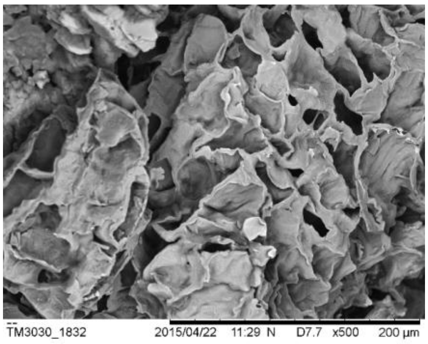

(c)

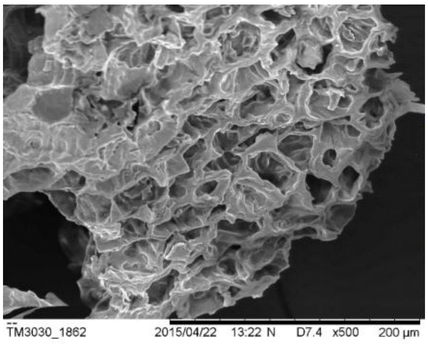

(d)

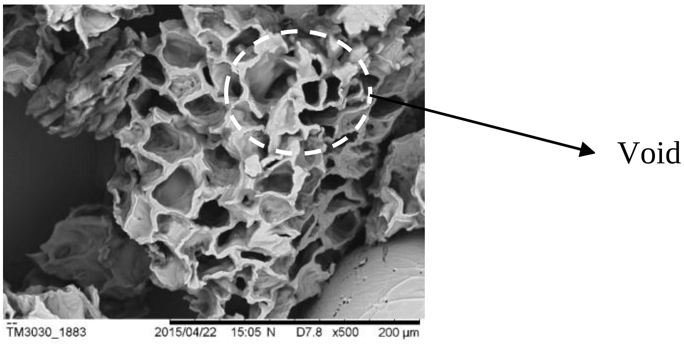

(e)

Figure 4.3: SEM images of 1%NaOH treated GCW as a function of treatment duration (a) non-treatment, (b) 1 hr c) 6 hr d) 12 hr and e) 24 hr

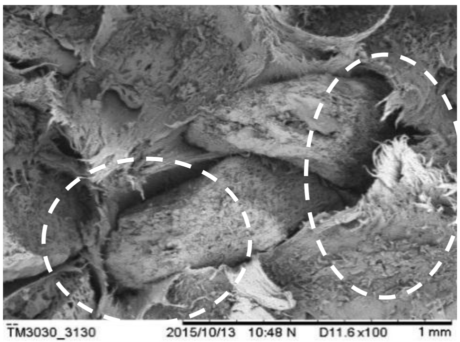

(a)

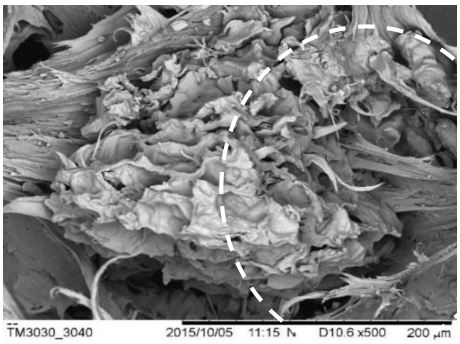

(b)

Figure 4.4: SEM images of breaking surface composites type a) untreated and b) NaOH GCW/oxo-HDPE composites (10% volume fraction)

4.1.3 Thermogravimetric analysis (TGA)

Figure 4.5 shows the thermogravimetric analysis (TGA) thermogram, of of oxo-HDPE, untreated GCW and NaOH treated GCW/oxo-HDPE composites. The first step degradation was found at approximately 250 ℃, followed by the second step at 440 ℃. The first step was due to the decomposition of pectin, wax, impurities and hemicellulose and the second step was due to the decomposition of lignin and cellulose. Lignocellulosic fibres were having complete thermal degradation above 400 ℃ (Nguyen et al., 2007). Hemicellulose was found to decompose at a maximum of 290 ℃, cellulose 370 ℃, lignin 280 ℃ to 520 ℃ (Kifani-Sahban et al., 1996; Nguyen et al., 2007). The temperature used for thermoforming HDPE was around 180 ℃ to 200 ℃ (Sibele Piedade & Luis Claudio, 2013). The inclusion of GCW into HDPE to form composite will not degrade the material since GCW has a high decomposition temperature. Figure 4.6 represents the peak of the main decomposition temperature of the composites or T_{max}. These peaks were attributed to the degradation of cellulose and lignin of the composites. Table 4.2 shows the initial degradation temperature (T_{onset}), maximum degradation temperature (T_{max}), final degradation temperature (T_{final}) and mass residue of the tested composites for TGA. T_{onset}, T_{max} and T_{final} of the untreated GCW and NaOH treated GCW composites remained very close to neat oxo-HDPE. Untreated GCW composites depicted the highest percentage of charred residue. Table 4.3 shows the percentage weight loss for both untreated GCW and NaOH treated GCW composites along with the neat oxo-HDPE. Both Table 4.2 and 4.3 shows that the degradation of untreated occurred earlier than treated GCW composite. NaOH treated composite slightly improved the thermal stability than the untreated. This attributed to the reduction of pectin, wax, hemicellulose, lignin and impurities content after NaOH treatment as observed in the FTIR spectra (Figure 4.2).

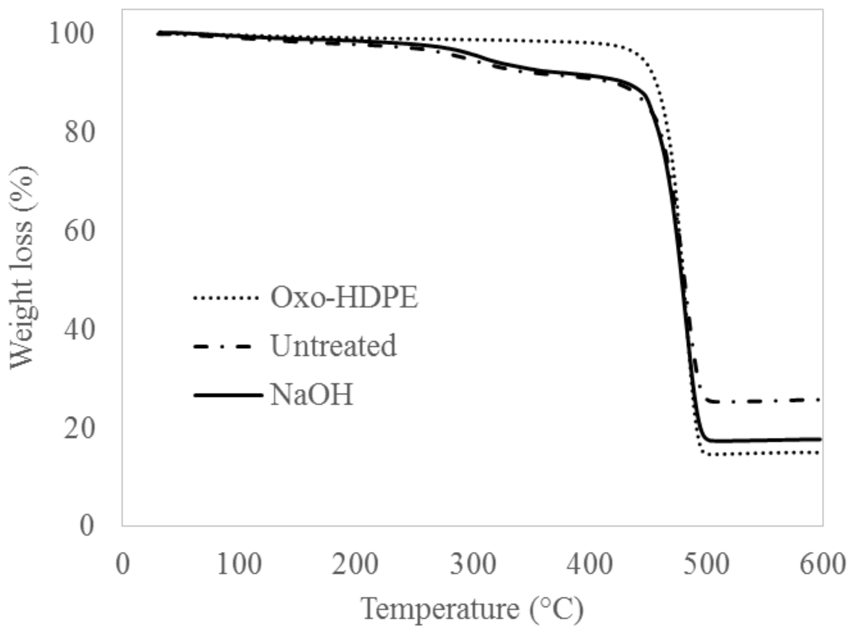

Figure 4.5: TGA thermogram of untreated GCW and NaOH treated GCW/oxo-HDPE composites (10% volume fraction)

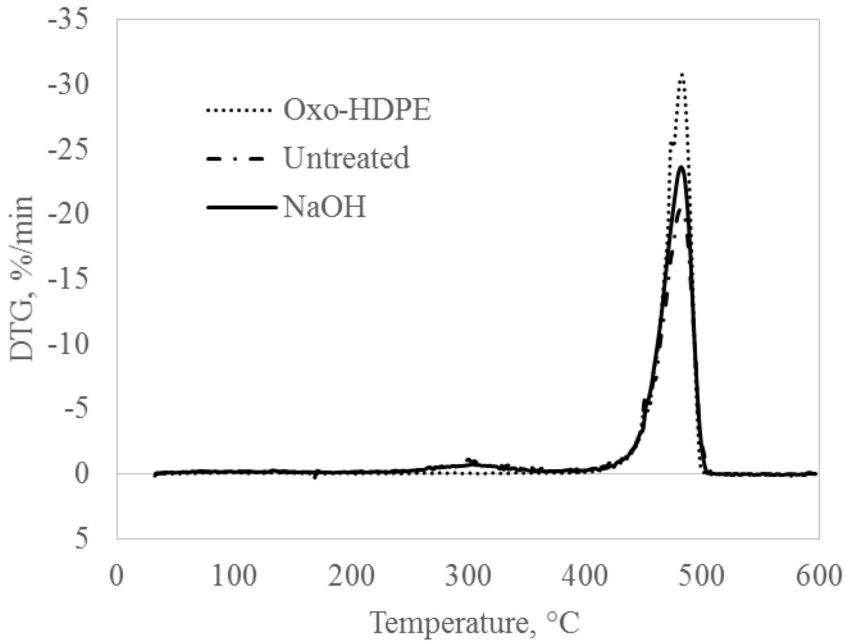

Figure 4.6: DTG thermogram of untreated GCW and NaOH treated GCW/oxo-HDPE composites (10% volume fraction)

Table 4.2: TGA data of oxo-HDPE, untreated and NaOH treated GCW/oxo-HDPE composites (10% volume fraction)

Composites	T_{onset} (℃)	T_{max} (℃)	T_{final} (℃)	Residue (%)
Oxo-HDPE	461.8	474.4	493.2	15.1
Untreated	460.4	481.9	492.4	25.8
NaOH	462.0	482.6	493.1	16.7

Table 4.3: Degradation temperature (in ℃) of oxo-HDPE, untreated and NaOH treated GCW/oxo-HDPE composites (10% volume fraction)

Composites	Temperature at 10% weight loss (℃)	Temperature at 15% weight loss (℃)	Temperature at 25% weight loss (℃)	Temperature at 50% weight loss (℃)
Oxo-HDPE	456.5	462.4	469.7	479.6
Untreated	422.1	450.4	464.6	478.0
NaOH	431.3	451.9	465.0	478.5

4.1.4 Differential scanning calorimetry (DSC)

Figure 4.7 depicts DSC curves of oxo-HDPE, untreated GCW and NaOH treated GCW/oxo-HDPE composites with endothermal peaks during the temperature scan. The peak of the curve represented crystalline melting temperature, T_m. Melting temperature of the composites tested remained in the range of 138 ℃ to 140 ℃. Heat fusion, ΔH_m was calculated using the area in Figure 4.7 while degree of crystallinity, X_c was calculated using Equation 3.5. As observed in Table 4.4, the degree of crystallinity increased slightly with the inclusion of both untreated and treated GCW into the composite. This may be owning to the nucleating ability of the GCW particle reinforcement for crystallisation of oxo-HDPE (Singha et al., 2013). NaOH treatment conducted had removed amorphous materials, such as hemicellulose and pectins supported by FTIR (Figure 4.2) from the GCW surface (Le Troedec et al., 2011). Thus, increased the crystalline components in GCW would resulted in a higher X_c composites.

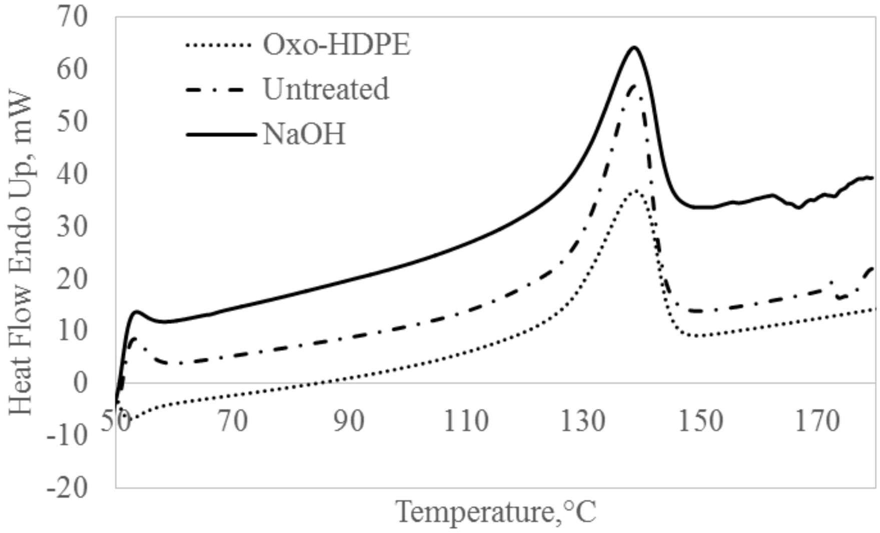

Figure 4.7: DSC curves of oxo-HDPE, untreated GCW and NaOH treated GCW/oxo-HDPE composites

Table 4.4: DSC data of oxo-HDPE, untreated GCW and NaOH treated GCW/oxo-HDPE composites

Composites	T_m (℃)	ΔH_m (J/g)	X_c (%)
Oxo-HDPE	138.9	142.4	49.1
Untreated	138.8	133.3	51.1
NaOH	139.7	140.1	53.7

4.1.5 Water absorption

The water absorption was conducted for 30 days. Figure 4.8 and Figure 4.9 represent the percentage weight gain as a function of the square root of time in seconds. As observed in Figure 4.8, the immersion time increased with increasing weight gain percentage of the composites. In addition, percentage weight gain of composite type C increased with volume fraction for 0.05%, 1.7%, 5.2%, 7.2% and 10.3%, respectively. This was due to the hydrophilic nature of GCW particles and poor adhesion between fibre and matrix. Figure 4.9 shows a comparison of water absorption of untreated and NaOH treated GCW reinforce oxo-HDPE at 10% volume fraction. NaOH treated GCW/oxo-HDPE composite was having a weight gain of 2.2%, a total of 57% reduction in water absorption compared to untreated. This has shown that alkaline treatment is able to increase the hydrophobicity of the GCW (Baghaei et al., 2014). Other than that, a better adhesion and reduction of the presence of void after the treatment contributed to the reduction of moisture absorption too.

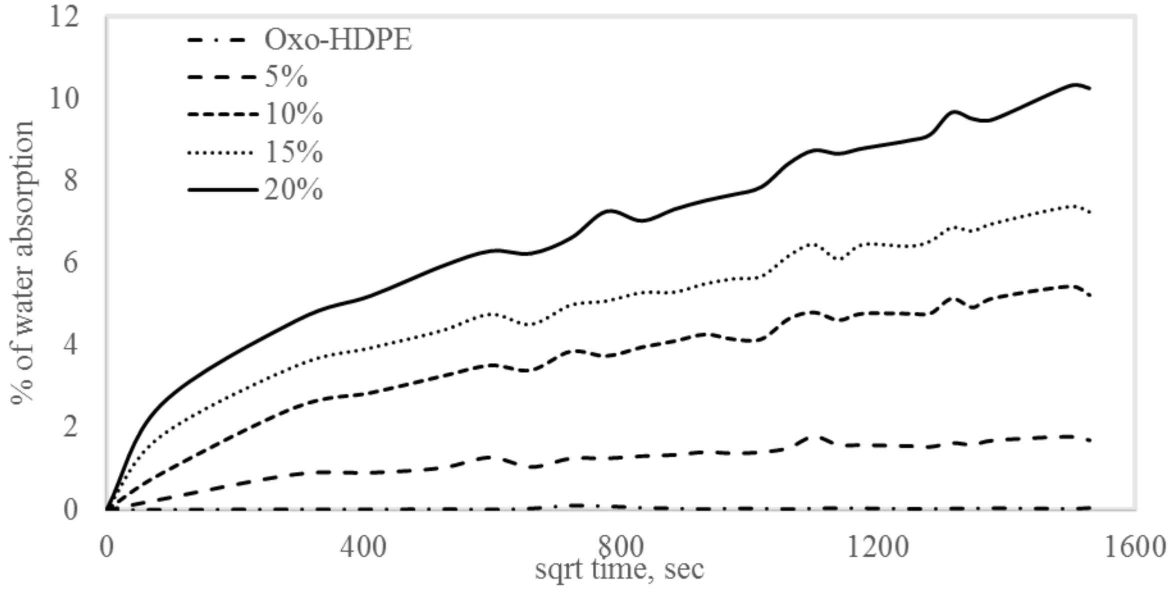

Figure 4.8: Percent mass gain due to the absorption of water for untreated GCW/oxo-HDPE composites by volume fraction

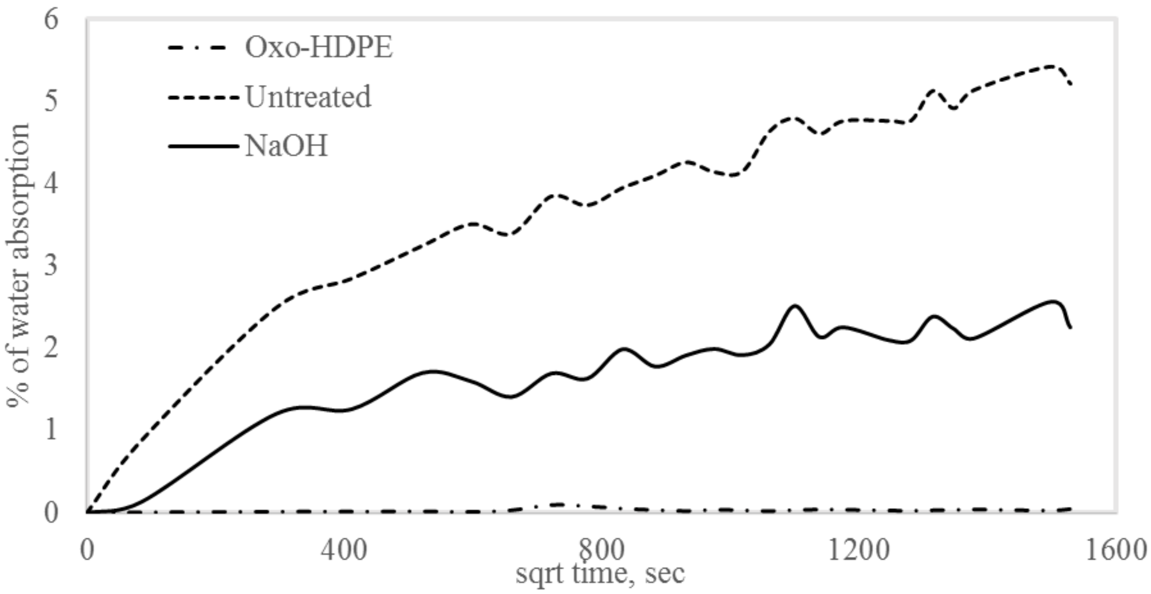

Figure 4.9: Percent weight gain due to the absorption of water of untreated and NaOH treated GCW/oxo-HDPE composites (10% volume fraction)

4.1.6 Tensile test

4.1.6.1 NaOH treatment by time

GCW were treated with 1% concentration of NaOH (0.25 Molarity) with different treatment time (0, 1, 6, 12 and 24 hours) for 10% volume fraction. As shown in Figure 4.10, Figure 4.11, Figure 4.12, Figure 4.13 and Figure 4.14, the result revealed the tensile properties increase with treatment time. Tensile strength showed an improvement of 32%, tensile modulus 23%, specific tensile strength 42%, specific tensile modulus 32% and ductility in the range of 12% to 23%. The mercerisation process removed surface impurities, natural fats, waxes, hemicellulose and a small amount of lignin (Bledzki & Gassan, 1999). This has increased the surface roughness of GCW as confirmed by FTIR and SEM result reported earlier. Thus, resulted in a higher intensity of hydroxyl group and other reactive functional groups on the surface. This had increased the surface roughness of GCW supported by FTIR and SEM (Valadez-Gonzalez et al., 1999). This suggested a better interaction and mechanical interlocking between NaOH treated GCW and oxo-HDPE matrix that provided higher tensile properties. Table 4.5 summarised the tensile results obtained.

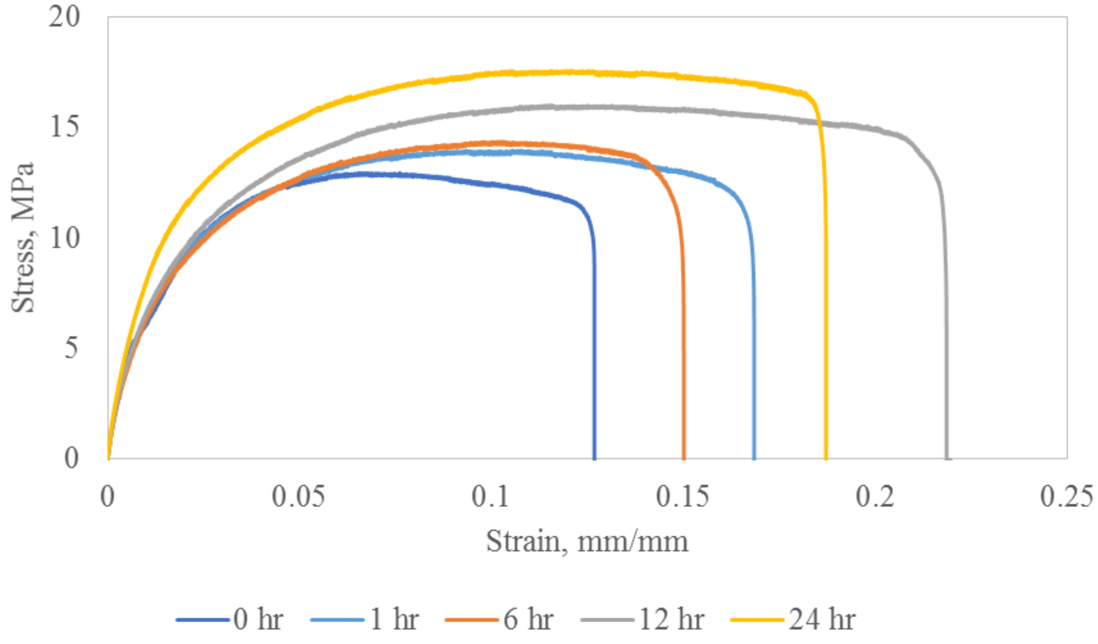

Figure 4.10: Stress-strain curves for NaOH treated GCW/oxo-HDPE composites at crosshead displacement rate of 1 mm/min by treatment time

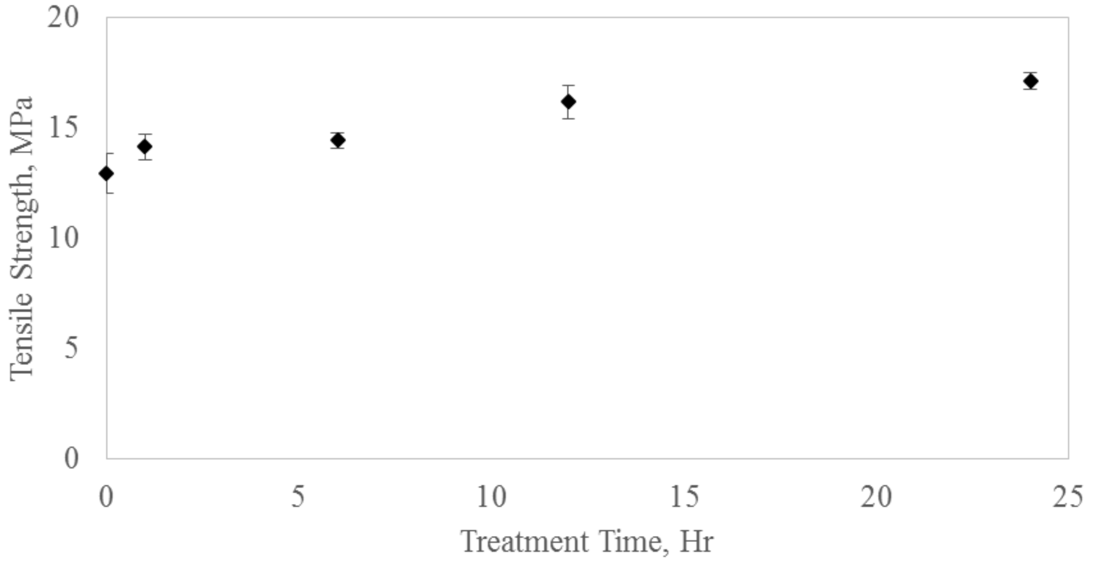

Figure 4.11: Tensile strength of NaOH treated GCW/oxo-HDPE composites at crosshead displacement rate of 1 mm/min by treatment time

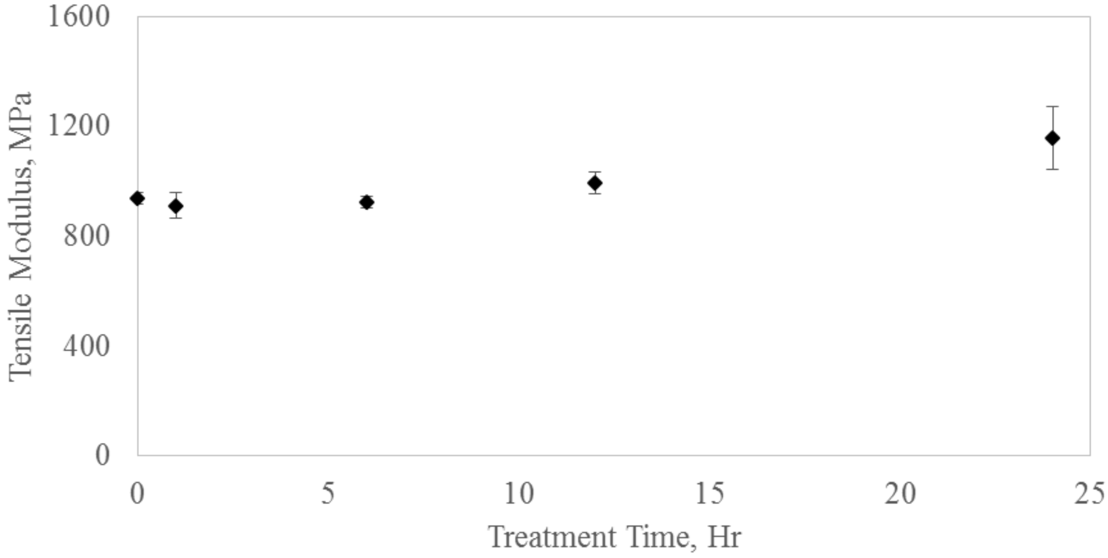

Figure 4.12: Tensile modulus of NaOH treated GCW/oxo-HDPE composites at crosshead displacement rate of 1 mm/min by treatment time

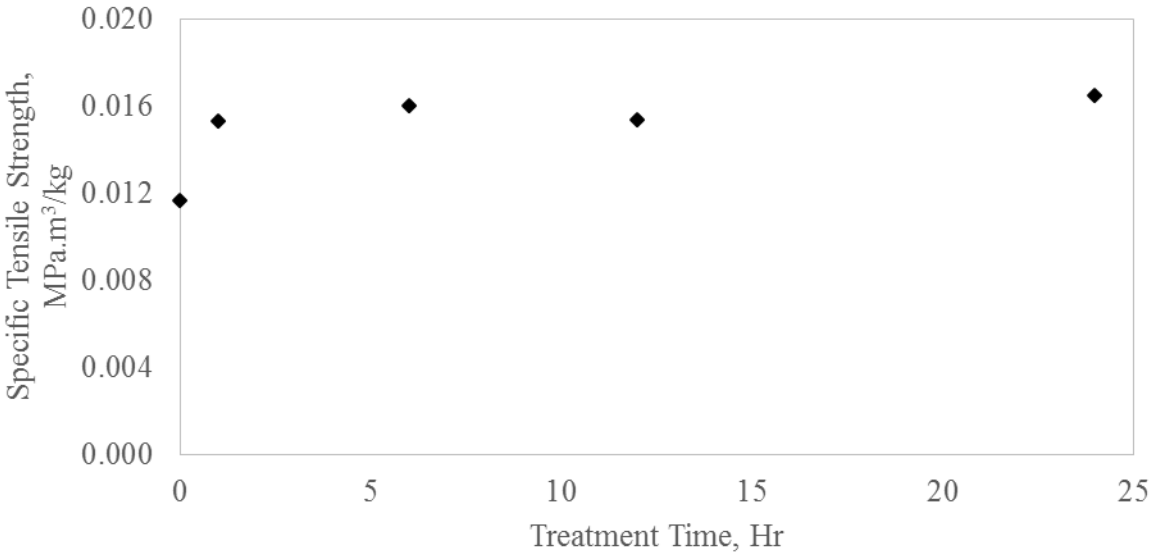

Figure 4.13: Specific tensile strength of NaOH treated GCW/oxo-HDPE composites at crosshead displacement rate of 1 mm/min by treatment time

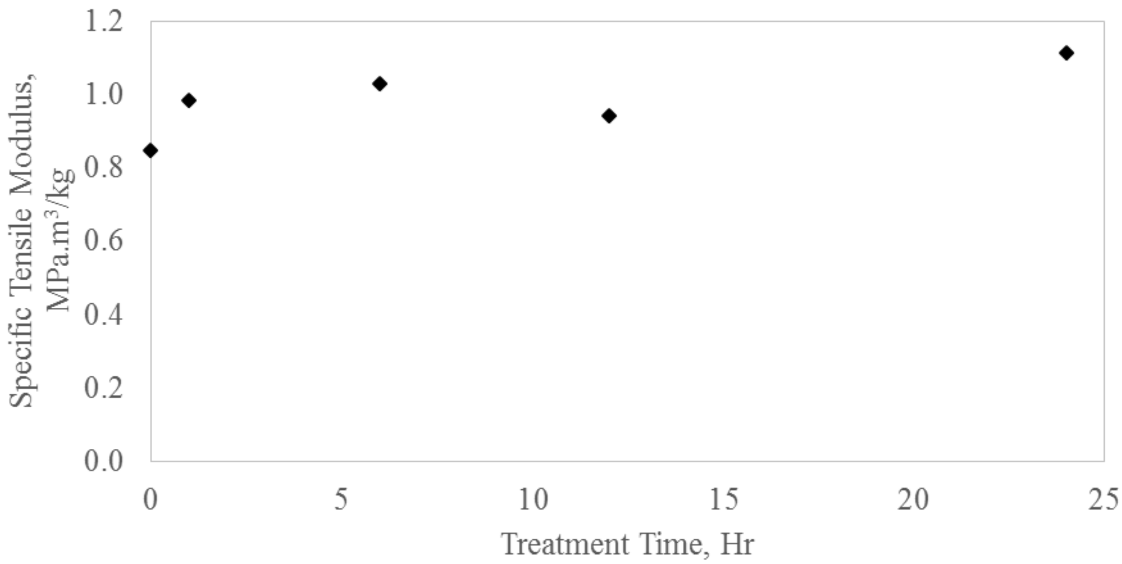

Figure 4.14: Specific tensile modulus of NaOH treated GCW/oxo-HDPE composites at crosshead displacement rate of 1 mm/min by treatment time

Table 4.5: Summary of tensile properties of NaOH treated GCW/oxo-HDPE composites by treatment time

Composite	**Treatment Time (Hr)**	**Tensile Strength (MPa)**	**Tensile Modulus (MPa)**	**Specific Tensile Strength (MPa.m^3/kg)**	**Specific Tensile Modulus (MPa.m^3/kg)**
	0	12.95 (0.89)	938.40 (20.86)	0.012	0.847
	1	14.15 (0.56)	911.42 (47.45)	0.015	0.985
Untreated	6	14.43 (0.37)	925.53 (21.29)	0.016	1.028
	12	16.18 (0.76)	993.57 (40.68)	0.015	0.943
	24	17.13 (0.39)	1157.73 (116.23)	0.017	1.115

4.1.6.2 Comparison of untreated and NaOH treated GCW/oxo-HDPE composites by volume fraction

Figure 4.15 and Figure 4.16 illustrates stress-strain curves of untreated and NaOH treated GCW/oxo-HDPE composites at crosshead displacement rates of 1 mm/min by volume fraction. Untreated GCW/oxo-HDPE composites showed a pattern of reduction in elongation at break with the addition of filler in HDPE composites from 18% to 8% (Khalaf, 2015). Meanwhile, the elongation at break for NaOH treated GCW/oxo-HDPE was around 19-20%. The treatment done led to a better interaction between GCW and oxo-HDPE thus improved the ductility of the composites.

Figure 4.17 and Figure 4.18 show tensile strength and modulus of untreated and NaOH treated GCW/oxo-HDPE composites with different volume fraction of GCW (0%, 5%, 10%, 15% and 20%). Untreated GCW/oxo-HDPE composites showed a decreasing trend of tensile properties with increasing volume fraction. Poor interaction can be seen in between untreated GCW and oxo-HDPE with a layer of impurities in SEM image (Figure 4.4a). For NaOH Treated GCW/oxo-HDPE composites, tensile strength and tensile modulus increased with 10% volume fraction. The highest tensile strength obtained was 17.14 MPa, an increment of 25% while tensile modulus of 1158 MPa shown an increment of 24% compared to untreated. The tensile modulus of NaOH Treated GCW/oxo-HDPE composites was 5% better than neat-oxo-HDPE. The inclusion of treated GCW was able to improve the stiffness of the composites. After the removal of hemicellulose, lignin, pectin, wax and impurities, the density and rigidity of interfibrillar region became less and were able to rearrange themselves along the direction of tensile deformation upon the applied load (Bledzki & Gassan, 1999). Thus, exhibited better tensile properties compare to untreated. Increasing the volume fraction of GCW would lead to a decrease in tensile properties (Yang et al., 2007). A large amount of

GCW particles would tend to agglomerate to form a bigger particle and cause a non-homogenous dispersion. Big particles tend to debond easily and thus result in poor mechanical properties. Similar tensile results were obtained by other researchers (Anbukarasi & Kalaiselvam, 2015; Fávaro et al., 2010; Singha et al., 2013; Stark & Rowlands, 2003).

Figure 4.19 and Figure 4.20 showed the specific tensile strength and modulus untreated and NaOH treated GCW/oxo-HDPE composites that determine strength and stiffness to weight ratio. The specific tensile strength of neat oxo-HDPE was 0.0175 MPa.m^3/kg while both untreated and NaOH treated showed lower specific tensile strength. On the other hand, the specific tensile modulus improved for 6% to 9% for NaOH treated (volume fraction of 5% and 10%). The improvement in specific tensile properties contributed to a reduction in CO_2 emission that is able to reduce the weight in transportation, ease the installation with less maintenance in the continuity of operation in the industrial application. It is suitable to be used in the applications where weight is paramount, such as cars body parts. Lighter vehicles will contribute to less fuel consumption. Summary of tensile results are shown in Table 4.6.

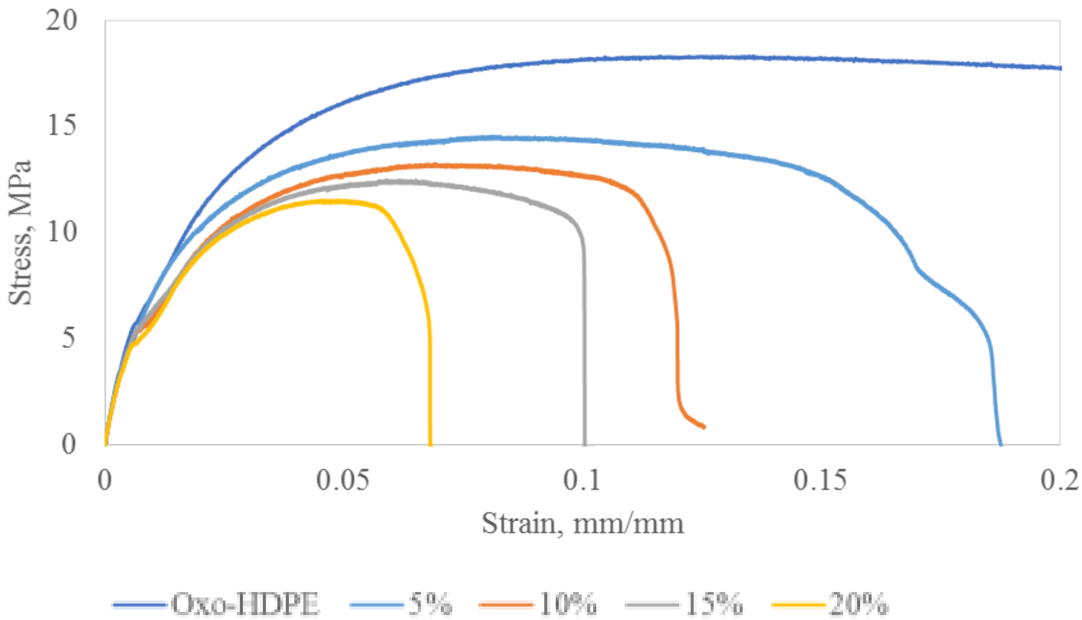

Figure 4.15: Stress-strain curves of untreated GCW/oxo-HDPE composites at crosshead displacement rates of 1 mm/min by volume fraction

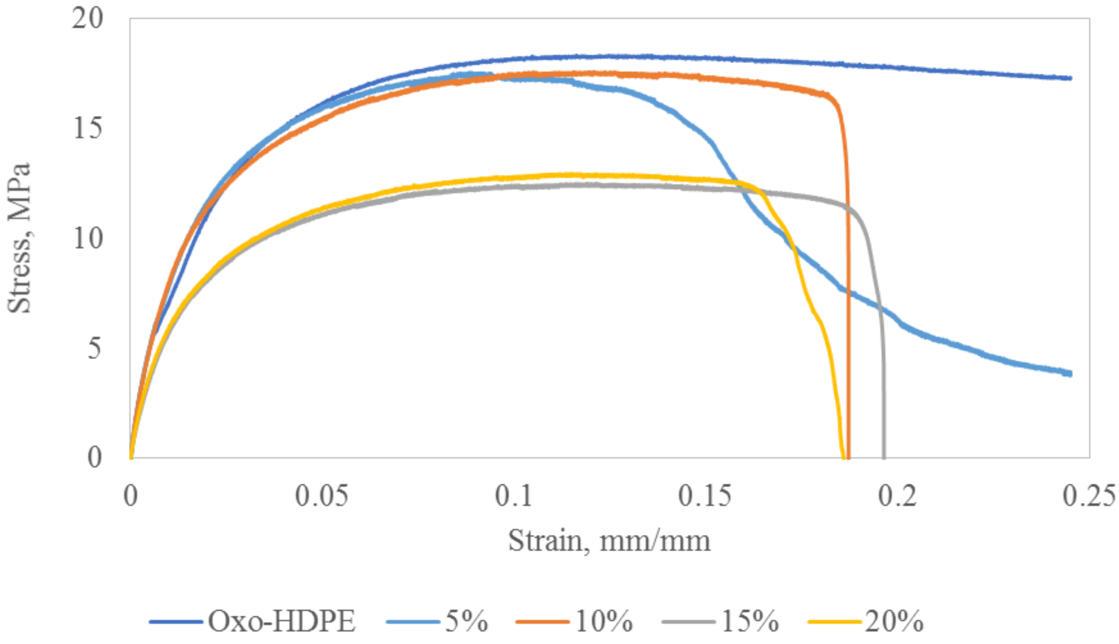

Figure 4.16: Stress-strain curves of NaOH treated GCW/oxo-HDPE composites at crosshead displacement rates of 1 mm/min by volume fraction

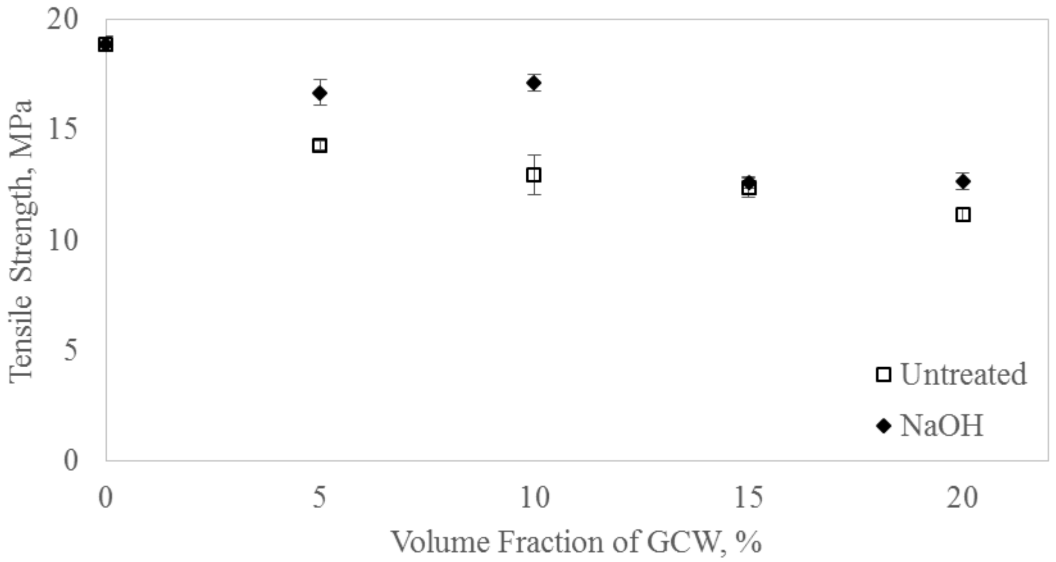

Figure 4.17: Tensile strength of untreated and NaOH treated GCW/oxo-HDPE composites at crosshead displacement rates of 1 mm/min by volume fraction

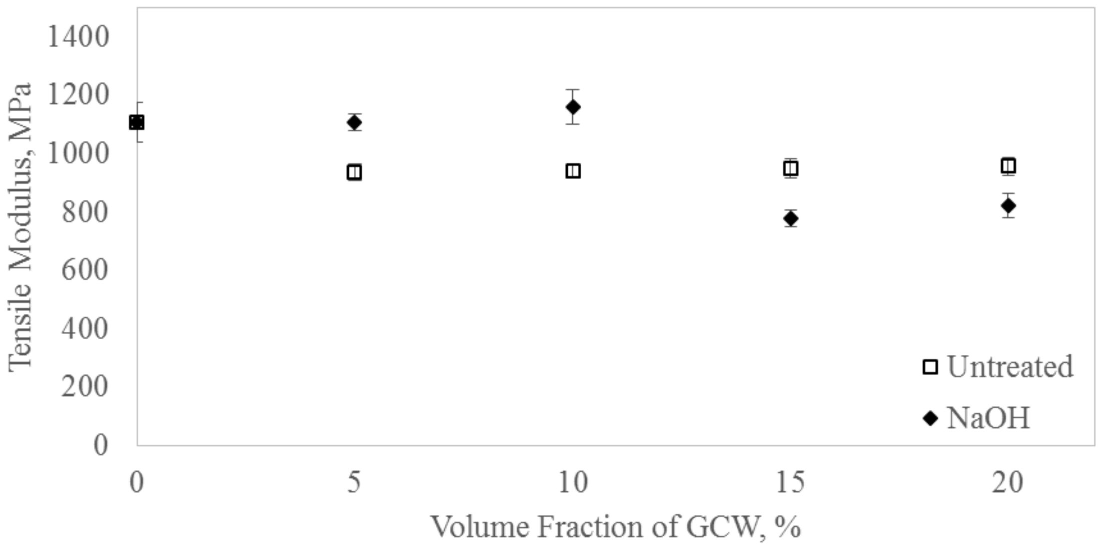

Figure 4.18: Tensile modulus of untreated and NaOH treated GCW/oxo-HDPE composites at crosshead displacement rates of 1 mm/min by volume fraction

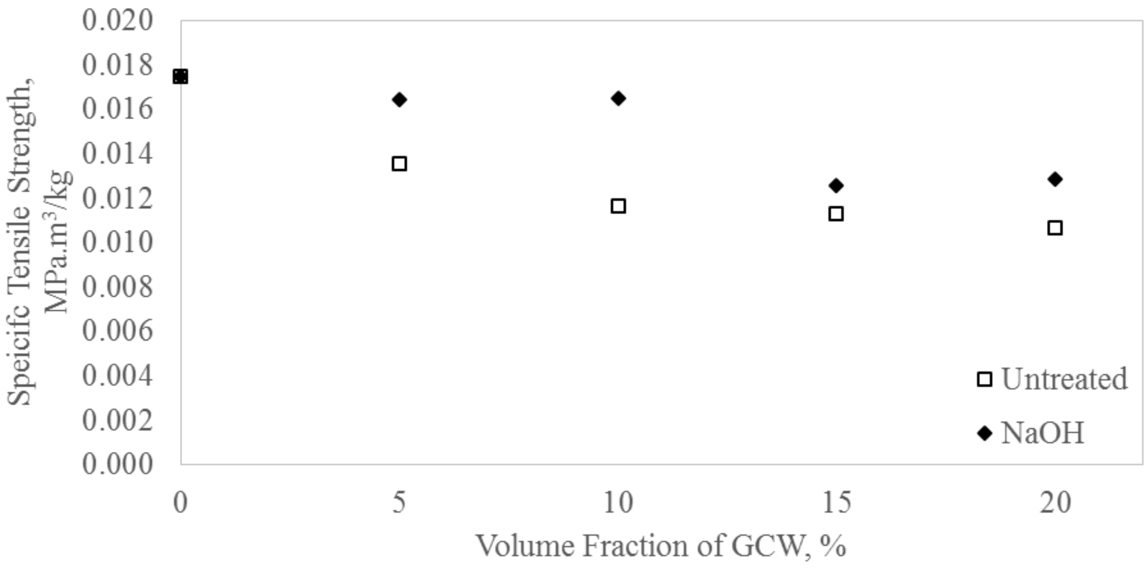

Figure 4.19: Specific tensile strength of untreated and NaOH treated GCW/oxo-HDPE composites at crosshead displacement rates of 1 mm/min by volume fraction

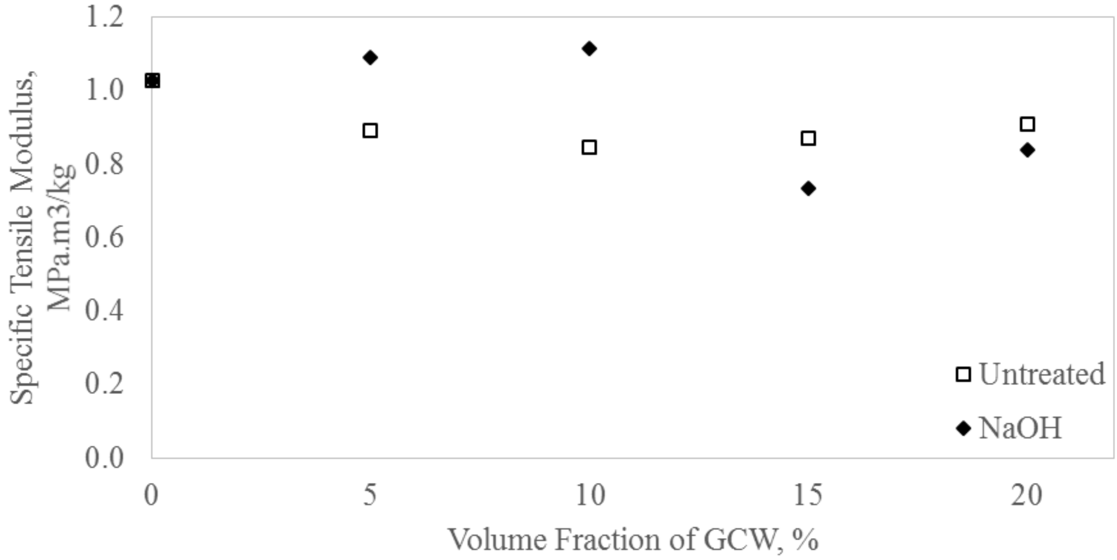

Figure 4.20: Specific tensile modulus of untreated and NaOH treated GCW/oxo-HDPE composites at crosshead displacement rates of 1 mm/min by volume fraction

Table 4.6: Tensile properties of oxo-HDPE, untreated and NaOH treated GCW/oxo-HDPE composites at crosshead displacement rates of 1 mm/min by volume fraction

Composite	Filler Vol. (%)	Tensile Strength (MPa)	Tensile Modulus (MPa)	Specific Tensile Strength (MPa.m^3/kg)	Specific Tensile Modulus (MPa.m^3/kg)
Oxo-HDPE	0	18.89 (0.35)	1107.18 (67.57)	0.018	1.026
Untreated	5	14.28 (0.22)	936.93 (28.58)	0.014	0.891
	10	12.95 (0.89)	938.40 (20.86)	0.012	0.847
	15	12.36 (0.43)	950.45 (33.38)	0.011	0.871
	20	11.19 (0.26)	955.81 (29.86)	0.011	0.910
NaOH	5	16.69 (0.56)	1107.37 (28.10)	0.017	1.092
	10	17.14 (0.39)	1157.73 (116.23)	0.017	1.115
	15	12.60 (0.26)	735.66 (79.61)	0.013	0.734
	20	12.66 (0.38)	822.31 (40.37)	0.013	0.837

4.1.7 Low velocity impact test

Impact test can be used to determine the amount of load, energy at maximum load and total absorption energy of a specimen. The stiffness untreated and NaOH treated GCW/oxo-HDPE composites were improved compared to neat oxo-HDPE as shown in the ascending part of the graph in Figure 4.21 and Figure 4.22. NaOH treated GCW/oxo-HDPE composites showed higher stiffness than untreated. Figure 4.23, Figure 4.24 and Figure 4.25 depict load, energy to maximum load and total energy absorbed by untreated and NaOH treated GCW/oxo-HDPE composites. The maximum load that can be sustained by untreated GCW/oxo-HDPE composites decreased with volume fraction. For NaOH treated GCW/oxo-HDPE composites, the maximum load can be sustained increased with volume fraction and reached a maximum at a volume fraction of 15%, an improvement of 6% compare to neat oxo-HDPE. Energy to maximum load is the energy absorbed by the samples with maximum load. It is the amount of energy that absorbed by a sample before failure. Results of energy to maximum load was showing a similar trend to maximum load that sustained by the composites. The decreasing curve of the graphs after maximum load represented the material's property. Impact load exhibited a drastic drop with increasing volume fraction for untreated GCW/oxo-HDPE composites. The brittleness of the composites increased with the volume fraction of GCW. On the other hand, the ductility behaviour increased for NaOH treated GCW/oxo-HDPE composites. This is explained in Figure 4.26 and Figure 4.27, where the fracture surface showed NaOH treated GCW/oxo-HDPE composites (15% volume fraction) was having better surface resistance than untreated with same volume fraction. The delamination of the composites occurred at the perforated area. The delamination area of NaOH treated GCW/oxo-HDPE composites was wider. The area of the graph is actually the total energy absorbed by the test specimens. The total energy absorbed by the untreated GCW/oxo-HDPE composites decreased as the volume fraction of GCW increased. Total energy absorbed by the composite is the sum of the energy consumed during plastic deformation. After the inclusion of GCW, the composites became harder, brittle and less ductile, so the total energy absorbed was lower compared to neat oxo-HDPE. In addition, less adhere between hydrophilic GCW and hydrophobic oxo-HDPE leading to less energy absorption too. Total energy absorption increased with increasing volume fraction reached its optimum condition at 15% for NaoH treated GCW/oxo-HDPE composites. Treated composites showed a better overall result compared to the untreated. This was due to better interphase between treated GCW and oxo-HDPE after the treatment as unwanted surface impurities had been removed, rougher surface and active sites exposed for interaction. Thus, provide better stress transfer. A similar trend of improvement of impact properties using alkaline treatment done by another researcher (Obasi et al., 2014). The summary data of impact properties are as shown in Table 4.7.

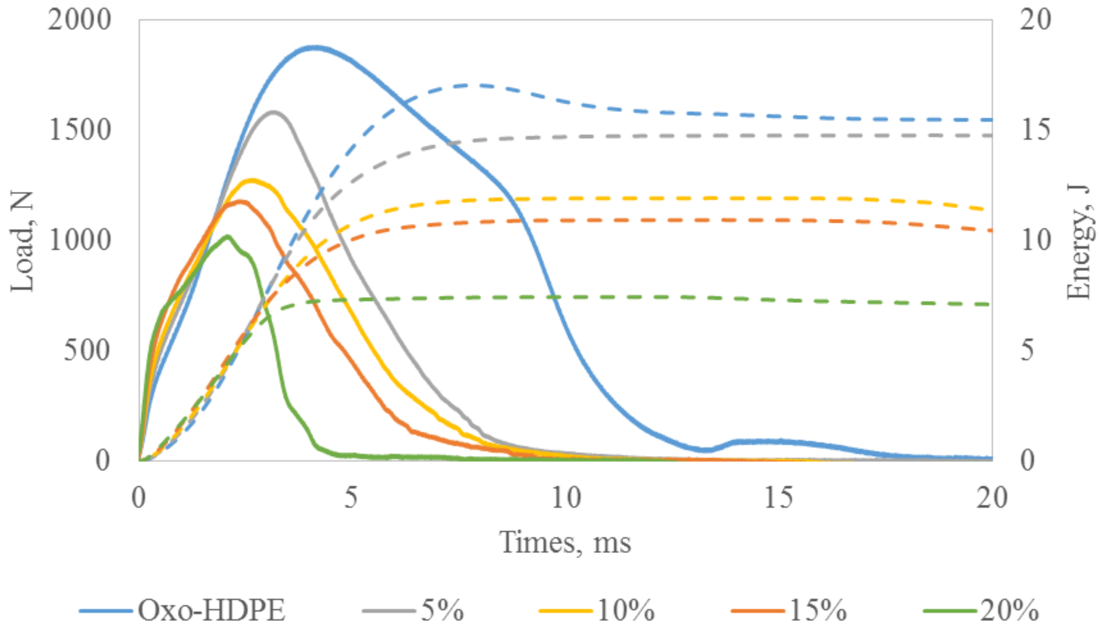

Figure 4.21: Load-energy-time graph of impact for untreated GCW/oxo-HDPE composites by volume fraction

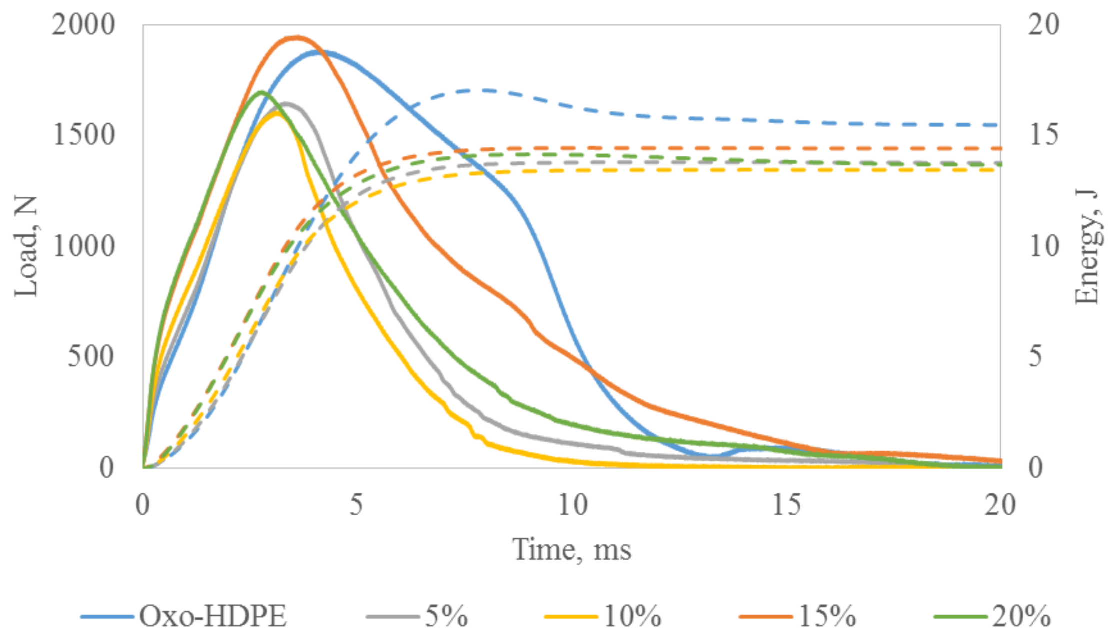

Figure 4.22: Load-energy-time graph of impact for NaOH treated GCW/oxo-HDPE by volume fraction

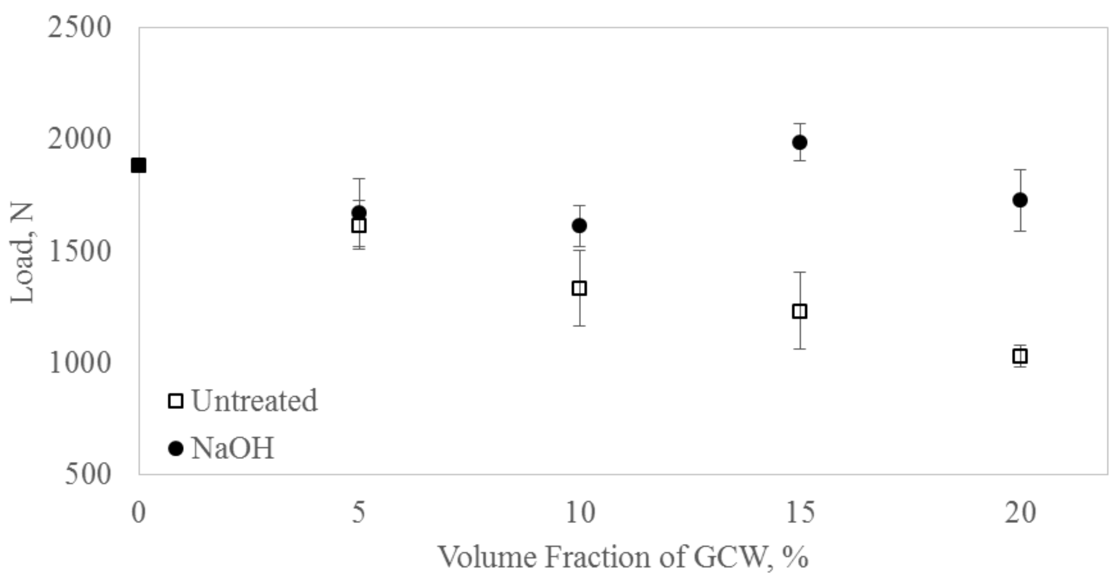

Figure 4.23: Comparison of different volume fraction of load for untreated and NaOH treated GCW/oxo-HDPE composites

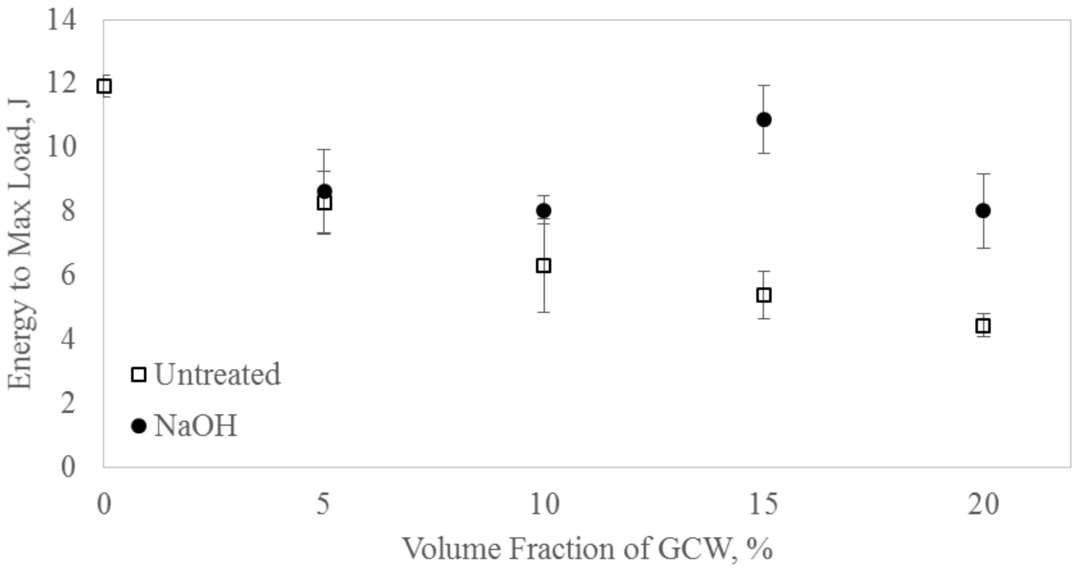

Figure 4.24: Comparison of different volume fraction of energy to maximum for untreated and NaOH treated GCW/oxo-HDPE composites

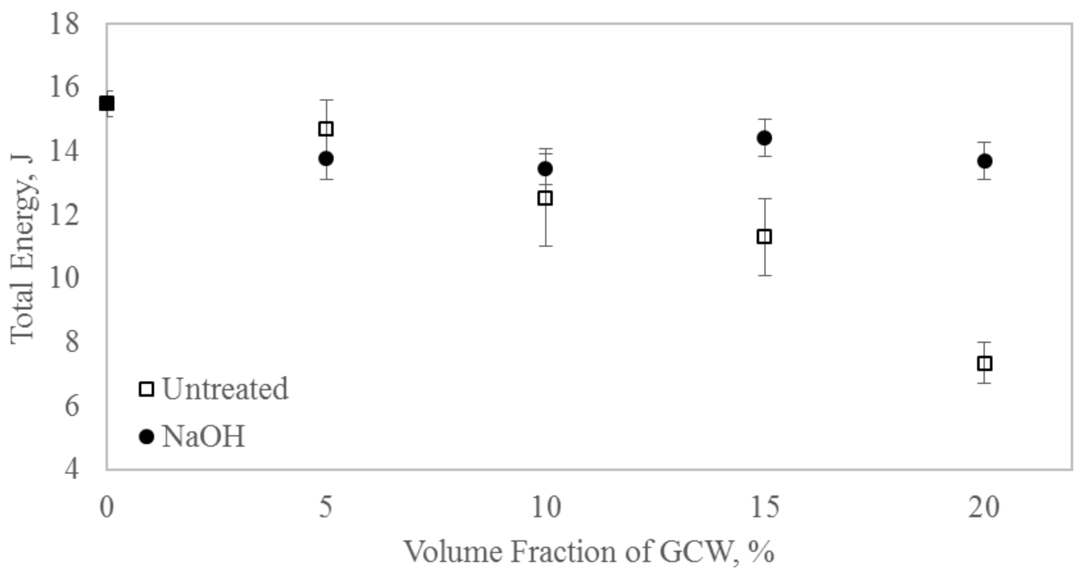

Figure 4.25: Comparison of different volume fraction of total energy for untreated and NaOH treated GCW/oxo-HDPE composites

Table 4.7: Impact properties of oxo-HDPE, untreated and NaOH treated GCW/oxo-HDPE composites

Composite	Filler Vol. (%)	Peak Load (N)	Energy to maximum load (J)	Total energy (J)
Oxo-HDPE	0	1885.98 (25.95)	11.91 (0.35)	15.49 (0.40)
Untreated	5	1617.73 (107.99)	8.25 (0.97)	14.72 (0.90)
	10	1334.74 (167.70)	6.30 (1.45)	12.54 (1.52)
	15	1232.40 (171.97)	5.36 (0.73)	11.31 (1.20)
	20	1031.01 (47.75)	4.42 (0.37)	7.35 (0.65)
NaOH	5	1673.33 (151.68)	8.61 (1.30)	13.79 (0.68)
	10	1614.73 (92.52)	8.04 (0.45)	13.44 (0.46)
	15	1988.58 (84.78)	10.87 (1.04)	14.41 (0.57)
	20	1727.76 (137.16)	8.01 (1.16)	13.70 (0.57)

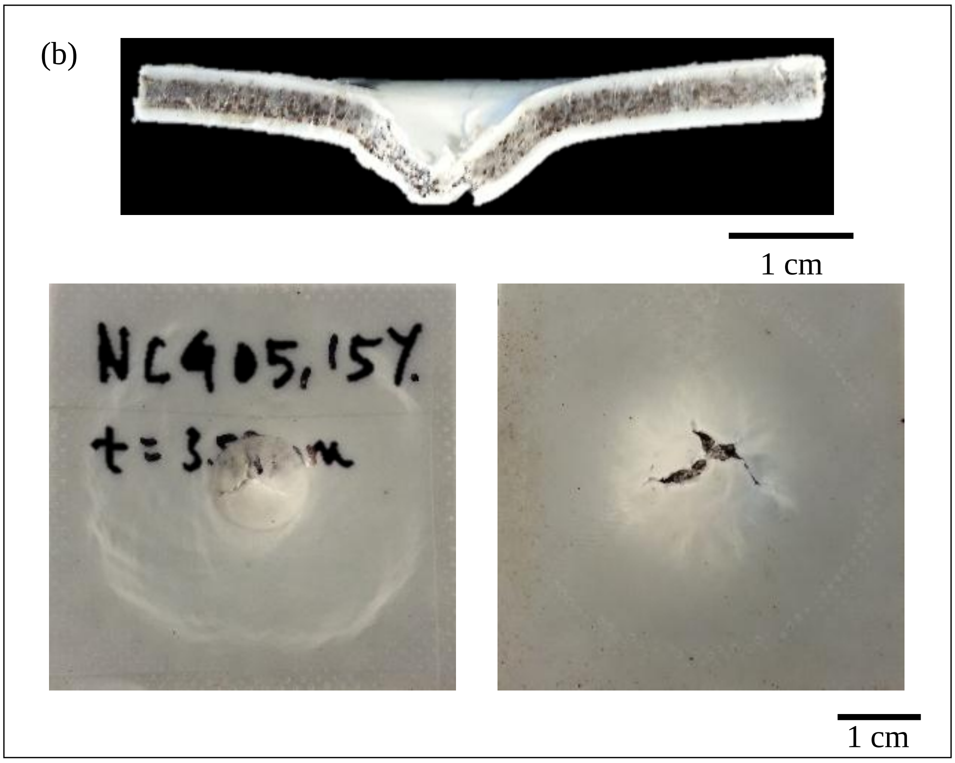

Figure 4.26: Fracture surface of impact test for a) untreated, b) NaOH treated GCW/oxo-HDPE composites (15% volume fraction)

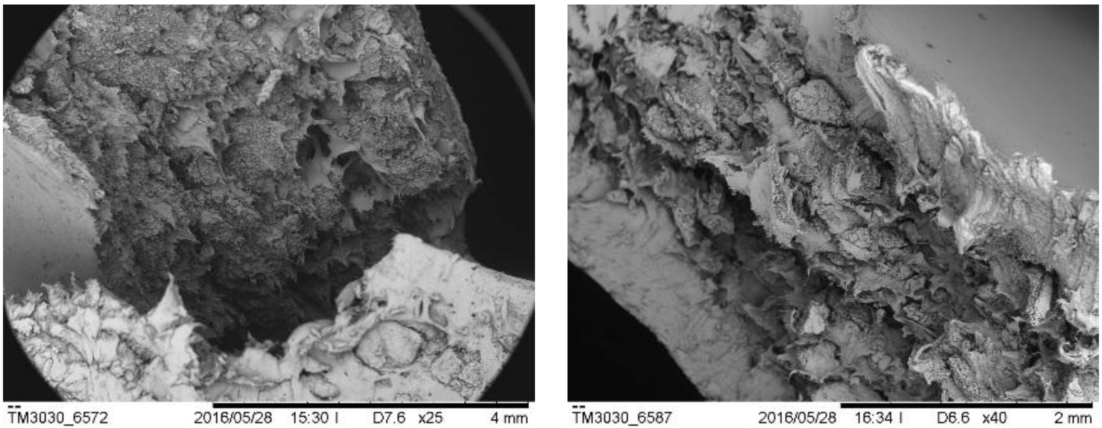

(a) (b)

Figure 4.27: SEM images of fracture surface of impact test for a) untreated, b) NaOH treated GCW/oxo-HDPE composites (15% volume fraction)

4.2 Comparison of composites type untreated, oil extracted and oil extracted + NaOH/oxo-HDPE composites

Soxhlet oil extraction is another method that had been employed to get rid of the oil on the surface of GCW. The extracted oil can be used to produce biodiesel, bioplastic or other industrial applications while the GCW left behind can be used as reinforcement of composite production. Thus, it can be utilised the waste to turn it into a value-added product.

4.2.1 Fourier transform infrared spectroscopy (FTIR)

FT-IR spectroscopy in Figure 4.28 shows exemplary peaks of untreated GCW, oil extracted GCW and oil extracted + NaOH GCW, respectively at 3351, 2923, 2859, 1733, 1444, 1367, 1238, 1120, 1031 cm^{-1}. The absorption band of 3351 cm^{-1} belongs to the absorption of –OH stretching vibrations on the GCW. The –OH compound consisted the presence of water, aliphatic primary and secondary alcohol found in cellulose, hemicellulose, lignin, extractives and carboxylic acids in extractives (Khan et al., 1993; Kolboe & Ellefsen, 1962). The decreasing area of this peak represented the removal of lipids. Peaks at 2859 and 2923 cm^{-1} recognised as asymmetric and symmetric stretching of C-H bonds in aliphatic chains that attributed to lipids (Cremer & Kaletunç 2003). The decreasing area of these peaks represented the removal of lipids. The characteristic GCW peak at 1733 cm^{-1} and 1238 cm^{-1} credited to the acetylated xylan (hemicellulose), aldehyde lignin or carbonyl lipid, pectin and wax (Faix, 1991; Matuana et al., 2001); 1444 cm^{-1} assigned to benzene ring stretching in lignin and $=CH_2$ vibration in polyoses (Hemicellulose) (Pervan et al., 2006); 1120 cm^{-1} attributed to the aromatic C-H in the plane deformation mode of the guaiacyl/syringyl units of lignin (Khan et al., 1993) disappeared after both treatments. The in-plane C-H bending in hemicellulose reduced with showing 1367 cm^{-1} after the treatments conducted (Fan et al., 2012). During 600-1100 cm^{-1} peak, the -OH concentration increasing from untreated GCW to oil extracted GCW followed by oil extracted + NaOH GCW, revealing a more active site that is available to intermingle between particle/matrix interfaces. Table 4.8 demonstrates the details of band wavelength and associated chemical group.

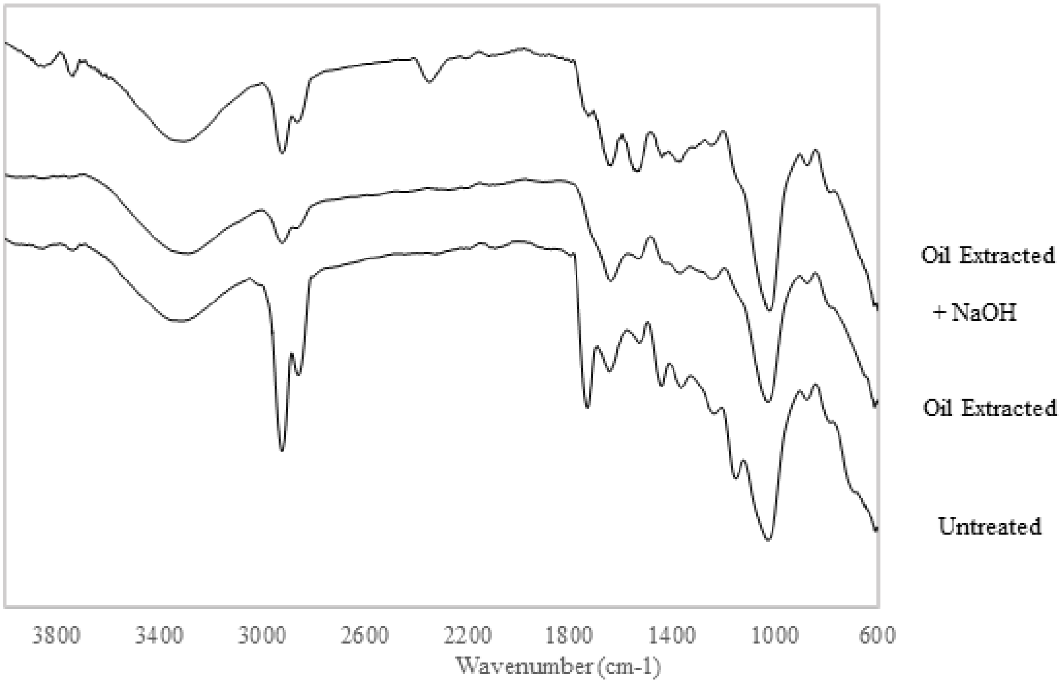

Figure 4.28: FTIR Spectra of untreated, oil extracted GCW and oil extracted + NaOH GCW

Table 4.8: FTIR results of untreated GCW, oil extracted GCW and oil extracted + NaOH GCW

Band wavelength (cm^{-1})	Associated chemical group	Untreated	Oil extracted	Oil extracted + NaOH
3351	-OH intensity	High	Low	Low
2923	Lipid peak	Present	Reduced	Reduced
2859	Lipid peak	Present	Reduced	Reduced
1733	Hemicellulose, Lignin, Lipid, pectin-wax peak	Present	-	-
1444	Lignin, hemicellulose peak	Present	-	-
1367	Hemicellulose peak	Present	Reduced	Reduced
1238	Hemicellulose, Lignin peak	Present	Reduced	Reduced
1120	Lignin peak	Present	-	-
600-1100	-OH intensity	Low	High	High

4.2.2 Scanning Electron Microscopy (SEM)

Surface morphology of untreated GCW, oil extracted GCW and oil extracted + NaOH GCW were shown in Figure 4.29. All of the GCW particles were having a dendritic appearance. Untreated GCW was having a layer of oil covered on its surface (Figure 4.29a). The SEM images illustrated that the modifications done on the GCW had increased its surface roughness. This had been proven by the FTIR and TGA of the removal of hemicellulose, lignin, pectin, wax, lipid and impurities on the GCW surface. As seen in Figure 4.29b, coarser surface revealed and cellulose microfibrils were exposed on oil extracted GCW surface after the oil had been extracted. In Figure 4.29c, oil extracted + NaOH GCW shown uneven concave and rougher surfaces with a less cellulose microfibrils exposure. Besides that, oil extracted + NaOH was more fragile as proven by the mechanical properties.

Figure 4.30 shows the SEM images conforming to fracture surfaces from tensile test of untreated, oil extracted and oil extracted + NaOH GCW/oxo-HDPE composites. For untreated

GCW/oxo-HDPE composites, the fractured surface showed a gap in between the GCW and oxo-HDPE resulted in poor particle/matrix adhesion. For oil extracted GCW/oxo-HDPE composites, a clearer and better interface between the oil extracted GCW and oxo-HDPE can be observed with a layer of removed lipid from GCW surface. The adhesion of oil extracted + NaOH GCW/oxo-HDPE composites was improved as it led to a better impregnation of the matrix into oil extracted + NaOH treated GCW. However, oil extracted + NaOH GCW became fragile and porous thus yielded lower mechanical properties.

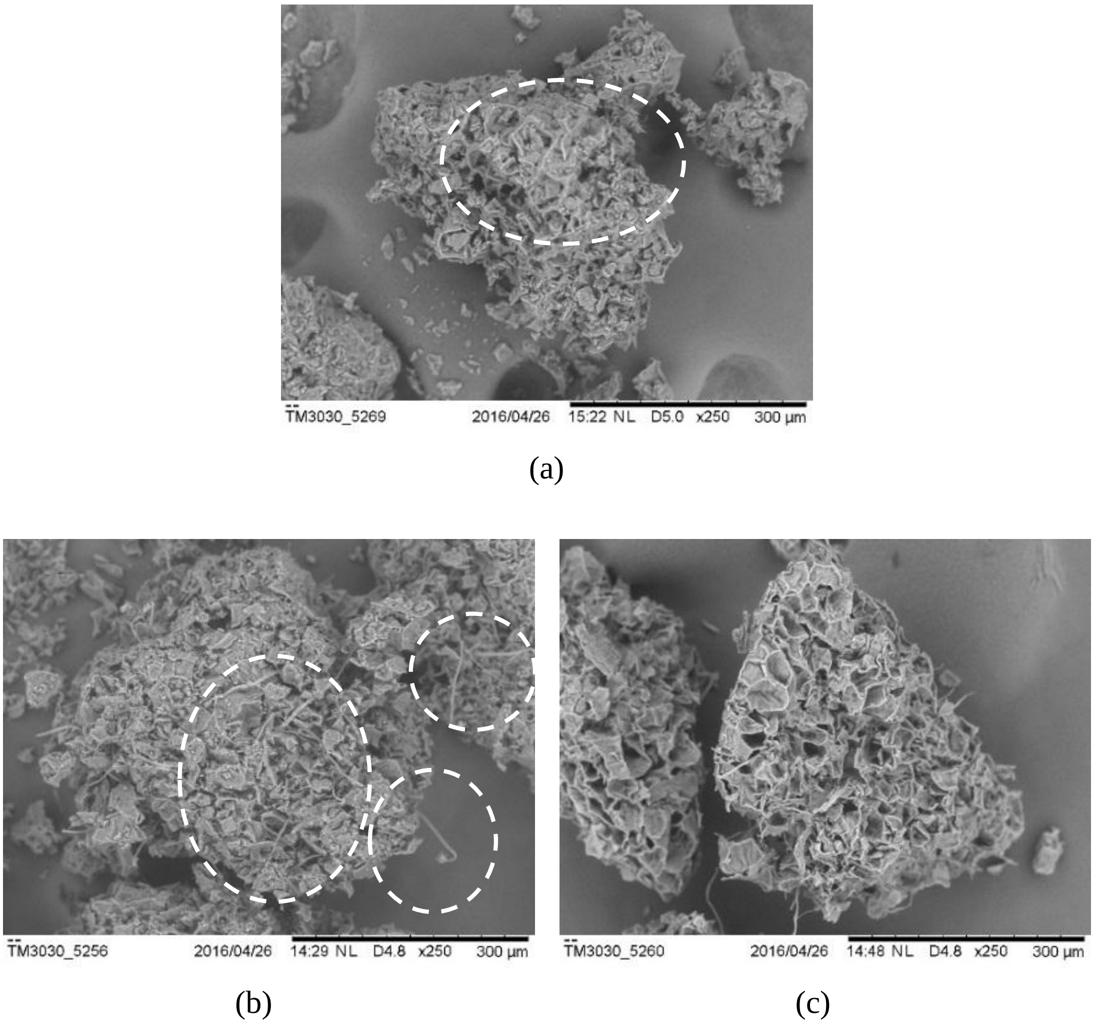

Figure 4.29: SEM images of GCW particle of a) untreated GCW, b) oil extracted GCW and c) oil extracted + NaOH GCW

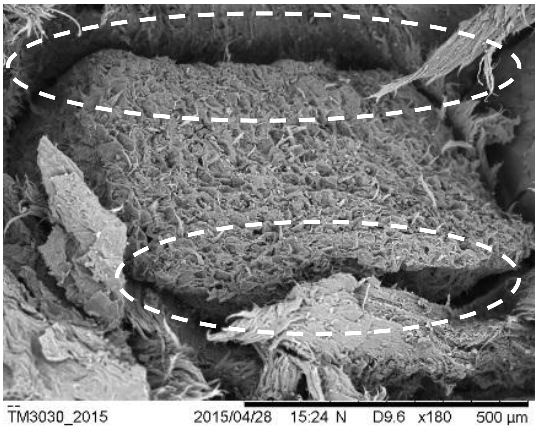

(a)

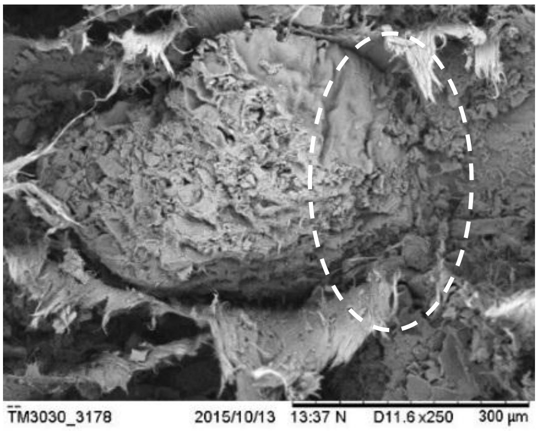

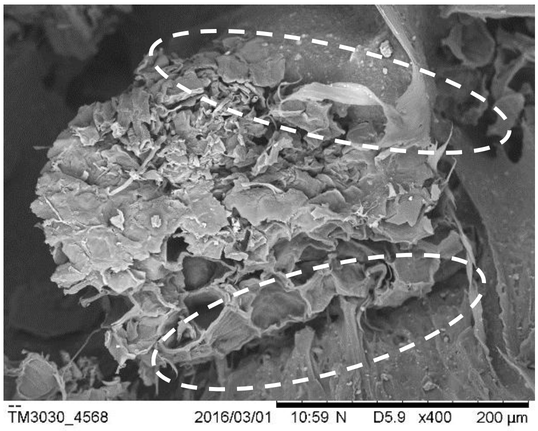

(b) (c)

Figure 4.30: SEM images of breaking surface for a) untreated b) oil extracted and c) oil extracted + NaOH GCW oxo-HDPE composites (10% volume fraction)

4.2.3 Thermogravimetric analysis (TGA)

Figure 4.31 and Figure 4.32 show the emblematic thermogravimetric analysis (TGA) thermogram and differential thermogravimetric analysis (DTG) thermogram of oxo-HDPE, untreated, oil extracted and oil extracted + NaOH GCW/oxo-HDPE composites at volume fraction of 10%. As shown in Table 4.9 and Table 4.10, the decomposition began at a lower temperature in the composites than in the neat oxo-HDPE due to the presence of GCW. However, the degradation temperature of oil extracted and oil extracted + NaOH treated

GCW/oxo-HDPE composites were higher than neat oxo-HDPE at 50% weight loss. Oil extractions and alkaline treatment done had improved their thermal stabilities. The thermal stability increased from composites type untreated, oil extracted and oil extracted + NaOH treated GCW/oxo-HDPE composites respectively. The percentage of charred residue decreased from composite type untreated to oil extracted and followed by oil extracted + NaOH treated GCW/oxo-HDPE composites. This has shown the effectiveness of the treatment as more unwanted impurities had been removed leading less charred residue. Weight loss before 100 ℃ was due to moisture absorption in the sample. The first step of degradation observed in the range of 250-400 ℃, remarked the degradation of hemicellulose, cellulose and a small amount of lignin (Castro et al., 2012). The second step of degradation which is also the main decomposition of GCW can be observed at approximately 440 ℃ contributed to the dramatic degradation of lignin as shown in DTG curve (Brebu & Vasile, 2010). The degradation temperature of the material was increased from hemicellulose < cellulose < lignin.

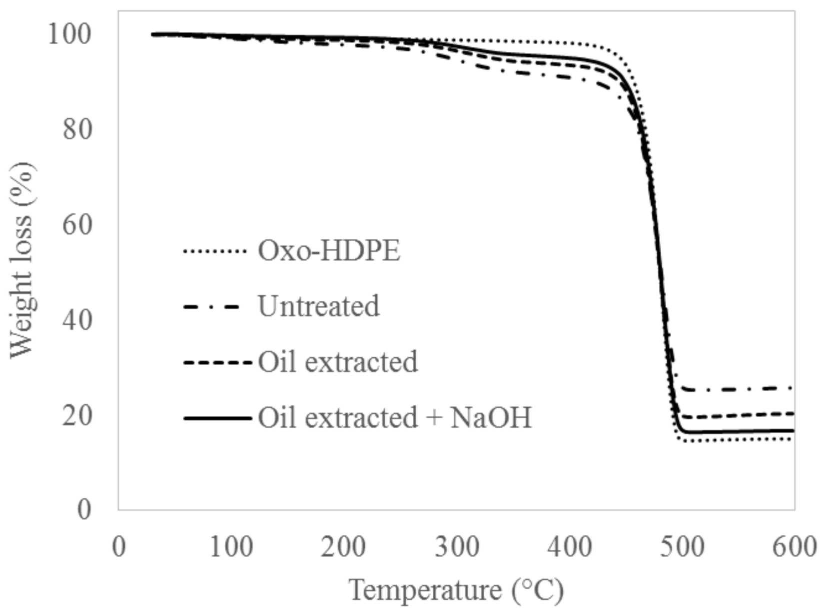

Figure 4.31: TGA thermogram of oxo-HDPE, untreated, oil extracted and oil extracted + NaOH treated GCW/oxo-HDPE composites (10% volume fraction)

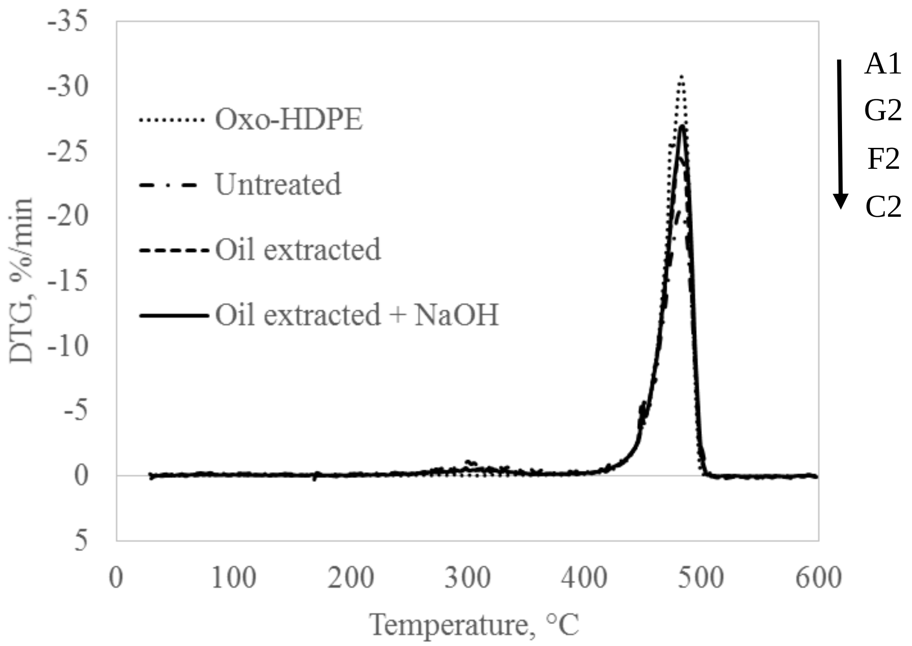

Figure 4.32: DTG thermogram of oxo-HDPE, untreated, oil extracted and oil extracted + NaOH treated GCW/oxo-HDPE composites (10% volume fraction)

Table 4.9: TGA data of untreated, oil extracted and oil extracted + NaOH treated GCW/oxo-HDPE composites

Composites	T_{onset} (℃)	T_{max} (℃)	T_{final} (℃)	Residue (%)
Oxo-HDPE	461.8	474.4	493.2	15.1
Untreated	460.4	481.9	492.4	25.8
Oil extracted	460.4	481.9	492.4	20.5
Oil extracted + NaOH	459.1	482.0	492.8	17.7

Table 4.10: Degradation temperature of untreated, oil extracted and oil extracted + NaOH treated GCW/oxo-HDPE composites

Composites	Temperature at 10% weight loss (℃)	Temperature at 15% weight loss (℃)	Temperature at 25% weight loss (℃)	Temperature at 50% weight loss (℃)
Oxo-HDPE	456.5	462.5	469.7	479.6
Untreated	422.1	450.4	464.6	478.0
Oil extracted	444.5	456.1	466.7	479.9
Oil extracted + NaOH	448.8	458.3	467.9	480.3

4.2.4 Differential scanning calorimetry (DSC)

The sample was first heated at a heating rate of 20 ℃ min^{-1}, from 50 ℃ to 180 ℃. When the sample reached 180 ℃, it was left for 2 minutes to cool to 50 ℃. The second cycle was to reheat the sample to 180 ℃ again. The curves exhibited endothermic peaks in Figure 4.33. These peaks attributed to the melting of crystalline domains of the oxo-HDPE matrix. Table 4.11 shows the important data of DSC measurement. The thermal characteristics such as crystalline melting temperature, T_m, melting enthalpy of composite according to the content of oxo-HDPE in the composite,ΔH_m and degree of crystallinity, X_c were identified. ΔH_m was calculated using area under the curve while X_c was determined based on the ratio ΔH_m to $\Delta H^0{}_m$, melting enthalpy of 100% crystalline HDPE (293 Jg^{-1}) (Perez et al., 2008). With regard to melt temperature the peaks were located in the same temperature range of 137 ℃-139 ℃. X_c increased with incorporation of GCW content in all composite formulations. In this case, GCW acted as nucleating agent and these produce crystals that increased the percentage of X_c of the composites. Nucleating effect had been detected as the result of low filler content. Other than that, the removal of lignin from the GCW after the treatment also contributed to the increase of X_c (Davachi et al., 2015).

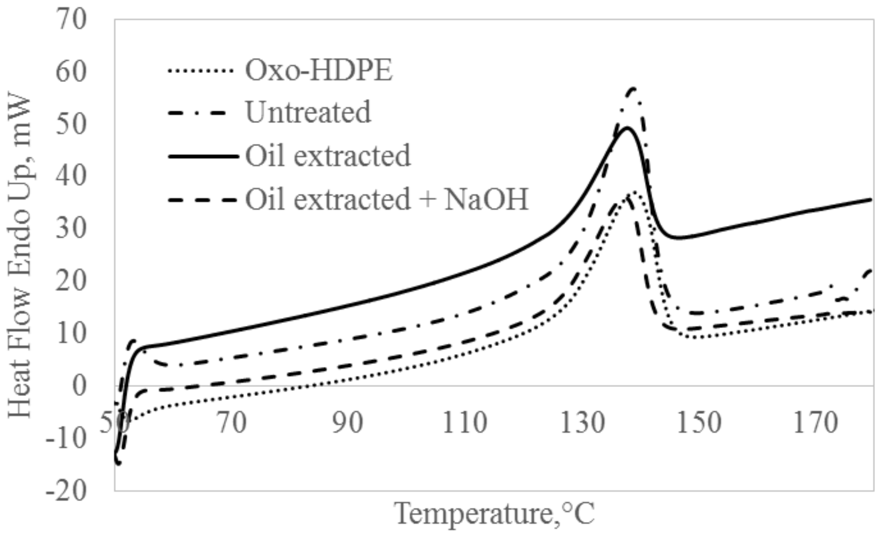

Figure 4.33: DSC curves of oxo-HDPE, untreated, oil extracted and oil extracted + NaOH treated GCW/oxo-HDPE composites (10% volume fraction)

Table 4.11: DSC data of oxo-HDPE, untreated, oil extracted and oil extracted + NaOH treated GCW/oxo-HDPE composites

Composites	T_m (℃)	ΔH_m (J/g)	X_c (%)
Oxo-HDPE	138.9	142.4	48.6
Untreated	138.9	133.3	51.1
Oil extracted	137.7	140.7	53.3
Oil extracted + NaOH	137.4	140.8	53.4

4.2.5 Water absorption

The water absorption proficiency of oxo-HDPE, untreated, oil extracted and oil extracted + NaOH treated GCW/oxo-HDPE composites are depicted in Figure 4.34. The water absorption results shown that the non-polar oxo-HDPE demonstrated the lowest water absorption. The percentage of water absorption increased from oxo-HDPE, oil extracted, oil extracted + NaOH treated and untreated GCW/oxo-HDPE composites at 0.05%, 3.22%, 3.80%, 5.22%, respectively. It was an improvement of 38% and 27% compared untreated GCW/oxo-HDPE composites. Treated GCW reinforced composites exhibited lower water absorption rate as it became more hydrophobic after the treatments. Other than that, a better interfacial adhesion of GCW/oxo-HDPE reduce the width of the interface area and diminish the water penetration to the inner parts of the material (Youssef et al., 2015).

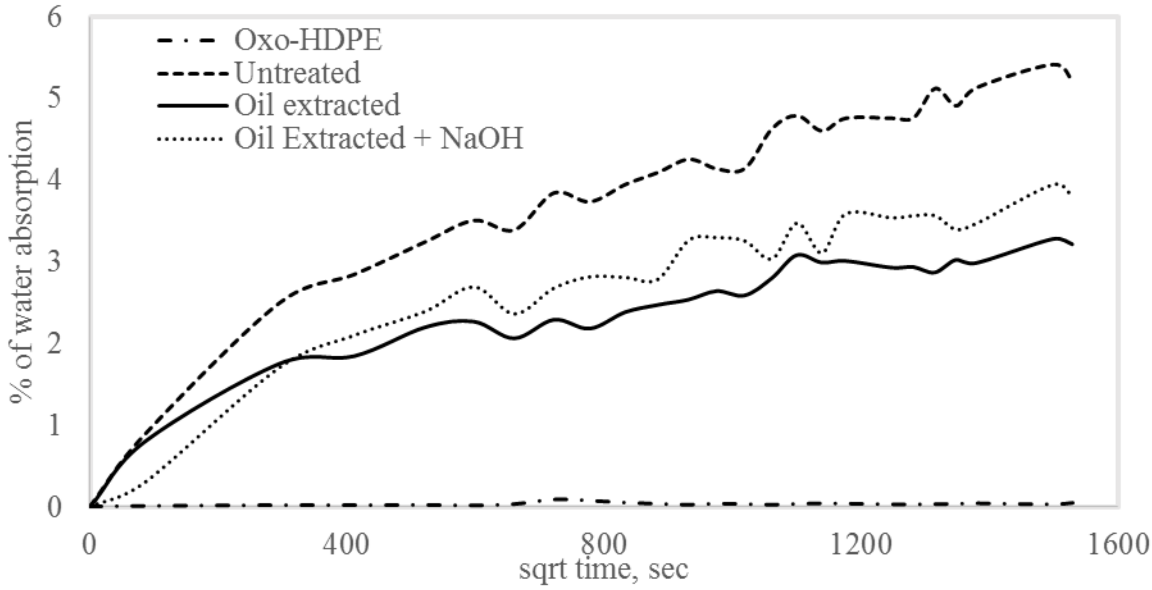

Figure 4.34: Percent mass gain due to the absorption of water oxo-HDPE, untreated, oil extracted and oil extracted + NaOH treated GCW/oxo-HDPE composites (10% volume fraction)

4.2.6 Tensile test

Figure 4.35 and Figure 4.36 show the stress strain curves of oil extracted and oil extracted + NaOH treated GCW/oxo-HDPE composites. The tensile properties were not as good as the neat oxo-HDPE after the inclusion of GCW. Reinforcement with uniform circular cross-section and aspect ratio more than its critical value will normally improve the strength of the composite. However, the irregular shape of GCW fillers with an aspect ratio of less than two cannot seem to well support the stress transferred from the polymer matrix (Fernandes et al., 2013). Thus, tensile strength is significantly reduced. Both oil extracted and oil extracted + NaOH treated GCW/oxo-HDPE composites showed improvement in tensile strength compared to untreated. The tensile strength increased from untreated < oil extracted + NaOH < oil extracted FCW/oxo-HDPE composites. (Figure 4.37). The tensile strength oil extracted GCW/oxo-HDPE composites increased and reached optimum during 10% volume fraction, 16.47 MPa, an increment of 27% compared to untreated then declined. A large amount of lipids is being removed for oil extracted GCW has discovered a coarser surface with cellulose microfibrils revealed on its surface supported by FTIR and SEM (Figure 4.28 & Figure 4.29b). The exposed cellulose microfibrils improved the effectiveness of contact surface area and thus giving better impregnation of GCW with the oxo-HDPE matrix. On the other hand, increasing volume fraction led to decreasing tensile strength for oil extracted + NaOH treated./oxo-HDPE composites (Figure 4.37). During 5% particle loading, its tensile strength was slightly better than the untreated, 15.49 MPa, with an improvement of 8%. This may due to less exposure of cellulose microfibrils after the treatment. In addition, oil extracted + NaOH GCW itself may become porous and weaker after alkaline treatment and therefore led to poor properties.

As observed in Figure 4.38, tensile modulus of oil extracted GCW/oxo-HDPE composites showed a slight improvement compared to neat oxo-HDPE during 5% and 10% particle volume fraction, which were 1263 MPa (+14%) and 1122 MPa (+1.4%) respectively. The chemical modification proved to provide a better homogeneous dispersion of GCW. The tensile properties showed a proportional increment with volume fraction until 10%. This was owing to the enhancement of load transfer between matrix and GCW interface. Nevertheless, composites declined in tensile properties beyond optimum values (>10%) as a result of agglomeration of GCW. Agglomerations create flaws and voids between GCW and matrix thus diminishing tensile properties (Yang et al., 2004). Other than that, aspect ratio plays a very important role. GCW had a very low aspect ratio of less than two resulted in insufficient stress transferred. Therefore, displayed low tensile modulus. In contrast, tensile modulus obtained for oil extracted + NaOH treated GCW/oxo-HDPE composites were lower than oxo-HDPE as oil extract + NaOH GCW had become weak after the treatment.

Figure 4.39 displays the specific tensile strength, known as strength to weight ratio. All of the treated GCW showed lower specific tensile strength. 5% and 10% volume fraction of oil extracted GCW/oxo-HDPE composites showed a slight decreased to 0.0173 MPa.m^3/kg (-1.1%), 0.0167 MPa.m^3/kg (-4.6%). Figure 4.40 illustrates specific tensile modulus, known as stiffness to weight ratio. The specific tensile modulus of neat oxo-HDPE was 1.0335 MPa.m^3/kg. Specific tensile modulus had improved 32% at 15% volume fraction for oil extracted GCW/oxo-HDPE composites. The inclusion of GCW contributed to a lighter weight composite. The specific tensile properties improved slightly as the composites had a lower density. Conversely, the specific tensile properties of oil extracted + NaOH treated GCW/oxo-HDPE composites did not improve due to the poor condition of oil extracted + NaOH treated GCW. Another researcher reported the same trend of results using oil extraction oil palm empty fruit bunch composite (Rozman et al., 2001). Tensile, flexural and toughness properties improved significantly than those without extraction. Summary of tensile properties of oxo-HDPE, untreated, oil extracted and oil extracted + NaOH treated GCW/oxo-HDPE composites are shown in Table 4.12.

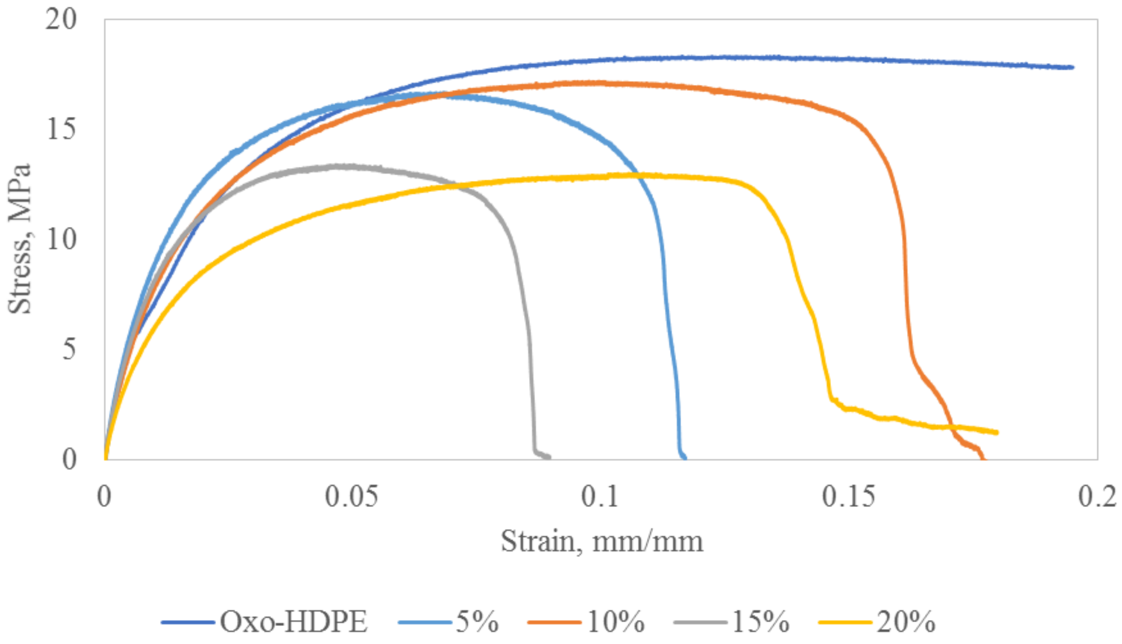

Figure 4.35: Stress-strain curves of oil extracted GCW/oxo-HDPE composites at crosshead displacement rates of 1 mm/min by volume fraction

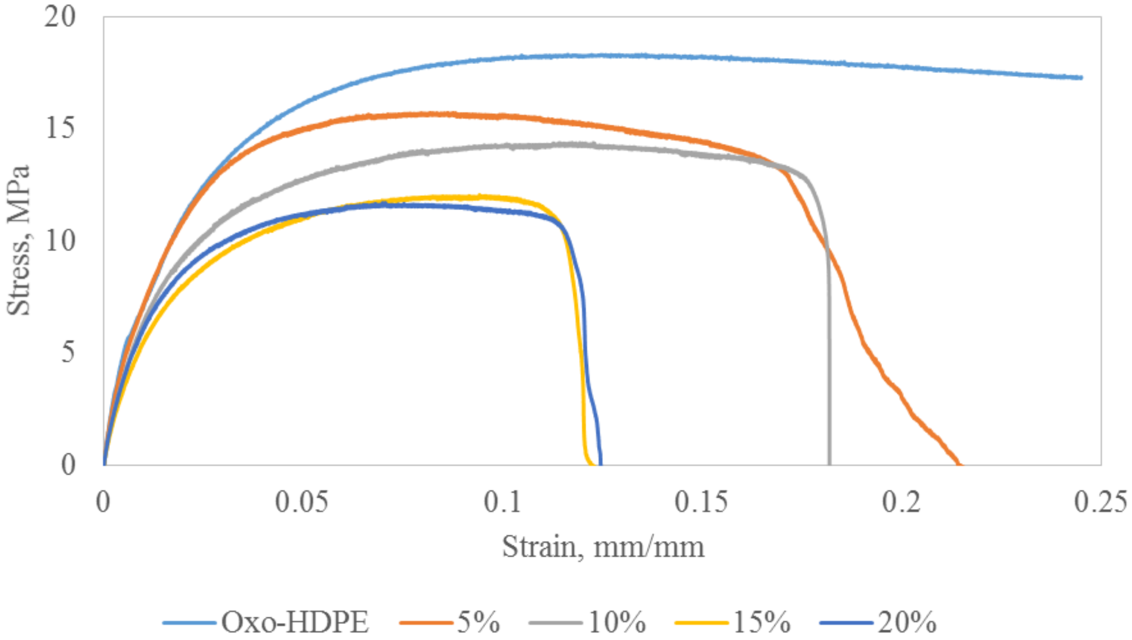

Figure 4.36: Stress-strain curves of oil extracted + NaOH treated GCW/oxo-HDPE composites at crosshead displacement rates of 1 mm/min by volume fraction

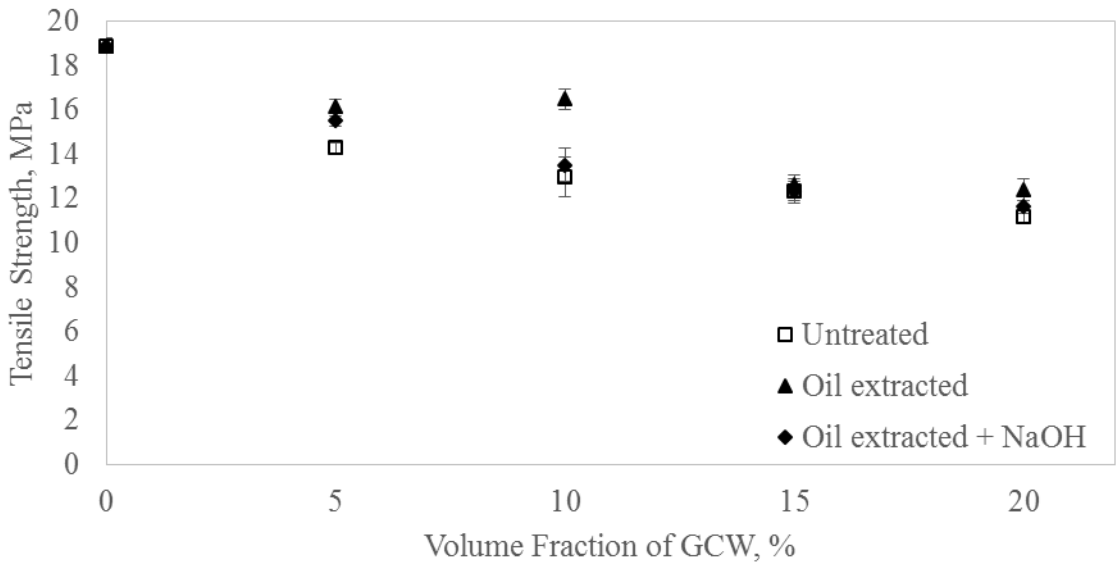

Figure 4.37: Tensile strength of untreated, oil extracted and oil extracted + NaOH treated GCW/oxo-HDPE composites at crosshead displacement rates of 1 mm/min by volume fraction

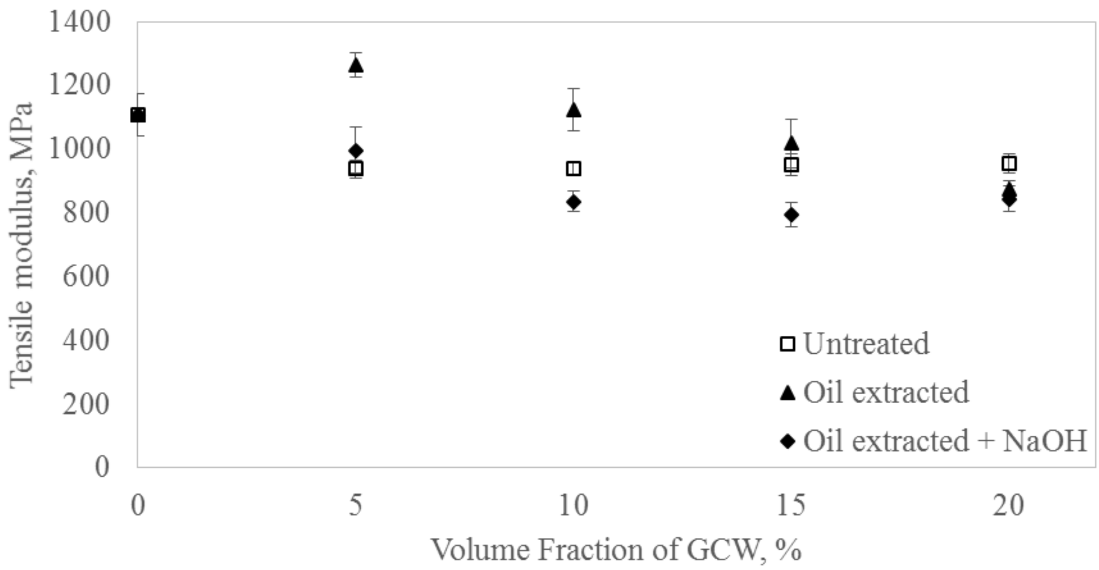

Figure 4.38: Tensile modulus of untreated, oil extracted and oil extracted + NaOH treated GCW/oxo-HDPE composites at crosshead displacement rates of 1 mm/min by volume fraction

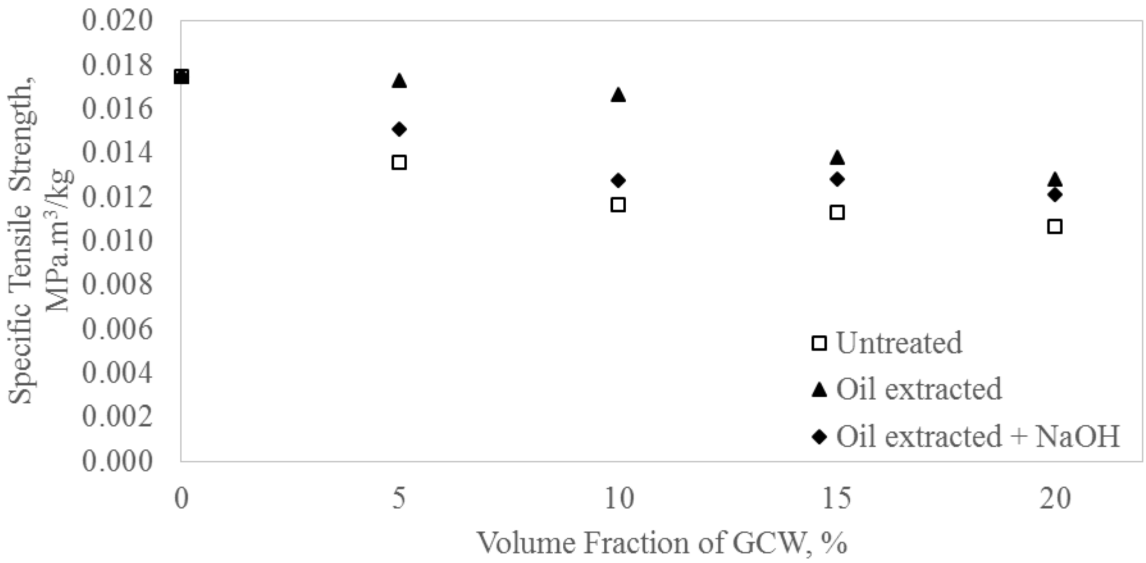

Figure 4.39: Specific tensile strength of untreated, oil extracted and oil extracted + NaOH treated GCW/oxo-HDPE composites at crosshead displacement rates of 1 mm/min by volume fraction

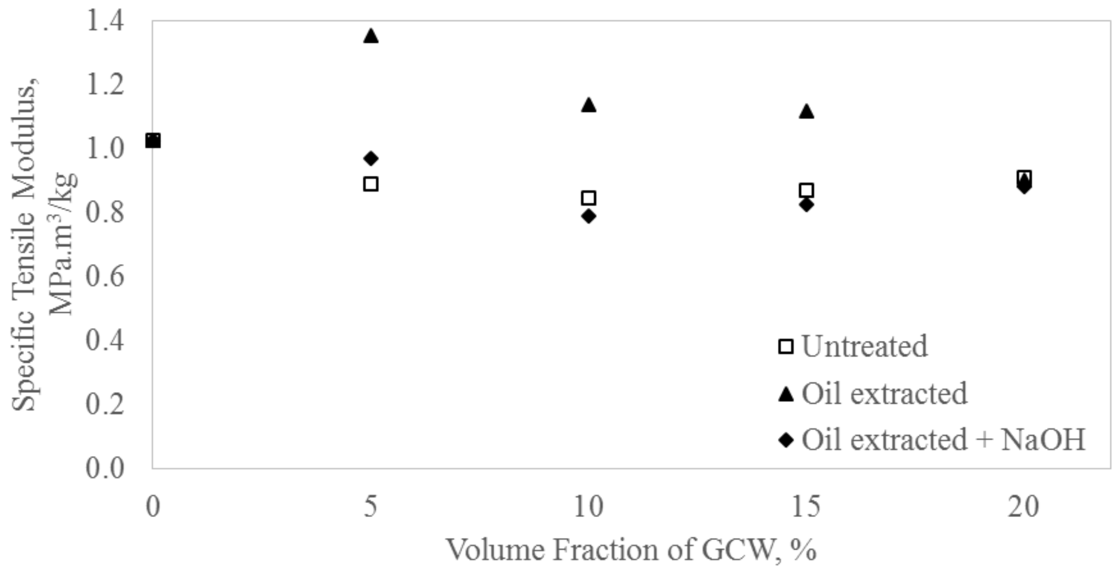

Figure 4.40: Specific tensile modulus of untreated, oil extracted and oil extracted + NaOH treated GCW/oxo-HDPE composites at crosshead displacement rates of 1 mm/min by volume fraction

Table 4.12: Tensile properties of oxo-HDPE, untreated, oil extracted and oil extracted + NaOH treated GCW/oxo-HDPE composites

Composite	Filler Vol. (%)	Average Tensile Strength (MPa)	Average Tensile Modulus (MPa)	Specific Tensile Strength (MPa.m^3/kg)	Specific Tensile Modulus (MPa.m^3/kg)
Oxo-HDPE	0	18.89 (0.35)	1107.18 (67.57)	0.018	1.026
Untreated	5	14.28 (0.22)	936.93 (28.58)	0.014	0.891
	10	12.95 (0.89)	938.40 (20.86)	0.012	0.847
	15	12.36 (0.43)	950.45 (33.38)	0.011	0.871
	20	11.19 (0.26)	955.81 (29.86)	0.011	0.910
Oil extracted	5	16.15 (0.30)	1263.34 (37.21)	0.017	1.353
	10	16.47 (0.45)	1121.62 (66.46)	0.017	1.136
	15	12.60 (0.47)	1018.19 (75.85)	0.014	1.117
	20	12.39 (0.51)	873.63 (27.21)	0.013	0.903
Oil extracted + NaOH	5	15.48 (0.23)	995.43 (72.45)	0.015	0.971
	10	13.51 (0.75)	835.31 (31.48)	0.013	0.790
	15	12.35 (0.54)	795.22 (37.96)	0.013	0.826
	20	11.61 (0.26)	843.24 (40.28)	0.012	0.880

4.2.7 Low velocity impact test

The dart drop weight impact test had been performed to study the impact response of untreated, oil extracted and oil extracted + NaOH treated GCW/oxo-HDPE composites. The results are shown in Figure 4.41, Figure 4.42, Figure 4.43 and Figure 4.44. The stiffness of the composites was represented with ascending curves in Figure 4.41. The stiffness of the composites increased from untreated, oil extracted and oil extracted + NaOH treated GCW/oxo-HDPE composites, respectively. The maximum impact force corresponds to the onset of material damage. The maximum load can be sustained by the composites before fracture increasing from untreated, oil extracted + NaOH treated and oil extracted GCW/oxo-HDPE composites, repectively with an improvement of 14 and 28% compared to untreated.

The energy to maximum load yielded similar trend of results with an improvement of 11% and 51% compared to untreated. The decreasing curve shows the materials' properties. The ductility of the composites experienced an alike trend of results to energy to maximum load. Total energy absorbed recorded similar pattern of results too with an improvement of 7% and 16%, respectively compared to untreated. Hydrophilic untreated GCW and hydrophobic oxo-HDPE were having poor interaction thus yielded lower impact resistance. Both treatments conducted had improved the impact resistance. After oil extraction, the fillers were dispersed more homogeneously. Besides that, the adhesion between filler and matrix was improved too. This contributed to a more uniform distribution of stress transfer thus more load and energy was required to perforate the samples. The treatments between matrix and reinforcement had significantly improved the toughness of the composite with showing the ability to absorb more energy and plastically deform before fracture. Oil extracted + NaOH treated GCW/oxo-HDPE composites yielded lower results than oil extracted. The reason was supported by the result discussed earlier where oil extracted + NaOH treated GCW itself had become weaker. Overall, the impact resistance of the composites enhanced from untreated, oil extracted + NaOH treated and oil extracted GCW/oxo-HDPE composites. Figure 4.45 displays the post impact fracture behaviour of the perforated composites. The failure implicates plastic deformation of the oxo-HDPE and debonding of the GCW filler within the composites. With the same volume fraction, it can be seen that treated GCW composites were having better plastic deformation than untreated GCW composite (Figure 4.45). The bottom face of the samples was having a bulging effect. The delamination only occurred at the perforated area. Similar impact result was obtained by another researcher (Anbukarasi & Kalaiselvam, 2015).

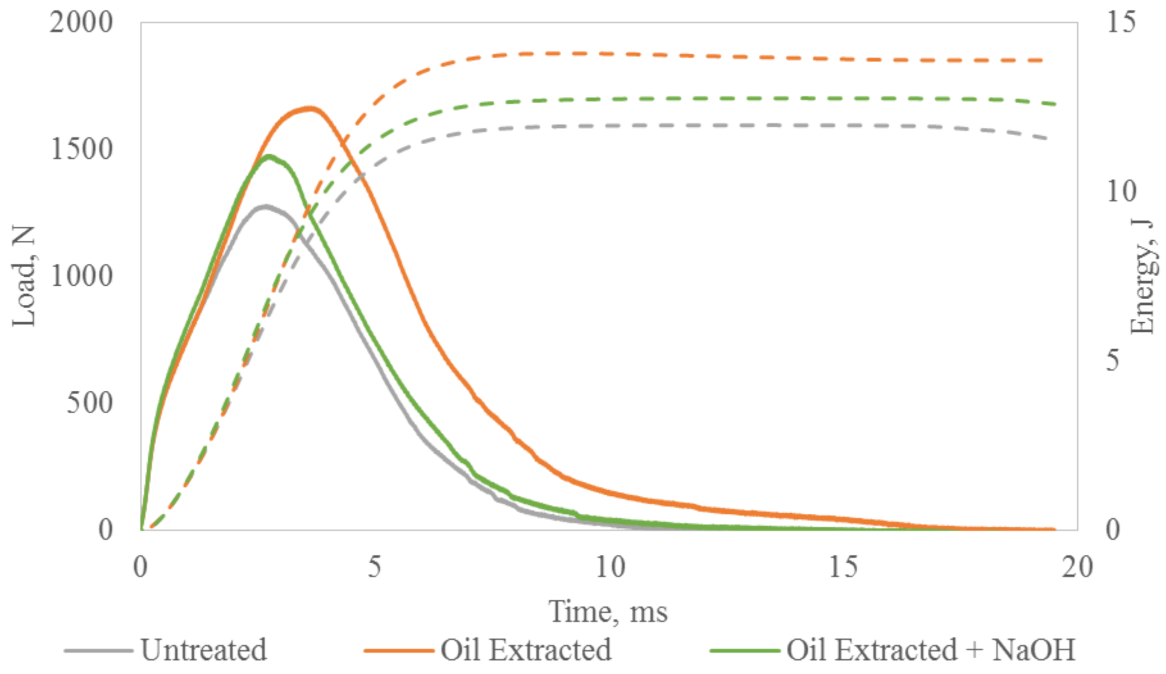

Figure 4.41: Load-energy-time graph of impact test for untreated, oil extracted and oil extracted + NaOH GCW/oxo-HDPE composites (10% volume fraction)

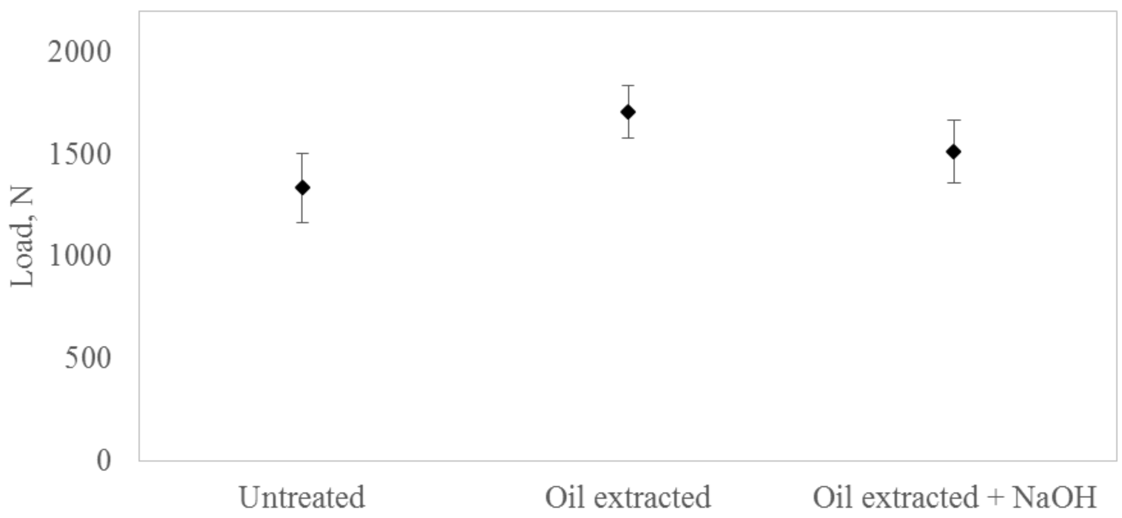

Figure 4.42: Comparison of load for untreated, oil extracted and oil extracted + NaOH GCW/oxo-HDPE composites (10% volume fraction)

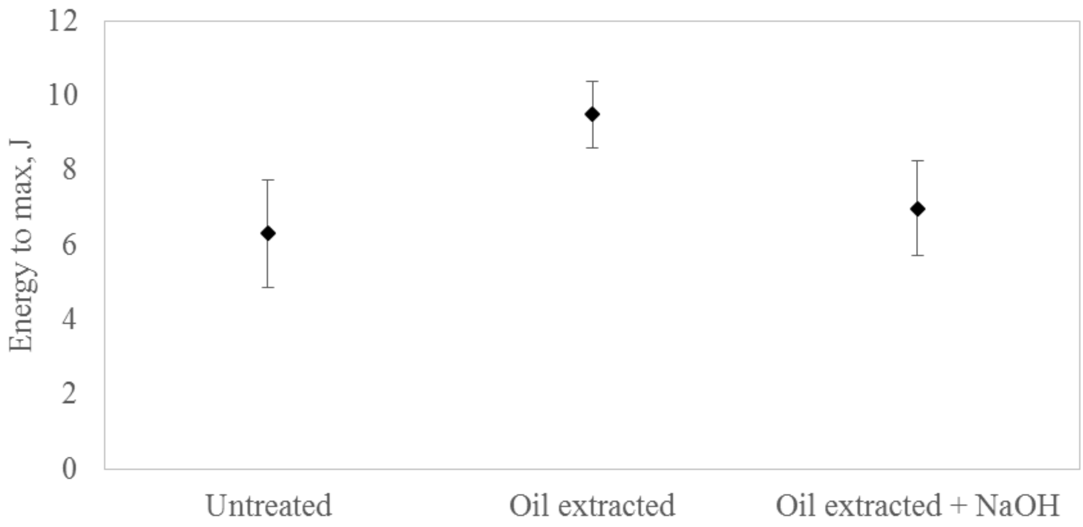

Figure 4.43: Comparison of energy to maximum load for untreated, oil extracted and oil extracted + NaOH GCW/oxo-HDPE composites (10% volume fraction)

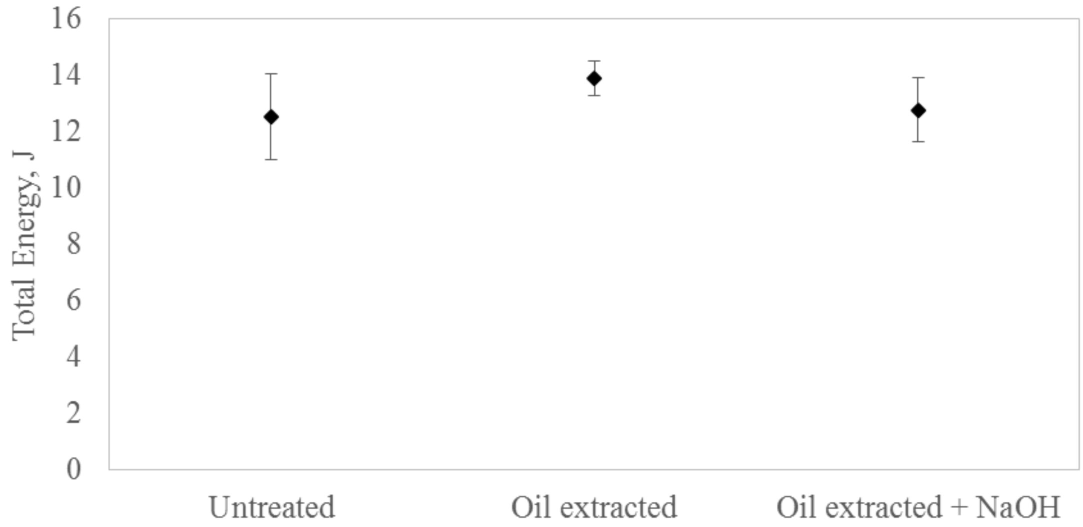

Figure 4.44: Comparison of total energy for for untreated, oil extracted and oil extracted + NaOH GCW/oxo-HDPE composites (10% volume fraction)

Table 4.13: Impact properties of untreated, oil extracted and oil extracted + NaOH GCW/oxo-HDPE composites (10% volume fraction)

Composite	**Filler Vol. (%)**	**Peak Load (N)**	**Energy to maximum load (J)**	**Total energy (J)**
Untreated	10	1334.74 (167.70)	6.30 (1.45)	12.54 (1.52)
Oil extraxted	10	1707.57 (129.90)	9.50 (0.89)	13.89 (0.59)
Oil extracted + NaOH	10	1515.30 (153.12)	6.98 (1.26)	12.77 (1.13)

(a)

(b)

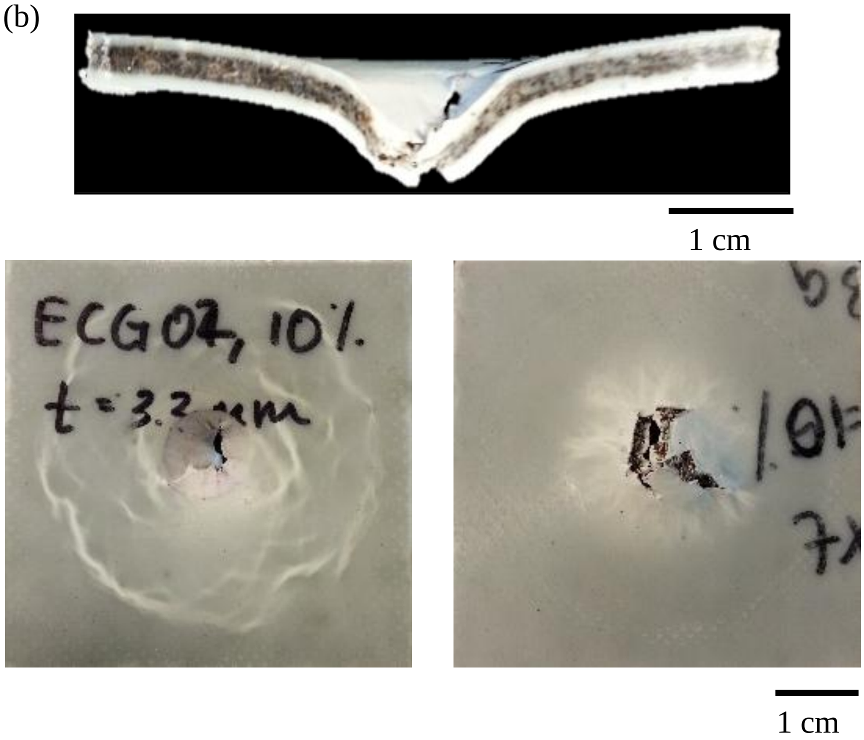

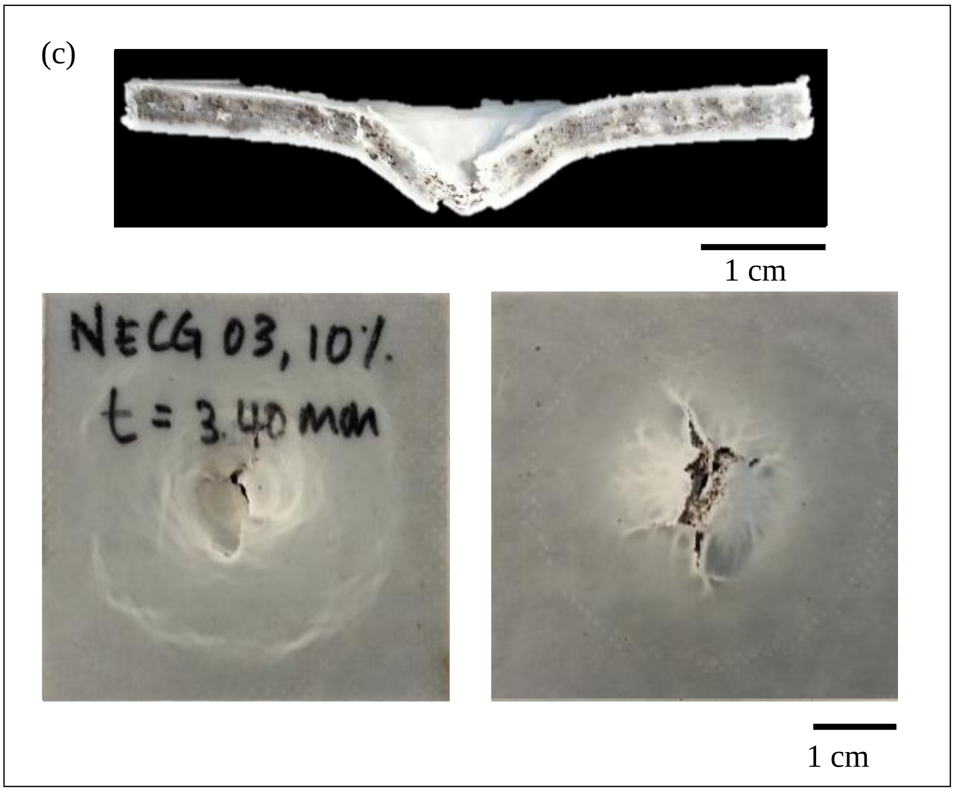

Figure 4.45: Fracture behaviour of perforated a) untreated, b) oil extracted and c) Oil extracted + NaOH treated GCW/oxo-HDPE composites

4.2 Overall comparison for all types of composites

Based on the results of different types of treatments, the overall comparison of all types of treatments was studied and discussed.

4.3.1 Tensile test

Figure 4.46 and Figure 4.47 show a comparison of overall tensile strength and modulus of all the untreated and treated GCW/oxo-HDPE composites. All of the treated GCW/oxo-HDPE composites showed improvement in tensile strength compared to untreated GCW/oxo-HDPE composites. The tensile strength of the composites was optimum for NaOH treated followed by oil extracted and oil extracted + NaOH treated GCW/oxo-HDPE composites, respectively.

Alternatively, optimum tensile modulus obtained during oil extracted GCW/oxo-HDPE composites followed by NaOH treated and oil extracted + NaOH treated GCW/oxo-HDPE composites, respectively. In comparison to filler volume fraction, tensile strength increased and reached a maximum at 10% while tensile modulus reached a maximum at 5% and 10%. Further increment led to the declination of tensile properties. In this case, 5% and 10% are the optimum filler volume fraction for this type of particle reinforcement as the addition of 10% or more may lead to a decrease in tensile properties.

Figure 4.48 and Figure 4.49 depict the comparison of overall specific tensile strength and modulus of the composites studied. The results of the specific tensile properties were having the same trend as tensile properties. Oil extracted + NaOH treated GCW/oxo-HDPE composites had the highest specific tensile strength and modulus. The specific tensile properties experienced slight improvement as the composites were lighter in weight. Table 4.14 shows the summary of the tensile properties all the composites.

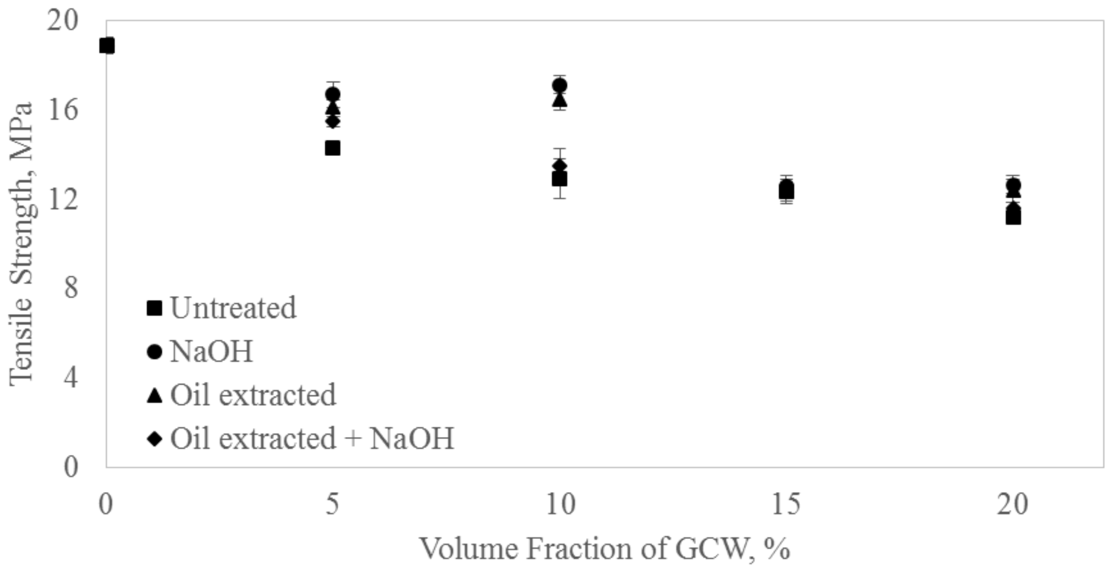

Figure 4.46: Comparison of tensile strength for all the composites

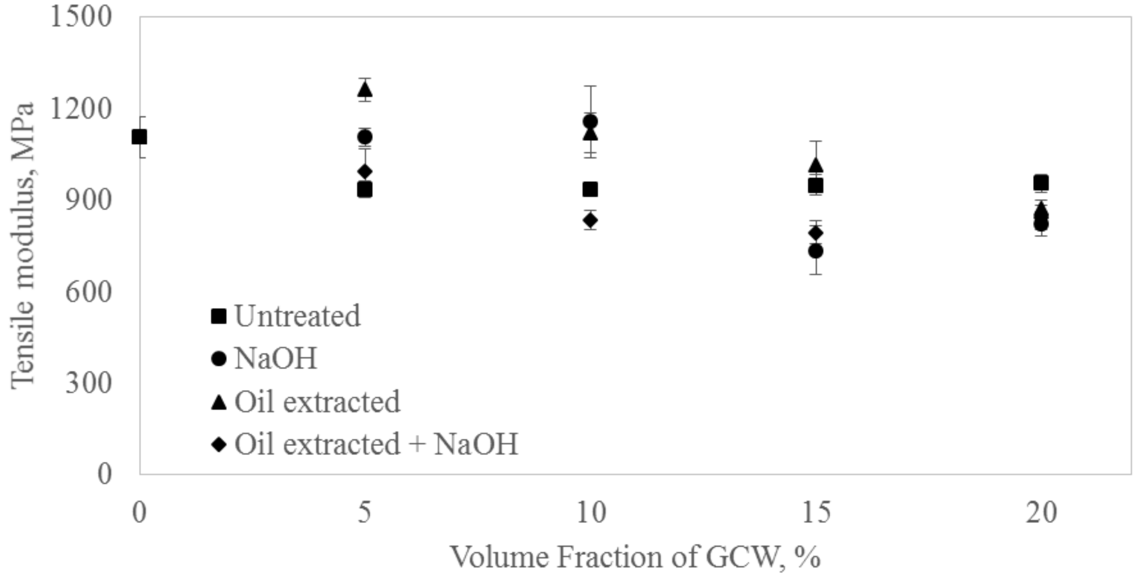

Figure 4.47: Comparison of tensile modulus for all the composites

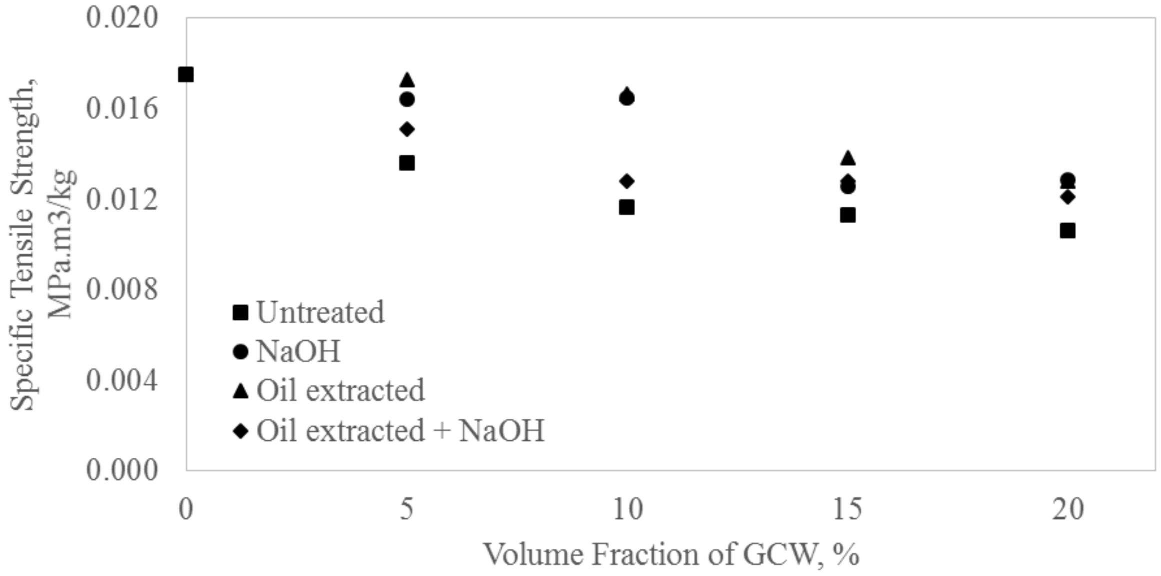

Figure 4.48: Comparison of specific tensile strength for all the composites

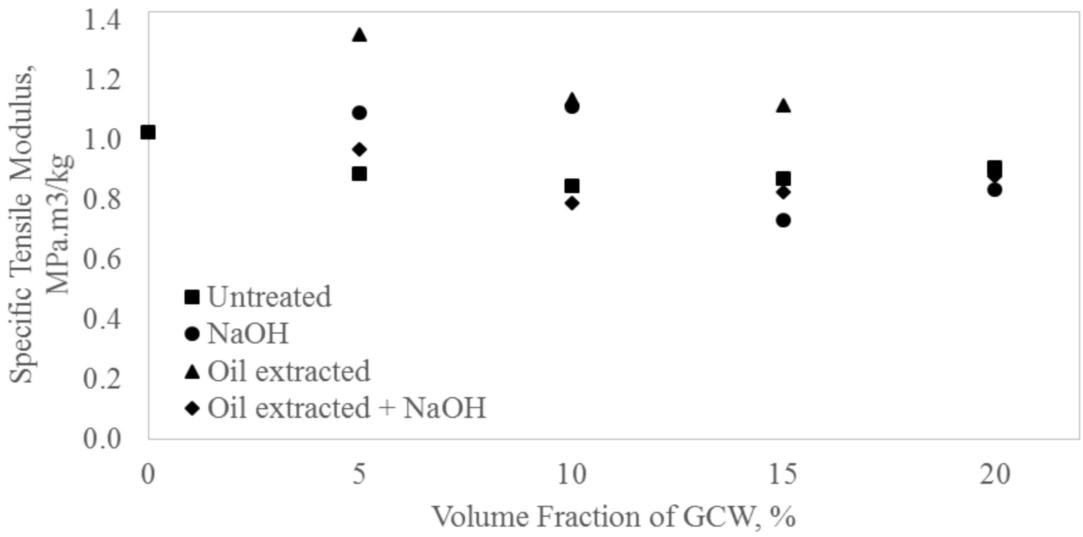

Figure 4.49: Comparison of specific tensile modulus for all the composites

Table 4.14: Summary of tensile data for all the composites

Composite	Filler Vol. (%)	Average Tensile Strength (MPa)	Average Tensile Modulus (MPa)	Specific Tensile Strength ($MPa.m^3/kg$)	Specific Tensile Modulus ($MPa.m^3/kg$)
Untreated	5	14.28 (0.22)	936.93 (28.58)	0.014	0.891
	10	12.95 (0.89)	938.40 (20.86)	0.012	0.847
	15	12.36 (0.43)	950.45 (33.38)	0.011	0.871
	20	11.19 (0.26)	955.81 (29.86)	0.011	0.910
NaOH	5	16.69 (0.56)	1107.37 (28.10)	0.017	1.092
	10	17.14 (0.39)	1157.73 (116.23)	0.017	1.115
	15	12.60 (0.26)	735.66 (79.61)	0.013	0.734
	20	12.66 (0.38)	822.31 (40.37)	0.013	0.837
Oil extracted	5	16.15 (0.30)	1263.34 (37.21)	0.017	1.353
	10	16.47 (0.45)	1121.62 (66.46)	0.017	1.136
	15	12.60 (0.47)	1018.19 (75.85)	0.014	1.117
	20	12.39 (0.51)	873.63 (27.21)	0.013	0.903
Oil extracted + NaOH	5	15.48 (0.23)	995.43 (72.45)	0.015	0.971
	10	13.51 (0.75)	835.31 (31.48)	0.013	0.790
	15	12.35 (0.54)	795.22 (37.96)	0.013	0.826
	20	11.61 (0.26)	843.24 (40.28)	0.012	0.880

4.3.2 Low velocity impact test

Figure 4.50 shows load, energy and time graph of impact test for untreated, NaOH treated, oil extracted and Oil extracted + NaOH treated GCW/oxo-HDPE composites at 10% volume fraction. Figure 4.51, Figure 4.52 and Figure 4.53 show load, energy to maximum and total energy absorbed of all the composites tested. In comparison to untreated GCW/oxo-HDPE composites, all of the treatments yielded better impact properties. oil extracted GCW/oxo-HDPE composites appeared to be the best sample. The 10% volume fraction composites were impact-tested to study the effect of different types of treatments.

The maximum load can be sustained by the composites before fracture increasing from composites type untreated < oil extracted + NaOH < NaOH < Oil extracted GCW/oxo-HDPE composites with an improvement of 14%, 21% and 28%, respectively. The results of the energy to maximum load was having the same trend showing 11%, 28% and 51% enhancement, respectively. Total energy can be absorbed during the complete test also increased from composite types untreated < oil extracted + NaOH < NaOH < Oil extracted GCW/oxo-HDPE composites with an improvement of 7%, 13% and 16%, respectively.

All of the treatments conducted had enhanced the impact resistance. The toughness of the composite was better after the treatment. Overall, the impact resistance improved from composites type untreated < oil extracted + NaOH < NaOH < Oil extracted GCW/oxo-HDPE composites. The data of impact properties of all the composite are summarised in Table 4.15.

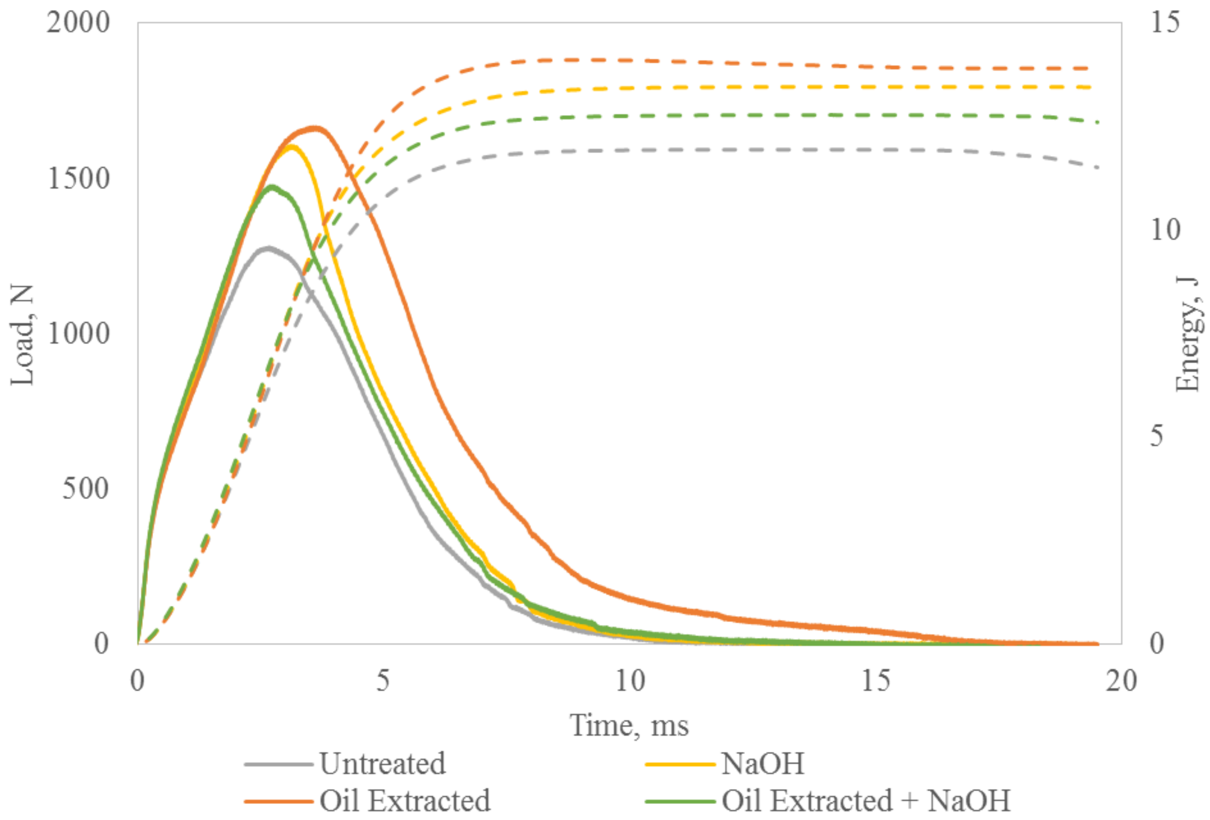

Figure 4.50: The variation of load-energy-time graph of impact for untreated, NaOH treated, oil extracted and Oil extracted + NaOH treated GCW/oxo-HDPE composites (10% volume fraction)

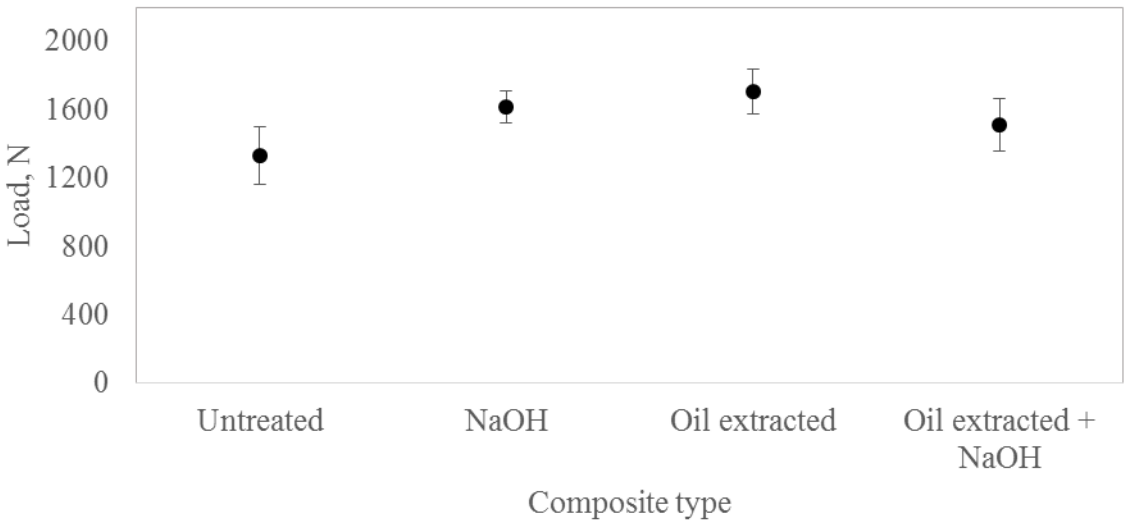

Figure 4.51: Comparison of load for untreated, NaOH treated, oil extracted and Oil extracted + NaOH treated GCW/oxo-HDPE composites (10% volume fraction)

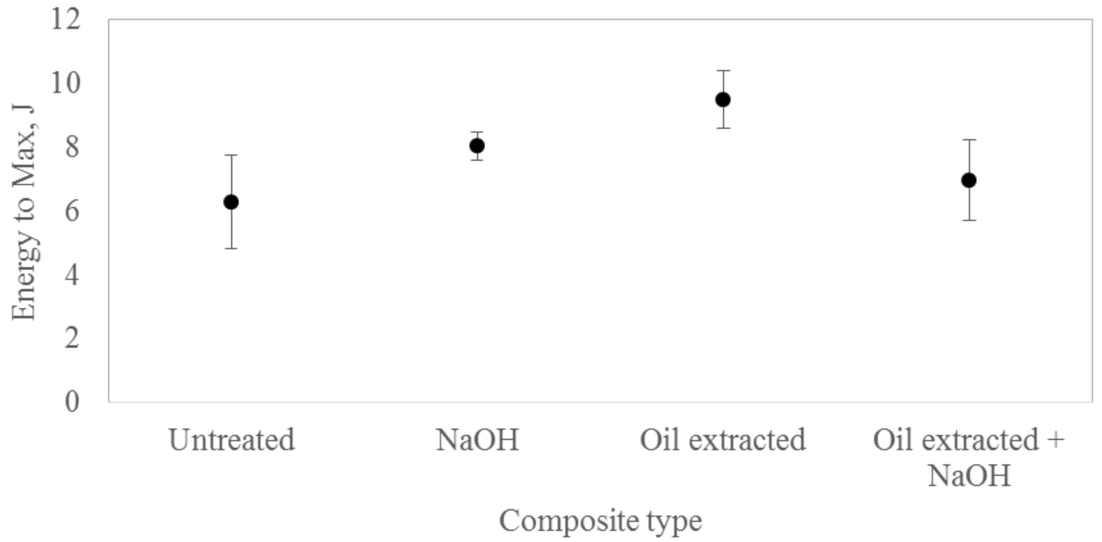

Figure 4.52: Comparison of energy to maximum for untreated, NaOH treated, oil extracted and Oil extracted + NaOH treated GCW/oxo-HDPE composites (10% volume fraction)

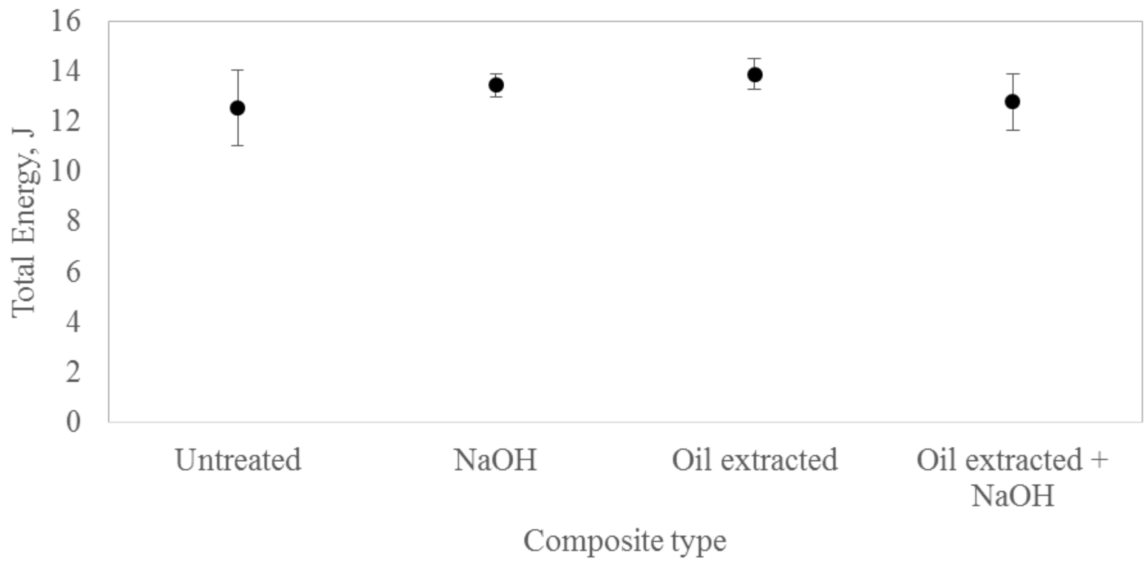

Figure 4.53: Comparison of total energy absorbed for untreated, NaOH treated, oil extracted and Oil extracted + NaOH treated GCW/oxo-HDPE composites (10% volume fraction)

Table 4.15: Summary of impact properties for all the composites

Composite	Filler Vol. (%)	Peak Load (N)	Energy to maximum load (J)	Total energy (J)
Untreated	10	1334.74 (167.70)	6.30 (1.45)	12.54 (1.52)
NaOH	10	1614.73 (92.52)	8.04 (0.45)	13.44 (0.46)
Oil extracted	10	1707.57 (129.90)	9.50 (0.89)	13.89 (0.59)
Oil extracted + NaOH	10	1515.30 (153.12)	6.98 (1.26)	12.77 (1.13)

Table 4.16 compares the properties from previous to current works done on natural composites. The properties of GCW/oxo-HDPE composites fabricated with compression moulding are comparable to lignocellulosic natural fibres reinforced thermoplastics fabricated with extrusion and injection moulding. Therefore, GCW exhibits good potentials to be used as reinforcement in producing green and eco-friendly composite. Further study can be conducted to design prototype GCW composites in engineering parts.

Table 4.16: Comparison of properties of current and previous work by other researchers

Reinforcement	Matrix	Fabrication method	Tensile (MPa)		Impact (J)	References
			Strength	Modulus		
GCW	**Oxo-HDPE**	**Manual sieving + compression moulding**	**17.0**	**1263.0**	**13.9**	**Current work**
Oil palm empty fruit bunch	PP	Extruder + compression moulding	13.0	750.0	-	(Rozman et al., 2001)
Rice husk	Post consumer PE	Extrusion + injection moulding	19.7	530.0	0.2-0.4	Fávaro et al., 2010
Wood flour	LDPE	Extrusion + injection moulding	14.4	767.0	0.2-0.4	Altun et al., 2013
Oil palm	HDPE	Extruder + compression moulding	15.0	1030.0	5.0 kJ/m^2	(Kakou et al., 2014)
Corn husk	LDPE	Extruder + compression moulding	24.7	456.0	-	(Youssef et al., 2015)
Palm leaf	HDPE	Mixer (Hakke) + compression moulding	24.0	150.0	20.0 kJ/m^2	(Khalaf, 2015)

CHAPTER 5

CONCLUSIONS AND RECOMMENDATIONS

5.1 Conclusions

Characterisation of oxo-biodegradable high density polyethylene (oxo-HDPE) and ground coffee waste (GCW) composites had been successfully investigated. These composites were divided into 7 categories. The blends were evaluated at different sizes (64-425 µm, 426-850 µm, 851-1180 µm and mixed size), volume fractions (5%, 10%, 15% and 20%) and surface treatments (untreated, mercerisation, oil extraction and a combination of oil extraction and mercerisation). The composites were fabricated with GCW reinforced oxo-HDPE films followed by a simple hot compression moulding. The fabricated composites were subjected to FTIR, SEM, TGA, DSC, water absorption, tensile and impact test.

FTIR spectrum indicated the eradication of lipids, hemicellulose, lignin and impurities of GCW particles after the treatments. SEM revealed the surface of the treated GCW were coarser and exposed microfibrils as impurities were removed. As a result, the composites exhibited better GCW/matrix interface. TGA was done to improve the thermal stability of the treated GCW composites (oil extracted + NaOH > Oil extracted > NaOH > untreated GCW/oxo-HDPE composites). DSC showed the increment in degree of crystallinity (oil extracted + NaOH > Oil extracted > NaOH > untreated GCW/oxo-HDPE composites). Water absorption demonstrated the treatments enhanced the hydrophobicity of the GCW particles. Water resistance improved from untreated < oil extracted + NaOH < Oil extracted < NaOH GCW/oxo-HDPE composites.

For mechanical properties, particle size of 64-850 μm showed the best tensile properties among the different particle size used. Based on the treatments conducted, NaOH treated GCW/oxo-HDPE composites exhibited the highest tensile strength (composites type NaOH > Oil extracted > Oil extracted + NaOH > untreated GCW/oxo-HDPE composites) while composite type F exhibited the highest tensile modulus (Oil extracted > NaOH > Oil extracted + NaOH > untreated GCW/oxo-HDPE composites). Specific tensile properties were further improved as the composites were lighter in weight. The study revealed that volume fraction of 5% and 10% exhibited the most impressive mechanical properties. For impact properties, the stiffness improved after the treatments. The load can be sustained, energy to maximum load, total energy absorbed by the composites and impact resistance during the complete impact test showed the best result for oil extracted GCW/oxo-HDPE composites. This is followed by composite type NaOH, Oil extracted + NaOH and untreated GCW/oxo-HDPE composites. The mechanical properties of the composites increased from composites type untreated < oil extracted + NaOH < NaOH < oil extracted GCW/oxo-HDPE composites.

Based on the study conducted, oil extracted GCW/oxo-HDPE composites exhibited the best result. The extraction had removed a large amount of lipids and other impurities from the surface of GCW that revealed cellulose microfibrils for better compatibility, adhesion and impregnation of GCW and matrix. Other than that, TGA and DSC done had improved its thermal stability and degree of crystallinity. In addition, the removal of the oil layer on the surface of GCW has increased the water resistance of the fabricated composited. Furthermore, oil extracted composite exhibited the highest mechanical properties of the composites studied. The increased in surface roughness and exposed microfibrils had led to a better adhesion and compatibility that provide a better mechanical and impact properties. Oil extracted GCW are dispersed more homogeneous during low filler (up to 10%). Thus, provide a better distribution of stress transfer within the composites leading to a better performance. When the volume fraction was more than 10%, the GCW tend to agglomerate. This created flaws and voids. Therefore, mechanical properties are declined.

Overall, the incorporation of GCW to oxo-biodegradable HDPE offers an environmentally friendly alternative to recycling the high volume of generated ground coffee waste in order to turn it into a value-added product, minimise the ecological damage and to reduce the production cost. The fabricated composites are able to degrade themselves at the end of their life cycle without leaving any negative effect on the environment. This particular type of green and eco-friendly composite has the potential to be in the application of consumable, packaging, gardening, furniture parts, door frame and profiles, and automotive components.

5.2 Future work

Along the process of completing this study, numerous suggestions can be made to improve the quality of work in the future.

- **Interfacial bonding**. Adhesion between fibre and matrix has a significant role in determining the mechanical properties of the composites. Other treatments such as coupling agent, compatiliser or enzyme treatment can be used to form a bond, to make the filler more hydrophobic and to provide better adhesion.
- **Particle size**. This study covers micro-particle with irregular shape and having low aspect ratio. Further study can be conducted to analyse nanoparticle GCW and increase its aspect ratio to improve the performance of the composites.
- **Biodegradability**. Biodegradability of oxo-HDPE can be studied such as burial in soil compos

REFERENCES

Aboul-Fadl, S. M., Zeronian, S. H., Kamal, M. M., Kim, M. S., & Ellison, M. S. (1985). Effect of Mercerization on the Relation Between Single Fiber Mechanical Properties and Fine Structure for Different Cotton Species. *Textile Research Journal*, *55*(8), 461–469.

Aga, E., Bryngelsson, T., Bekele, E., & Salomon, B. (2003). Genetic diversity of forest arabica coffee (Coffea arabica L.) in Ethiopia as revealed by random amplified polymorphic DNA (RAPD) analysis. *Hereditas*, *138*(1), 36–46.

Agrawal, R., Saxena, N., Sharma, K., Thomas, S., & Sreekala, M. (2000). Activation energy and crystallization kinetics of untreated and treated oil palm fibre reinforced phenol formaldehyde composites. *Materials Science and Engineering: A*, *277*(1-2), 77–82.

Akil, H. M., Omar, M. F., Mazuki, A. A. M., Safiee, S., Ishak, Z. A. M., & Abu Bakar, A. (2011). Kenaf fiber reinforced composites: A review. *Materials & Design*, *32*(8-9), 4107–4121.

Altun, Y., Doğan, M., & Bayramli, E. (2013). Comparative study of maleated and glycidyl methacrylate functionalized terpolymers as compatibilizers for low-density polyethylene-wood flour composites. *Journal of Applied Polymer Science*, *127*(2), 1010–1016.

Anbukarasi, K., & Kalaiselvam, S. (2015). Study of effect of fibre volume and dimension on mechanical , thermal , and water absorption behaviour of luffa reinforced epoxy composites. *Materials and Design*, *66*, 321–330.

Ang, T. N., Yoon, L. W., Lee, K. M., Ngoh, G. C., Chua, A. S. M., & Lee, M. G. (2011). Efficiency of Ionic Liquids in the Dissolution of Rice Husk. *Bioresources*, *6*(4), 4790–4800.

Arbelaiz, A., Fernández, B., Ramos, J. A., Retegi, A., Llano-Ponte, R., & Mondragon, I. (2005). Mechanical properties of short flax fibre bundle/polypropylene composites: Influence of matrix/fibre modification, fibre content, water uptake and recycling. *Composites Science and Technology*, *65*(10), 1582–1592.

Arrakhiz, F. Z., Malha, M., Bouhfid, R., Benmoussa, K., & Qaiss, A. (2013). Tensile, flexural and torsional properties of chemically treated alfa, coir and bagasse reinforced polypropylene. *Composites Part B: Engineering*, *47,* 35–41.

ASTM D3039/D3039M. (2000). Standard Test Method for Tensile Properties of Polymer Matrix Composite Materials. *Annual Book of ASTM Standards*.

ASTM D3763. (2012). ASTM D3763: Standard Test Method for High Speed Puncture Properties of Plastics Using Load and Displacement Sensors. *ASTM International*.

ASTM D570-98. (2010). ASTM D570-10: Standard Test Method for Water absorption of Plastics.

Avella, M., Bogoeva-Gaceva, G., Bužarovska, A., Errico, M. E., Gentile, G., & Grozdanov, A. (2008). Poly(lactic acid)-based biocomposites reinforced with kenaf fibers. *Journal of Applied Polymer Science*, *108*(6), 3542–3551.

Baek, B. S., Park, J. W., Lee, B. H., & Kim, H. J. (2013). Development and Application of Green Composites: Using Coffee Ground and Bamboo Flour. *Journal of Polymers and the Environment, 21*(3), 702–709.

Baghaei, B., Skrifvars, M., Salehi, M., Bashir, T., Rissanen, M., & Nousiainen, P. (2014). Novel aligned hemp fibre reinforcement for structural biocomposites: Porosity, water absorption, mechanical performances and viscoelastic behaviour. *Composites Part A: Applied Science and Manufacturing*, *61*, 1–12.

Ballesteros, L. F., Teixeira, J. A., & Mussatto, S. I. (2014). Chemical, Functional, and Structural Properties of Spent Coffee Grounds and Coffee Silverskin. *Food and Bioprocess Technology*, *7*(12), 3493–3503.

Beckermann, G. W., & Pickering, K. L. (2009). Engineering and evaluation of hemp fibre reinforced polypropylene composites: Micro-mechanics and strength prediction modelling. *Composites Part A: Applied Science and Manufacturing*, *40*(2), 210–217.

Bera, M., Alagirusamy, R., & Das, A. (2010). A study on interfacial properties of jute-PP composites. *Journal of Reinforced Plastics and Composites*, *29*(20), 3155–3161.

Bernhard, J., & Elmar, W. (2013). *Composites Market Report 2013: Market Developments, Trends,* *Challenges and Opportunities*. Europe.

Berthaud, J., & Charrier, A. (2008). *Coffee: Recent Developments*. (R. Clarke & O. G. Vitzthum, Eds.). John Wiley & Sons.

Biagiotti, J., Puglia, D., & Kenny, J. M. (2004). A Review on Natural Fibre-Based Composites-Part I. *Journal of Natural Fibers*, *1*(2), 37–68.

Bisanda, E. T. N., & Ansell, M. P. (1992). Properties of sisal-CNSL composites. *Journal of Materials Science*, *27*(6), 1690–1700.

Bismarck, A., Mishra, S., & Lampke, T. (2005). Plant fibers as reinforcement for green composites. In A. K. Mohanty, M. Misra, & L. T. Drzal (Eds.), *Natural Fibers, Biopolymers, and Biocomposites*. Boca Raton, Florida: CRC Press.

Bledzki, A. K., & Gassan, J. (1997). Natural Fiber Reinforced Plastics. In P. Cheremisinoff (Ed.), *Handbook of Engineering Polymeric Materials* (p. 787). New Jersey: CRC Press.

Bledzki, A. K., & Gassan, J. (1999). Composites reinforced with cellulose based fibres. *Progress in Polymer Science*, *24*(2), 221–274.

Bledzki, A. K., Mamun, A. A., Lucka-Gabor, M., & Gutowski, V. S. (2008). The effects of acetylation on properties of flax fibre and its polypropylene composites. *Express Polymer Letters*, *2*(6), 413–422.

Bledzki, A. K., Reihmane, S., & Gassan, J. (1996). Properties and modification methods for vegetable fibers for natural fiber composites. *Journal of Applied Polymer Science*, *59*(8), 1329–1336.

Bledzki, A., Mamun, A., Jaszkiewicz, A., & Erdmann, K. (2010). Polypropylene composites with enzyme modified abaca fibre. *Composites Science and Technology*, *70*(5), 854–860.

Brebu, M., & Vasile, C. (2010). Thermal degradation of Lignin - A review. *Cellulose Chemistry and Technology*, *44*(9), 353–363.

Caetano, N. S., Silvaa, V. F. M., & Mata, T. M. (2012). Valorization of coffee grounds for biodiesel production. *Chemical Engineering Transactions*, *26*, 267–272.

Callister, W. D., & Rethwisch, D. G. (2012). *Fundamentals of Materials Science and Engineering: An Integrated Approach*. John Wiley & Sons.

Castro, D. O., Ruvolo-Filho, a., & Frollini, E. (2012). Materials prepared from biopolyethylene and curaua fibers: Composites from biomass. *Polymer Testing*, *31*(7), 880–888.

Chand, N., & Rohatgi, P. K. (1994). *Natural Fibres and Their Composites*. *Periodical Experts Book Agency*. Delhi, India: Periodical Experts Book Agency.

Clark, J. H., & Deswarte, F. (2014). *Introduction to Chemicals from Biomass*. Cornwall: Wiley.

Clyne, T. W., & Withers, P. J. (1995). *An Introduction to Metal Matrix Composites*. Cambridge University Press.

Coats, A. W., & Redfern, J. P. (1963). Thermogravimetric analysis. A review. *The Analyst*, *88*(1053), 906.

Craig, A. P., Franca, A. S., & Oliveira, L. S. (2012). Evaluation of the potential of FTIR and chemometrics for separation between defective and non-defective coffees. *Food Chemistry*, *132*(3), 1368–1374.

Cremer, D. R., & Kaletunç, G. (2003). Fourier transform infrared microspectroscopic study of the chemical microstructure of corn and oat flour-based extrudates. *Carbohydrate Polymers*, *52*, 53–65.

Davachi, S. M., Kaffashi, B., Davoodi, S., Pouresmaeel-Selakjani, P., Bakhtiari, S., Mohammadi-Rovshandeh, J., & Yousefi, A. (2015). Investigating the Effect of Treated Rice Straw in PLLA/Starch Composite: Mechanical, Thermal, Rheological, and Morphological Study. *Advances in Polymer Technology*, *00*(0), 1–12.

de Candolle, M. A. P. (1813). *Theorie Elementaire de la Botanique ou Exposition des Principes de la Classification Naturelle et de l'Art de Decrire et d'Etudier les Vegetaux*. Paris: Deterville.

De, S. K., & White, J. R. (1996). *Short fibre polymer composite*. England: Woodhead Publishing Limited.

Dittenber, D. B., & Gangarao, H. V. S. (2012). Critical review of recent publications on use of natural composites in infrastructure. *Composites Part A: Applied Science and Manufacturing*, *43*(8), 1419–1429.

Edwin, R., Sanker, P., Sekar, T., & Munusamy, T. S. (2006). *Botany*. Chennai, India: Government of

Tamil Nadu.

Enamul Hossain, M. (2011). The current and future trends of composite materials: an experimental study. *Journal of Composite Materials*, *45*(May), 2133–2144.

Eucia. (2011). *Composites Recycling Made Easy. European Composites Industry Association*. Brussel, Belgium.

Faix, O. (1991). Classification of Lignins from Different Botanical Origins by FT-IR Spectroscopy. *Holzforschung*, *45*(s1), 21–28.

Fan, M., Dai, D., & Huang, B. (2012). Fourier Transform Infrared Spectroscopy for Natural Fibres. In Salih Mohammed Salih (Ed.), Fourier Transform - Materials Analysis (pp. 45–68). InTech.

Faruk, O., Bledzki, A. K., Fink, H. P., & Sain, M. (2012). Biocomposites reinforced with natural fibers:2000-2010. *Progress in Polymer Science*, *37*(11), 1552–1596.

Faruk, O., Bledzki, A. K., Fink, H., & Sain, M. (2012). Progress in Polymer Science Biocomposites reinforced with natural fibers : 2000 – 2010. *Progress in Polymer Science*, *37*(11), 1552–1596.

Fávaro, S. L., Lopes, M. S., Vieira de Carvalho Neto, A. G., Rogério de Santana, R., & Radovanovic, E. (2010). Chemical, morphological, and mechanical analysis of rice husk/post-consumer polyethylene composites. *Composites Part A: Applied Science and Manufacturing*, *41*(1), 154–160.

Fernandes, E. M., Mano, J. F., & Reis, R. L. (2013). Hybrid cork-polymer composites containing sisal fibre: Morphology, effect of the fibre treatment on the mechanical properties and tensile failure prediction. *Composite Structures*, *105*, 153–162.

Fidelis, M. E. A., Pereira, T. V. C., Gomes, O. da F. M., Silva, F. de A., & Filho, R. D. T. (2013). The effect of fiber morphology on the tensile strength of natural fibers. *Journal of Material Research and Technology*, *2*(2), 149–157.

Fiol, N., Escudero, C., & Villaescusa, I. (2008). Re-use of Exhausted Ground Coffee Waste for Cr(VI) Sorption. *Separation Science and Technology*, *43*(3), 582–596.

Focher, B. (1992). Physical characteristics of flax fibre. In H. S. Sharma (Ed.), *The biology and* *processing of flax* (pp. 11–32). Belfast, UK: M. Publications.

Franco-Marquès, E., Méndez, J. A., Pèlach, M. A., Vilaseca, F., Bayer, J., & Mutjé, P. (2011). Influence of coupling agents in the preparation of polypropylene composites reinforced with recycled fibers. *Chemical Engineering Journal*, *166*(3), 1170–1178.

Fu, D., Mazza, G., & Tamaki, Y. (2010). Lignin extraction from straw by ionic liquids and enzymatic hydrolysis of the cellulosic residues. *Journal of Agricultural and Food Chemistry*, *58*(5), 2915–22.

Fu, S. Y., Feng, X.Q., Lauke, B., & Mai, Y.W. (2008). Effects of particle size, particle/matrix interface adhesion and particle loading on mechanical properties of particulate–polymer composites. *Composites Part B: Engineering*, *39*(6), 933–961.

Fu, S. Y., & Lauke, B. (1998). Characterization of tensile properties behavior of hybrid short glass fibre calcite particle ABS composites. *Composite Part A*, *29A*, 575–583.

García, D., López, J., Balart, R., Ruseckaite, R. A., & Stefani, P. M. (2007). Composites based on sintering rice husk-waste tire rubber mixtures. *Materials and Design*, *28*(7), 2234–2238.

Garcia-Garcia, D., Carbonell, A., Samper, M. D., & Balart, G. R. (2015). Green composites based on polypropylene matrix and hydrophobized spend coffee ground (SCG) powder. *Composites Part B*, *78*, 256–265.

Geethamma, V. G., Thomas Mathew, K., Lakshminarayanan, R., & Thomas, S. (1998). Composite of short coir fibres and natural rubber: effect of chemical modification, loading and orientation of fibre. *Polymer*, *39*(6-7), 1483–1491.

Gho, J. G., Ballingham, E. P. N., Chiellini, E., Swift, G., Wiles, D., & Katsaros, N. (2008). EPI’s Oxo-biodegradable Plastics Guidebook (Vol. 1). Canada: EPA Environmental Products Inc.

Goda, K., Sreekala, M. S., Gomes, A., Kaji, T., & Ohgi, J. (2006). Improvement of plant based natural fibers for toughening green composites—Effect of load application during mercerization of ramie fibers. *Composites Part A: Applied Science and Manufacturing*, *37*(12), 2213–2220.

Gomes, A., Matsuo, T., Goda, K., & Ohgi, J. (2007). Development and effect of alkali treatment on tensile properties of curaua fiber green composites. *Composites Part A: Applied Science and*

Manufacturing, *38*(8), 1811–1820.

Hansen, N. M. L., & Plackett, D. (2008). Sustainable films and coatings from hemicelluloses: a review. *Biomacromolecules, 9*(6), 1493–505.

Harlan, J. R. (1969). Ethiopia: A center of diversity. *Economic Botany*, *23*(4), 309–314.

He, & Pei. (2013). *On the structure-property correlation and the evolution of Nanofeatures in 12-13.5% Cr oxide dispersion strengthened ferritic steels*. KIT Scientific Publishing.

Ho, M., Wang, H., Lee, J.H., Ho, C.-K., Lau, K.T., Leng, J., & Hui, D. (2012). Critical factors on manufacturing processes of natural fibre composites. *Composites Part B*, *8*(8), 3549–3562.

Höhne, G., Hemminger, W., & Flammersheim, H.J. (2003). *Differential Scanning Calorimetry*. Springer Science & Business Media.

Holbery, J., & Houston, D. (2006). Natural-fiber-reinforced polymer composites in automotive applications. *JOM*, *58*(11), 80–86.

Hsueh, C.-H. (1989). Effects of Aspect Ratios of Ellipsoidal Inclusions on Elastic Stress Transfer of Ceramic Composites. *Journal of the American Ceramic Society*, *72*(2), 344–347.

Hull, D., & Clyne, T. W. (1996). *An Introduction to Composite Materials*. Cambridge University Press.

Hung, K. C., Wu, T. L., Chen, Y. L., & Wu, J. H. (2016). Assessing the effect of wood acetylation on mechanical properties and extended creep behavior of wood/recycled-polypropylene composites. *Construction and Building Materials*, *108*, 139–145.

Ibrahim, N. A., Hadithon, K. A., & Abdan, K. (2010). Effect of Fiber Treatment on Mechanical Properties of Kenaf Fiber-Ecoflex Composites. *Journal of Reinforced Plastics and Composites, 29*(14), 2192–2198.

Illy, A., & Viani, R. (2005). *Espresso Coffee: The Science of Quality*. Academic Press.

International Coffee Organization. (2014). *Coffee Consumption in East and Southeast Asia: 1990-2012.*

International cotton advisory committee (2012). *Overview of World Fibre Production*. *Discover*

Natural Fibre Initiative, Washington, USA.

Islam, M. S., Pickering, K. L., & Foreman, N. J. (2010). Influence of alkali treatment on the interfacial and physico-mechanical properties of industrial hemp fibre reinforced polylactic acid composites. *Composites Part A: Applied Science and Manufacturing*, *41*(5), 596–603.

Jawaid, M., & Abdul Khalil, H. P. S. (2011). Cellulosic/synthetic fibre reinforced polymer hybrid composites: A review. *Carbohydrate Polymers*, *86*(1), 1–18.

Joseph, K., James, B., Thomas, S., & Carvalho, L. H. De. (1999). A review on sisal fiber reinforced polymer. *Revista Brasileira de Engenharia Agr ćola E Ambiental*, *3*(3), 367–379.

Joseph, S., Sreekala, M. S., Oommen, Z., Koshy, P., & Thomas, S. (2002). A comparison of the mechanical properties of phenol formaldehyde composites reinforced with banana fibres and glass fibres. *Composites Science and Technology*, *62*(14), 1857–1868.

Kabir, M. M., Wang, H., Lau, K. T., Cardona, F., & Aravinthan, T. (2012). Mechanical properties of chemically-treated hemp fibre reinforced sandwich composites. *Composites Part B: Engineering*, *43*(2), 159–169.

Kakou, C. A., Arrakhiz, F. Z., Trokourey, A., Bouhfid, R., Qaiss, A., & Rodrigue, D. (2014). Influence of coupling agent content on the properties of high density polyethylene composites reinforced with oil palm fibers. *Materials & Design*, *63*, 641–649.

Kalia, S., Kaith, B. S., & Kaur, I. (2009). Pretreatments of Natural Fibers and their Application as Reinforcing Material in Polymer Composites — A Review. *Polymer Engineering and Science*, *49*(7), 1253–1272.

Kang, J. T., Park, S. H., & Kim, S. H. (2014). Improvement in the adhesion of bamboo fiber reinforced polylactide composites. *Journal of Composite Materials*, *48*(21), 2567–2577.

Kemsley, E. K., Ruault, S., & Wilson, R. H. (1995). Discrimination Between Coffea-Arabica and Coffea-Canephora Variant Robusta Beans Using Infrared-Spectroscopy. *Food Chemistry*, *54*(3), 321–326.

Khalaf, M. N. (2015). Mechanical Properties of filled high density polyethylene. *Journal of Saudi*

Chemical Society, *19*, 88–91.

Khan, M. A., Ali, K. M. I., & Basu, S. C. (1993). IR studies of wood plastic composites. *Journal of Applied Polymer Science*, *49*(9), 1547–1551.

Kifani-Sahban, F., Belkbir, L., & Zoulalian, A. (1996). Study of the slow pyrolysis of Moroccan eucalyptus by thermal analysis. *Thermochimica Acta*, *2*(284), 341–349.

Kim, M., & Day, D. F. (2011). Composition of sugar cane, energy cane, and sweet sorghum suitable for ethanol production at Louisiana sugar mills. *Journal of Industrial Microbiology & Biotechnology*, *38*(7), 803–807.

Kingston, C., Zepp, R., Andrady, A., Boverhof, D., Fehir, R., Hawkins, D., Roberts, J., Sayre, P., Shelton, B., Sultan, Y., Vejins, V., & Wohlleben, W. (2014). Release characteristics of selected carbon nanotube polymer composites. *Carbon*, *68*, 33–57.

Kolboe, S., & Ellefsen, O. (1962). Infrared investigations of lignin. A discussion of some recent results. *Tappi*, *45*, 163–166.

Kondo, T. (2004). Hydrogen Bonds in Cellulose and Cellulose Derivatives. In S. Dumitriu (Ed.), *Structural Diversity and Functional Versatility* (2nd Ed). New York, USA: CRC Press.

Kumar, S., Kothari, U., Kong, L., Lee, Y. Y., & Gupta, R. B. (2011). Hydrothermal pretreatment of switchgrass and corn stover for production of ethanol and carbon microspheres. *Biomass and Bioenergy*, *35*(2), 956–968.

Le Troedec, M., Rachini, A., Peyratout, C., Rossignol, S., Max, E., Kaftan, O., Ferry, A., & Smith, A. (2011). Influence of chemical treatments on adhesion properties of hemp fibres. *Journal of Colloid and Interface Science*, *356*(1), 303–310.

Lee, H. K., Park, Y. G., Jeong, T., & Song, Y. S. (2015). Green nanocomposites filled with spent coffee grounds. *Journal of Applied Polymer Science*, *132*(23), 2–7.

Lee, K. M., Ngoh, G. C., Seak, A., Chua, M., Yoon, L. W., Ang, T. N., & Lee, M. (2014). Comparison Study of Different Ionic Liquid Pretreatments in Maximizing Total Reducing Sugars Recovery. *Bioresources.com*, *9*(1), 1552–1564.

Li, X., Tabil, L. G., & Panigrahi, S. (2007). Chemical treatments of natural fiber for use in natural fiber-reinforced composites: A review. *Journal of Polymers and the Environment*, *15*(1), 25–33.

Liang, J. Z., Li, R. K. Y., & Tjong, S. C. (1997). Tensile fracture behaviour and morphological analysis of glass bead filled low density polyethylene composites. *Plastics Rubber and Composites Processing and Applications*, *26*, 278–282.

Lipp-Symonowicz, B., Tańska, B., Wołukanis, A., & Wrzosek, H. (2004). Influence of Enzymatic Treatment on the Flax Fibre Morphological Structure, Physico - Chemical Properties and Metrological Parameters of Yarn. *Fibres & Textiles in Eastern Europe*, *1*(45), 61–65.

Liu, L., Yu, J., Cheng, L., & Qu, W. (2009). Mechanical properties of poly(butylene succinate) (PBS) biocomposites reinforced with surface modified jute fibre. *Composites Part A: Applied Science and Manufacturing*, *40*(5), 669–674.

Malkapuram, R., & Kumar, V. (2008). Recent Development in Natural Fiber Reinforced Polypropylene Composites. *Journal of Reinforced Plastics and Composites*, *28*(10), 1169–1189.

Malkapuram, R., Kumar, V., & Yuvraj Singh Negi, Y. S. (2009). Recent Development in Natural Fiber Reinforced Polypropylene Composites. *Journal of Reinforced Plastics and Composites*, *28*(10), 1169–1189.

Mamun, A. A., & Bledzki, A. K. (2013). Micro fibre reinforced PLA and PP composites: Enzyme modification, mechanical and thermal properties. *Composites Science and Technology*, *78*, 10–17.

Matuana, L. M., Balatinecz, J. J., Sodhi, R. N. S., & Park, C. B. (2001). Surface characterization of esterified cellulosic fibers by XPS and FTIR spectroscopy. *Wood Science and Technology*, *35*(3), 191–201.

Medronho, B., & Lindman, B. (2014). Competing forces during cellulose dissolution: From solvents to mechanisms. *Current Opinion in Colloid & Interface Science*, *19*(1), 32–40.

Mérot-L'Anthoëne, V., Mangin, B., Lefebvre-Pautigny, F., Jasson, S., Rigoreau, M., Husson, J., Lambot, C., & Crouzillat, D. (2014). Comparison of three QTL detection models on biochemical, sensory, and yield characters in Coffea canephora. *Tree Genetics & Genomes*, *10*(6), 1541–1553.

Michell, A. J., & Willis, D. (1978). Cellulosic fibres for reinforcement [use of wood fibres in structural materials]. *Appita*.

Mohanty, A. ., Khan, M. ., & Hinrichsen, G. (2000). Influence of chemical surface modification on the properties of biodegradable jute fabrics—polyester amide composites. *Composites Part A: Applied Science and Manufacturing*, *31*(2), 143–150.

Mohanty, A. K., Misra, M., & Drzal, L. T. (2001). Surface modifications of natural fibers and performance of the resulting biocomposites: An overview. *Composite Interfaces*, *8*(5), 313–343.

Mussatto, S. I., Ballesteros, L. F., Martins, S., & Teixeira, J. A. (2011a). Extraction of antioxidant phenolic compounds from spent coffee grounds. *Separation and Purification Technology*, *83*, 173–179.

Mussatto, S. I., Machado, E. M. S., Martins, S., & Teixeira, J. A. (2011b). Production, Composition, and Application of Coffee and Its Industrial Residues. *Food and Bioprocess Technology*, *4*(5), 661–672.

Mussig, J. (2010). *Industrial Applications of Natural Fibres: Structure, Properties and Technical Applications*. United Kingdom: John Wiley & Sons.

Mwaikambo, L. Y., & Ansell, M. P. (1999). The effect of chemical treatment on the properties of hemp, sisal, jute and kapok for composite reinforcement. *Die Angewandte Makromolekulare Chemie*, *272*(1), 108–116.

Mwaikambo, L. Y., & Ansell, M. P. (2002). Chemical modification of hemp, sisal, jute, and kapok fibers by alkalization. *Journal of Applied Polymer Science*, *84*(12), 2222–2234.

Nam, T. H., Ogihara, S., Tung, N. H., & Kobayashi, S. (2011). Effect of alkali treatment on interfacial and mechanical properties of coir fiber reinforced poly(butylene succinate) biodegradable composites. *Composites Part B: Engineering*, *42*(6), 1648–1656.

Nekhlaoui, S., Essabir, H., Bensalah, M. O., Fassi-Fehri, O., Qaiss, A., & Bouhfid, R. (2014). Fracture study of the composite using essential work of fracture method: PP–SEBS–g–MA/E1 clay. *Materials & Design*, *53*, 741–748.

Nelson, D. L., & Cox, M. M. (2013). *Lehninger Principles of Biochemistry*. Portland: Macmillan learning.

Nguyen, T., Zavarin, E., & barrall, E. M. (2007a). Thermal Analysis of Lignocellulosic Materials. *Journal of Macromolecular Science, Part C*, *20*(1), 1–65.

Nguyen, T., Zavarin, E., & Barrall, E. M. (2007b). Thermal Analysis of Lignocellulosic Materials. Part II. Modified Materials. *Journal of Macromolecular Science, Part C*, *21*(1), 1–60.

Nicolet, T., & All, C. (2001). *Introduction to Fourier Transform Infrared Spectrometry*. *A Thermo Electron Bussines*.

Nishiyama, Y., Langan, P., & Chanzy, H. (2002). Crystal Structure and Hydrogen-Bonding System in Cellulose Iβ from Synchrotron X-ray and Neutron Fiber Diffraction. *Journal of the American Chemical Society*, *124*(31), 9074–9082.

Obasi, H. ., Iheaturu, N. C., Onuoha, F. . ., Akanbi, M. N., & Ezeh, V. O. (2014). Influence of Alkali Treatment and Fibre Content on the Properties of Oil Palm Press Fibre Reinforced Epoxy Biocomposites. *American Journal of Engineering Research*, *3*(02), 117–123.

Ou, Y., Yang, F., & Yu, Z. Z. (1998). A new conception on the toughness of nylon6/silica nano composite prepaid via in situ polymerization. *Journal of Polymer Science Part B: Polymer Physics*, *36*, 789–795.

Padmapriya, R., Tharian, J. A., & Thirunalasundari, T. (2013). Coffee waste management-An overview. *Int J Curr Sci*, *9*, 83–91.

Panthapulakkal, S., Sain, M., & Law, S. (2005). Effect of coupling agents on rice-husk-filled HDPE extruded profiles. *Polymer International*, *54*(1), 137–142.

Paradkar, M. M., & Irudayaraj, J. (2002). Rapid determination of caffeine content in soft drinks using FTIR-ATR spectroscopy. *Food Chemistry*, *78*(2), 261–266.

Peng, F., Bian, J., Peng, P., Guan, Y., Xu, F., & Sun, R. C. (2012). Fractional separation and structural features of hemicelluloses from sweet sorghum leaves. *BioResources*, *7*(4), 4744–4759.

Perez, I. S. B., Manrich, S., & Manrich, S. (2008). The effect of different block copolymers on post consumer HDPE/HIPS Blends: phase morphology and thermal properties. *Pol ́meros*, *18*(3), 207–214.

Pervan, S., Prekrat, S., Gorisek, Z., Straze, A., & Humar, M. (2006). Effect of Steaming on Colour and Chemistry of Cherrywood (Prunus Avium L .). In S. Kurjatko, J. Kudela, & J. Lagana (Eds.), *Wood Structure and Properties '06* (pp. 331–336). Zvolen, Slovakia: Arbora Publisher.

Pickering, K. L., Efendy, M. G. A., & Le, T. M. (2016). A review of recent developments in natural fibre composites and their mechanical performance. *Composites Part A: Applied Science and Manufacturing*, *83*, 98–112.

Pickering, K., Li, Y., & Farrell, R. (2007). Interfacial modification of hemp fiber reinforced composites using fungal and alkali treatment. *Journal of Biobased Materials and Bioenergy*, *1*(1), 109–117.

Preethu, D. C., Prakash, B. N. U. H., Srinivasamurthy, C. A., & Vasanthi, B. G. (2007). Maturity indices as in index to evaluate the quality of compost of coffee waste blended with other organic wastes. In *Proceedings of the International Conference on Sustainable Solid Waste Management* (pp. 270–275). Chennai, India.

Pujol, D., Liu, C., Gominho, J., Olivella, M. À., Fiol, N., Villaescusa, I., & Pereira, H. (2013). The chemical composition of exhausted coffee waste. *Industrial Crops and Products*, *50*, 423–429.

Pukánszky, B. (1993). Interfacial interactions in particulate filled thermoplastics: Mechanism, strength, properties. *Makromolekulare Chemie. Macromolecular Symposia*, *70-71*(1), 213–223.

Pukánszky, B., & Móczó, J. (2004). Morphology and Properties of Particulate Filled Polymers. *Macromolecular Symposia*, *214*(1), 115–134.

Pukanszky, B., & Voros, G. (1996). No TitleStress distribution around inclusions, interaction and mechanical properties of particulate-filled composites. *Polymer Composites*, *17*(3), 384–392.

Raj, R. G., Kokta, B. V., Maldas, D., & Daneault, C. (1989). Use of wood fibers in thermoplastics. VII. The effect of coupling agents in polyethylene–wood fiber composites. *Journal of Applied Polymer Science*, *37*(4), 1089–1103.

Ramawat, K. G., Mérillon, J.-M., & Ahuja, M. R. (2014). *Tree Biotechnology*. Boca Raton: CRC Press.

Reis, N., Franca, A. S., & Oliveira, L. S. (2013). Discrimination between roasted coffee, roasted corn and coffee husks by Diffuse Reflectance Infrared Fourier Transform Spectroscopy. *LWT - Food Science and Technology*, *50*(2), 715–722.

Reviews, C. T. (2012). *e-Study Guide for: Introduction to the Principles of Materials Evaluation: Chemistry, Materials science*. Cram101.

Riley, A. M., Paynter, C. D., McGenity, P. M., & Adams, J. M. (1990). Factors affecting the impact properties of mineral filled polypropylene. *Plastics and Rubber Processing and Applications, 14*(2), 85–93.

Rokbi, M., Osmani, H., Imad, A., & Benseddiq, N. (2011). Effect of chemical treatment on flexure properties of natural fiber-reinforced polyester composite. *Procedia Engineering*, *10*, 2092–2097.

Rong, M. Z., Zhang, M. Q., Liu, Y., Yang, G. C., & Zeng, H. M. (2001). The effect of fiber treatment on the mechanical properties ofunidirectional sisal-reinforced epoxy composites. *Composites Science and Technology*, *61*(10), 1437–1447.

Rothon, R. N. (2007). The high performance fillers market and the position of precipitated calcium carbonate and silica. In *proceedings of high performance fillers*. Hamburg, Germany.

Rowell, R. M., Sanadi, A. R., Caulfield, D. F., & Jacobson, R. E. (1997). Utilization of Natural Fibers in Plastic Composites : Problems and Opportunities. *Lignocellulosic-Plastic Composites*, 23–51.

Rozman, H. D., Ismail, H., Jaffri, R. M., Aminullah, a., & Mohd Ishak, Z. A. (1998). Mechanical Properties of Polyethylene-Oil Palm Empty Fruit Bunch Composites. *Polymer-Plastics Technology and Engineering*, *37*(4), 495–507.

Rozman, H. D., Tay, G. S., Kumar, R. N., Abusamah, A., Ismail, H., & Mohd Ishak, Z. A. (2001). The effect of oil extraction of the oil palm empty fruit brunch on the mechanical properties of polypropylene-oil palm empty fruit bunch-glass fibre hybrid composites. *Polymer-Plastics Technology and Engineering*, *40*(2), 103–115.

Saechtling, H. (1995). *Saechtling international plastics handbook : for the technologist, engineer, and user*. Munich ; Hanser Publishers.

Saheb, D. N., & Jog, J. P. (1999). Natural fiber polymer composites: A review. *Advances in Polymer Technology*, *18*(4), 351–363.

Saleem, Z., Rennebaum, H., Pudel, F., & Grimm, E. (2008). Treating bast fibres with pectinase improves mechanical characteristics of reinforced thermoplastic composites. *Composites Science and Technology*, *68*(2), 471–476.

Sawpan, M. A., Pickering, K. L., & Fernyhough, A. (2011). Improvement of mechanical performance of industrial hemp fibre reinforced polylactide biocomposites. *Composites Part A: Applied Science and Manufacturing*, *42*(3), 310–319.

Scott, G. (2009). Oxo-biodegradable plastic. *Bioplastics Magazine*, 28–30.

Sheltami, R. M., Abdullah, I., Ahmad, I., Dufresne, A., & Kargarzadeh, H. (2012). Extraction of cellulose nanocrystals from mengkuang leaves (Pandanus tectorius). *Carbohydrate Polymers*, *88*(2), 772–779.

Shinoj, S., Visvanathan, R., Panigrahi, S., & Kochubabu, M. (2011). Oil palm fiber (OPF) and its composites: A review. *Industrial Crops and Products*, *33*(1), 7–22.

Sibele Piedade, C., & Luis Claudio, M. (2013). Thermal properties and morphology of high-density polyethylene filled with coffee dregs. *Journal of Thermal Analysis and Calorimetry*, *114*(1), 1–4.

Singha, A. S., Rana, A. K., & Jarial, R. K. (2013). Mechanical, dielectric and thermal properties of Grewia optiva fibers reinforced unsaturated polyester matrix based composites. *Materials and Design*, *51*, 924–934.

Siracusa, V., Rocculi, P., Romani, S., & Rosa, M. D. (2008). Biodegradable polymers for food packaging: a review. *Trends in Food Science and Technology*, *19*(12), 634–643.

Sjostrom, E. (1993). *Wood Chemistry: Fundamentals and Applications*. San Diego, California: Acadamic Press Inc.

Spence, K. L., Venditti, R. a., Habibi, Y., Rojas, O. J., & Pawlak, J. J. (2010). The effect of chemical composition on microfibrillar cellulose films from wood pulps: Mechanical processing and physical properties. *Bioresource Technology*, *101*(15), 5961–5968.

Sreekala, M. S., Kumaran, M. G., Joseph, S., Jacob, M., & Thomas, S. (2000). Oil Palm Fibre Reinforced Phenol Formaldehyde Composites: Influence of Fibre Surface Modifications on the Mechanical Performance. *Applied Composite Materials*, *7*(5/6), 295–329.

Sridhar, M. K., Basavarajappa, G., Kasturi, S. G., & Balasubramanian, N. (1982). Evaluation of jute as a reinforcement in composites. *Indian J Fibre Text Res*, *7*, 87–92.

Stamboulis, A., Baillie, C. A., & Peijs, T. (2001). Effects of environmental conditions on mechanical and physical properties of flax fibers. *Composites Part A: Applied Science and Manufacturing*, *32*(8), 1105–1115.

Stark, N. M., & Rowlands, R. E. (2003). Effects of wood fiber characteristics on mechanical properties of wood/polypropylene composites. *Wood and Fibre Science*, *35*(2), 167–174.

Suetsugu, Y., Kikutani, T., Kyu, T., & White, J. L. (1990). An experimental technique for characterizing dispersion in compounds of particulates in thermoplastics using small-angle light scattering. *Colloid & Polymer Science*, *268*(2), 118–131.

Sun, R., Fang, J. M., Mott, L., & Bolton, J. (1999). Fractional Isolation and Characterization of Polysaccharides from Oil Palm Trunk and Empty Fruit Bunch Fibres. *Holzforschung*, *53*(3), 253–260.

Sun, R., Fang, J. M., Mott, L., & Bolton, J. (1999). ractional isolation and characterization of Polysaccharides from oil palm trunk and empty fruit bunch fibres. *Hozforschung*, *53*(3), 253–260.

Tan, C. L. (2010). Bags that break down. *The Star Online*. Retrieved from http://www.thestar.com.my/story/?file=%2F2010%2F12%2F7%2Flifefocus%2F7548373&sec=lifefocus

Tan, I. A. W., Wu, W. H., Chan, R. A., & Lim, L. L. P. (2014). Effect of Mercerization and Acetylation on Properties of Coconut Fiber and its Influence on Modified Bitumen. *UNIMAS E-Journal of Civil Engineering*, 5(1), 17–22.

Taşdemır, M., Biltekin, H., & Caneba, G. T. (2009). Preparation and characterization of LDPE and PP-Wood fiber composites. *Journal of Applied Polymer Science*, *112*(5), 3095–3102.

Thakur, V. K. (2013). *Green Composites from Natural Resources*. Boca Raton, Florida: CRC Press.

Thermogravimetric Analysis (TGA) A Beginner's Guide. (2010). *PerkinElmer, Inc*. USA.

Thomas, E. T., & Dobkin, A. B. (1972). Untoward effects of muscle relaxant drugs. *International Anesthesiology Clinics*, *10*(1), 207–25.

Thomas, S., Paul, S. A., Pothan, L. A., & Deepa., B. (2011). Natural fibres: structure, properties and applications. In S. K. Kalia (Ed.), *Cellulose fibres: bio- and nano-polymer composites: green chemistry technology*. New York, USA: Springer-Verlag Berlin Heidelberg.

Tsai, W.-T., Liu, S.-C., & Hsieh, C.-H. (2012). Preparation and fuel properties of biochars from the pyrolysis of exhausted coffee residue. *Journal of Analytical and Applied Pyrolysis*, *93*, 63–67.

Tsoumis, G. (1991). *Science and Technology of Wood: Structure, Properties, Utilization*. New York, USA: Van Nostrand Reinhold.

UK Food Standards Agency. (2003). *Safe Upper Levels for Vitamins and Minerals*. *Expert Group on Vitamins and Minerals*.

Valadez-Gonzalez, A., Cervantes-Uc, J. M., Olayo, R., & Herrera-Franco, P. J. (1999). Effect of fiber surface treatment on the fiber–matrix bond strength of natural fiber reinforced composites. *Composites Part B: Engineering*, *30*(3), 309–320.

Varma, D. S., Varma, M., & Varma, I. K. (1984). Coir Fibers: Part I: Effect of Physical and Chemical Treatments on Properties. *Textile Research Journal*, *54*(12), 827–832.

Varma, D. S., Varma, M., & Varma, I. K. (1986). Thermal behaviour of coir fibres. *Thermochimica Acta*, *108*, 199–210.

Varshney, V. K., & Naithani, S. (2011). *Cellulose Fibers: Bio- and Nano-Polymer Composites*. (S. Kalia, Ed.). Springer-Verlag Berlin Heidelberg.

Wambua, P., Ivens, J., & Verpoest, I. (2003). Natural fibres: Can they replace glass in fibre reinforced plastics? *Composites Science and Technology*, *63*(9), 1259–1264.

Willats, W. G. ., Knox, J. P., & Mikkelsen, J. D. (2006). Pectin: new insights into an old polymer are starting to gel. *Trends in Food Science & Technology*, *17*(3), 97–104.

Wu, C. S. (2015). Renewable resource-based green composites of surface-treated spent coffee grounds and polylactide: Characterisation and biodegradability. *Polymer Degradation and Stability*, *121*, 51–59.

Yang, H. S., Kim, H. J., Son, J., Park, H. J., Lee, B. J., & Hwang, T. S. (2004). Rice-husk flour filled polypropylene composites; mechanical and morphological study. *Composite Structures*, *63*(3-4), 305–312.

Yang, H. S., Wolcott, M. P., Kim, H. S., Kim, S., & Kim, H. J. (2007). Effect of different compatibilizing agents on the mechanical properties of lignocellulosic material filled polyethylene bio-composites. *Composite Structures*, *79*(3), 369–375.

Yang, Q. (2014). Global Fibres Overview. In *Synthetic fibre raw materials committee meeting at APIC 2014*. Pattaya, Thailand.

Youssef, A. M., El-Gendy, A., & Kamel, S. (2015). Evaluation of corn husk fibers reinforced recycled low density polyethylene composites. *Materials Chemistry and Physics*, *152*, 26–33.

Yu, T., Jiang, N., & Li, Y. (2014). Study on short ramie fiber/poly(lactic acid) composites compatibilized by maleic anhydride. *Composites Part A: Applied Science and Manufacturing*, *64*, 139–146.

Zahran, M. K., & Rehan, M. F. (2006). Grafting of acrylic acid onto flax fibers using Mn(IV)-citric acid redox system. *Journal of Applied Polymer Science*, *102*(3), 3028–3036.

APPENDIX

List of Publications

Colloquium:

Tan, M. Y., & Kuan, H. T. N. "Characterisation of ground coffee waste based bio-composites" North Borneo Research Colloquium 2016, 18th – 19th April 2016, Curtin University Sarawak, Malaysia.

Conference:

Tan, M. Y., Kuan, H. T. N., & Khan, A. A. "Tensile properties of ground coffee waste reinforced polyethylene composite", 4th Asia Conference of Mechanical and Material Engineering (ACMME 2016), 14th – 18th July 2016, Hotel Melia, Kuala Lumpur, Malaysia.

Journal:

Tan, M. Y., Kuan, H. T. N., & Khan, A. A. (2017). Tensile properties of ground coffee waste reinforced polyethylene composite. *Material Science Forum, 880*, 73–76.

Tan, M. Y., Kuan, H. T. N., & Lee, M. C. (2017). Characterisation of alkaline treatment and fiber content on the physical, thermal and mechanical properties of ground coffee waste/oxo-biodegradable HDPE Biocomposites. *International Journal of Polymer Science*, 2017.